UNIVERSITÀ DEGLI STUDI DI PALERMO

Dipartimento Scienze Agrarie, Alimentari e Forestali

Dottorato di Ricerca in Scienze Agrarie, Alimentari e Forestali - XXXIV ciclo

Identification and characterization of nitrate-related genes in durum wheat (*Triticum turgidum* L. subsp. *durum* Desf.) to improve Nitrogen Use Efficiency

Dottorando:

Guglielmo Puccio

Tutor:

Prof. Gaetano Amato

Co-tutor:

Prof. Dario Giambalvo

Dott. Francesco Mercati

Table of Contents

Abstract

The increasing foods demand caused by the increasing world population posed new challenges to the modern agriculture. In recent years, many strategies have been adopted to cope with these needs and satisfy these demands. Among these, the improvement of agronomic techniques and plant selection and breeding are crucial for a sustainable improvement of crop production.

Nitrogen (N) is an essential nutrient for plant growth and development due to its important role in several biochemical pathways, constituting 2-5 % of plant dry matter. The excessive use of N fertilizer led to high environmental pollution with impacts on both ecosystems and human health. Therefore, N inputs reduction is one of the most important challenges to develop more sustainable agricultural systems. The selection of genotypes with a high Nitrogen Use Efficiency (NUE) is crucial to achieve this goal. Indeed, NUE is a complex trait governed by both environmental and genetic factors and their interaction. To reach a deep understanding of the molecular mechanisms involved in NUE and their role in plant selection for the complex trait is a common goal for crops.

Wheat is one of the most important cereal crops worldwide due to its adaptability to a wide range of environments. Durum wheat (*Triticum turgidum* L. subsp. *durum* (Desf.) Husn. syn. *Triticum durum*) account for almost 5% of the total world wheat production with more than half belonging to the Mediterranean area. The recent complete durum wheat genome assembly report allows for a deeper and easier genetic investigation of more complex traits and their regulation, including NUE-related genes. A better understanding of the induction and the regulation of N-related genes might assist both breeding molecular assisted programs and the selection of novel high NUE genotypes. The high genome duplication and its being allopolyploid as well as the large size of the durum wheat genome pose further challenges for the identification of putative target genes. The aim of this work was the identification of key genes involved in N-related pathways responsible for NUE differences between genotypes and the characterization of transcriptional patterns underlying nitrate uptake, remobilization, and assimilation dynamics and their regulatory network.

To achieve these goals, nine genotypes, chosen for their large variability in terms of plant growth habits, grain yield potential, and year of release were adopted for NUE evaluation (Chapter 2). Here, we focused on the identification of durum wheat genotypes highly contrasting for NUE. A first trial was performed in pots and in a controlled environment, using labeled ^{15}N fertilizer mainly to quantify Nitrogen Uptake Efficiency (NUpE). The second trial, performed in field with high and low N supply, showed high variability for the complex trait allowing us to select four genotypes (Senatore Cappelli, Orizzonte, Antalis, and Appio) characterized for contrasting NUE. These genotypes were then used for a comparative transcriptomic analysis in a time-course design under different nitrogen availability.

We further focused on the characterization of the two main gene families involved in the nitrate transport, NPF (formerly, NRT1) and NRT2, in the durum wheat genome (Chapter 3). NPF and NRT2

families are of large importance for nitrate uptake from the soil, its translocation and remobilization in different plant tissues as well as for nitrate signaling. Here, for the first time, we identified two-hundreds eleven (211) *Triticum durum NPF* (*TdNPF*) and twenty (20) *TdNRT2s*, providing a deep annotation of their protein sequences and conserved domains. We further described their evolutionary relationships and the putative Transcription Factors (TFs) involved in their regulation, mainly MYB and MYC and ABA related TFs for *TdNRT2s* and *TdNPFs*, respectively.

High salinity in soil also affects the availability of nutrients, their uptake, translocation or portioning within the plant. Thus, we also investigated the salt-stress tolerance aided by Arbuscular Mycorrhizal Fungi (AMF) in durum wheat comparing AMF-inoculated and uninoculated plants (Chapter 4). AMF hyphae have been reported to supply up to 25% plant N, enhancing N uptake through a higher membrane stability. The study of AMF-induced genes might help to detect key genes involved in stress-response and nutrient uptake. In our experiment, the expression of genes involved in trehalose metabolism, RNA processing, vesicle trafficking, cell wall organization, and signal transduction was significantly enhanced by the AMF fungi symbiosis. Furthermore, many transcription factors, including WRKY, NAC, and MYB, known for their key role in plant abiotic stress response appeared differentially expressed between treatments. We further described the co-expression relationship between these genes and how these may affect the plant stress response.

Finally, the four genotypes previously selected for their contrasting NUE, were adopted for a high-depth comparative RNA sequencing to describe the expression profiles in response to both high and low N supply to detect genotype-specific expression patterns potentially involved in their different NUE (Chapter 5). We were able to precisely supply nitrate in both high and low concentrations by using a hydroponic system, focusing on both short- (8h) and long-term (96h) plant responses to N supply. To cluster Differential Expressed Genes (DEGs) and identify functional pathways involved in nitrate metabolism, a Weighted Genes Co-expression Analysis (WGCNA) were carried out able also to detect modules of co-expression among genotypes and treatments. The comparison between contrasting genotypes allowed us to select candidate genes related to high NUE and its components. The analysis was performed on both root and shoot to break down the expression patterns involved in N uptake from the soil as well as N translocation and assimilation. Forty and thirty-four thousand DEGs were detected in root and shoot, respectively, clustered in 21 and 28 co-expression modules that were functionally characterized using GO terms enrichments. Genes involved in peptide biosynthesis, transmembrane transport, translation, oxoacid and carboxylic acid metabolisms were highly induced in root in response to N treatments whereas genes involved in photosynthesis, isoprenoid and terpenoid biosynthesis, lipid, carbohydrate and oxoacid metabolism were up-regulated in shoot. Furthermore, TFs and regulatory genes (such as Protein Kinases) involved in the N response were characterized. We also detected genotype specific expression variation inside the co-expression modules and among *TdNPFs* and *TdNRT2s*. In detail, the two older varieties, Cappelli and Appio showed a higher and faster induction of many genes related to oxidative stress response, transmembrane transport and amino acid transport as

well as many *TdNPFs*, mainly in root. This study provided new insights into the molecular mechanisms of durum wheat in response to N supply and revealed many functional pathways involved in N uptake, translocation and assimilation in durum wheat. Furthermore, the utilization of contrasting genotypes for NUE aided the identification of several candidate genes for improving the complex trait in durum wheat.

Chapter 1: Introduction

1.1 Wheat, a relevant crop species

Wheat is one of the most important cereal crops worldwide owing to its adaptability to a wide range of environments (Reynolds et al., 2012a; Snape, 1998). It has an important role in the human diet being the main source of calories for the world population (Barros et al., 2020). 65% of wheat world production (760 MT) is used for human nutrition while the rest is used for livestock feed and for the food industry (FAO-AMIS, 2018). Hexaploid bread wheat, *Triticum aestivum* (2n = 6x = 42, genome AABBDD) and tetraploid durum wheat, *Triticum turgidum* L. subsp. *durum* (Desf.) Husn. (syn. *Triticum durum*) (2n = 4x = 28, genome AABB) are the main cultivated wheat species. Flours obtained from durum wheat are mainly used for pasta and couscous production while those obtained from common wheat are widely used for bakery products like bread. Wheat constitutes over 20% of the total calories consumed by humans today, making it the most commonly produced grain in the world. About 5% of the overall wheat production comes from durum wheat which represents the 8% of all wheat cultivated areas (De Vita et al., 2019). Although less used in absolute terms, durum wheat is the main culture for a wide number of Mediterranean regions.

The three subgenomes A, B, and D of bread wheat derive from the hybridization of three ancestral diploid species with similar but distinct genomes that diverged between 2.5 and 6 million years ago (Peng et al., 2011; Marcussen et al., 2014). Durum wheat, in fact, evolved from domesticated emmer wheat, *Triticum turgidum* L. subsp. *dicoccon* and its hybridization with *Aegilops tauschii* (2n = 2x = 14, genome DD) gave birth to the hexaploid bread wheat (Faris, 2014). The wide utilization and cultivation of bread wheat has been attributed to the plasticity of the hexaploid genome, which could allow a broader adaptability capacity compared with tetraploid wheat (Dubcovsky et al., 2007). More than eight thousand years of independent evolution have allowed the accumulation of significant variation between the A and B genomes of the two species. To highlight these differences Lv and colleagues (2019) constituted a novel plant type, namely, Extracted Tetraploid Wheat (ETW) by extracting the AABB subgenomes from a hexaploid cultivar (TAA10) through the first cross with durum wheat and subsequent multiple backcrosses with TAA10. The ETW genome, containing only the A and B genomes of the hexaploid parent TAA10, displayed multiple abnormal phenotypes that were restored after re-introducing the D genome (Lv et al., 2019). These findings emphasize the differences between durum and bread wheat.

Both species have a large genome size (16 Gb for bread wheat and 11 Gb for durum wheat) compared to other crop species (e.g. *Zea mays*: 2.4 Gb; *Sorghum bicolor*: 730 Mb; *Glycine max*: 1 Gb). The three subgenomes share high sequence similarity and an abundance of repetitive elements (about 85% of the genome). The first bread wheat genome assembly was published for the first time in 2012 by Brenchley and colleagues (5.4 Gb). In 2014, the International Wheat Genome Sequencing Consortium (IWGSC) published an improved version of the genome, which covered two-thirds of the genome (10.2 Gb). The

last version released by IWGSC in 2018 is a full 21 chromosome ordered assembly of almost 14.5 Gb (Appels et al., 2018). In 2019 Maccaferri and colleagues published for the first time a 10.45 Gb assembly of the durum wheat genome (cv. Svevo). This represents an essential tool for the study of durum wheat genetics, evolution, gene function and regulation.

1.2 Nitrogen in the soil

Protein content and gluten quality are two of the most important factors for determining pasta cooking quality. Both grain quality and yield are highly influenced by genotype, environment, and by their interactions (Asthir et al., 2017). Among the environmental variables, seasonal temperature and rainfall variations together with N availability in soil are the most relevant factors for both grain quality and yield (Troccoli et al., 2000; Rharrabti et al., 2001). Nitrogen (N) is an essential nutrient for both growth and development of plants due to its important role in various biochemical pathways (e.g. amino acid synthesis, nucleic acid synthesis) and it constitutes between 2 and 5 percent of plants' dry matter. Its main form in the atmosphere is dinitrogen (N_2) which is converted to various forms, mainly ammonium and nitrate by prokaryotic organisms. In soil, N is found in three main forms: organic matter, primarily plant material and humus; soil organisms and microorganisms; mineral N forms like ammonium ions (NH_4^+), nitrate (NO_3^-), and low concentrations of nitrite (NO_2^-) (Cameron et al., 2013). In aerated soils, nitrate is the main form of inorganic N whereas, in acidic or anaerobic soils, ammonium is the major form (Xu et al., 2012). Nitrate is generated by the microbial conversion of soil N forms and this process occurs via intermediates, such as NH_4^+ and NO_2^-, that are usually only found in the soil at very low concentrations. Global annual biological N_2 fixation in various agricultural systems accounts for approximately 50-70 million tonnes (Tg) of N input (Herridge et al., 2008). In most agricultural systems the N requirement to produce 1 kg of dry biomass is between 20 and 50 g. This is usually not available through only natural supply of soil N, resulting in a limiting factor for plant yields (Robertson and Vitousek, 2009). The production and application of chemical N fertilizers during the past fifty years have greatly increased global food production (Ju et al., 2009).

1.3 Nitrogen fertilizers and their limitations

In 2015 the total global consumption of nitrogen fertilizer was 112.5 million tons. This is likely to increase with world population growth that may reach 10.5 billion people in 2050 (Hirel et al., 2011). Over the last 40 years, the amount of N applied to agricultural crops increased by 7.4 times, with only 2.4 times increase in grain yield (Tiaman et al., 2002). Among N fertilizers, urea is the major N form supplied with about 56% of the world's share. In soil, urea is rapidly degraded to ammonium (NH_4^+) ions and CO_2 by urease. Other N fertilizers commonly applied to cultivated soils are anhydrous ammonia (NH_3), ammonium sulfate $(NH_4)_2SO_4$, and ammonium nitrate (NH_4NO_3). Both urea and ammonia are converted to nitrate which is the main form of N uptake.

Due to the difficulty in accurately predicting N fertilizer requirements and soil N content, fertilizer rates exceeding the plant's needs are often applied. The excessive utilization of N fertilizer has a high environmental pollution effect and can affect both ecosystems and human health. Only 30-50% of the applied N was estimated to be absorbed by most crop plants and used for grain production while the remaining part is lost (Fageria et al., 2014). In agricultural and horticultural systems, mineral-N is mainly lost through ammonia volatilization, leaching, and denitrification to N_2. These mechanisms can lead to surface and underwater contamination (leaching), acidification, and eutrophication of freshwater (volatilization) (Cameron et al., 2013). Furthermore, the production of N fertilizers, through the Haber-Bosch process, has a substantial energetic impact responsible for about 1-2% of the global energy consumption and 1.44% of CO_2 emissions (Kyriakou et al., 2020).

Therefore, reducing N inputs in agroecosystems without limiting their production is crucial to improve their sustainability and reducing environmental pollution. This can be done with numerous of the so-called Best Management Practices (BMP) like fertilizer management techniques (e.g., deep placement, controlled release materials), better prediction of the overall N content of soils, correct timing of application, utilization of cover crops, and conservation tillage practices. Fertilizer N management is one of the most impacting ways to reduce N inputs and N loss in the short term. For example, the use of urease inhibitors in urea-based fertilizer was effective in reducing NH_3 and N_2O emissions (Singh et al., 2013).

Another key strategy for sustainable use of N fertilizers and to help face the rising global demand for food is the use of N utilization efficient genotypes.

1.4 NUE in crops

The ability of plants to recover N in various forms from soil varies greatly among species and among varieties of the same species. Nitrogen Use Efficiency (NUE) was defined as the yield of grain per unit of available N (Moll et al. 1982), although numerous definitions have been used during the last thirty years (Cormier et al., 2016, Congreves et al., 2021). NUE defined in this way is the product of Nitrogen Uptake Efficiency (NUpE) and Nitrogen Utilization Efficiency (NUtE) (Nyikako et al., 2014) NUE is a complex trait highly influenced by the interaction of multiple environmental and genetic factors. A plant's ability to recover and utilize N is highly influenced by physiological, metabolical, and developmental factors.

NUE is usually quantified using plant's grain yield (Grain Weight, Gw, kg ha^{-1}) and N supply (N supply, Ns, kg N ha^{-1}):

$$NUE=Gw/Ns$$

NUpE and NUtE are defined as the percentage of available soil N (Ns + soil N) that is uptaken by the plant and the grain produced (Gw) per total nitrogen acquired (Nupt, kg ha^{-1}) respectively. They are usually evaluated using the indices:

$$NUpE = Nupt / Ns + soil\ N \qquad NUtE = Gw/Nupt$$

Many studies focused on the topic of NUE, predominately facing how to improve crop NUE via agricultural management or breeding innovations. Although breeding allowed for the selection of numerous wheat genotypes with high NUE (Ortiz-Monasterio et al., 1997; Gaju et al., 2014; Muurinen et al., 2006) the selection of high NUE genotypes is often conducted in high N environments. This results in the selection of genotypes that perform well in optimal conditions but may suffer in N-limiting conditions. A certain genetic variability for NUE has been detected in wheat. Differences in NUE among genotypes have often been related to the year of release of the varieties, with modern ones being able to intercept a higher percentage of the administered N. For example, numerous studies have found that NUpE has increased with the introduction of improved varieties (Le Gouis et al., 2000; Brancourt-Hulmel et al., 2003; Guarda et al., 2004; Guttieri et al., 2017). In contrast, other studies have found that modern wheat varieties are less efficient at recovering soil N than older varieties when no N fertilizer is applied and are more efficient only when N is applied profusely (Rfoulkes et al., 1998). Barraclough et al. (2010) highlighted the variability in NUpE and NUtE when applying variable N rates using 39 wheat varieties in a 4-year trial. Variability in NUpE was highest at low N inputs (50 kg ha^{-1}) and decreased at higher N rates (Fig. 1A). Furthermore, NUtE variability was lowest at low N rates and it increased with higher N rates (Fig. 1B). This seems to suggest that grain yield under high N inputs

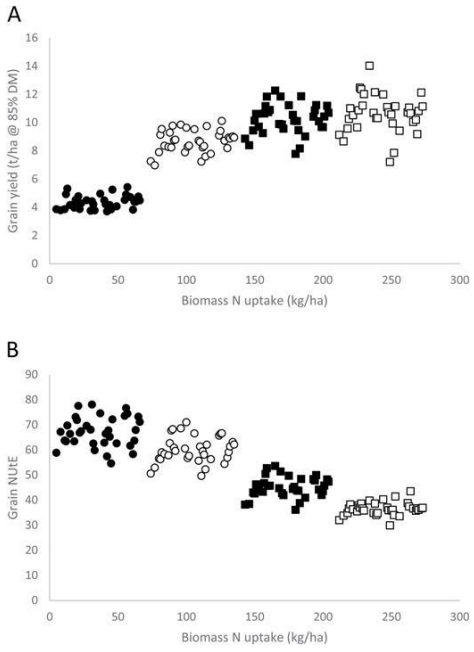

Figure 1 Variation in grain yields (A) and NUtE (B) as a function of variation in nitrogen uptake at four N rate levels: 0 (filled circles), 100 (open circles), 200 (filled squares) and 350 kg ha^{-1} (open squares). Mean yields for between 3 and 13 years of data for 40 wheat varieties are represented. (Barraclough et al., 2010).

conditions may create a bias in the selection of high NUE genotypes, especially in N-limiting conditions. Although a high number of works have focused on the selection of NUE efficient genotypes in crop plants, the genetics underlying this trait is still unclear. The utilization of NUE efficient and inefficient genotypes is a key instrument to try to identify key genes and regions that may affect both N uptake and N utilization.

1.5 Molecular insights into Nitrogen Uptake

Plants uptake inorganic N through roots both in the form of nitrate and ammonium ions (NO_3^-, NH_4^+) which then undergo complex systems of assimilation, transformation, and mobilization within plants. To cope with the variations in nitrate and ammonium concentrations, which may range from 10 μM to 100 mM in highly fertilized soils, plant roots have uptake systems for both NO_3^- and NH_4^+ with different affinities. These systems allow a fine tuning of N uptake rhythms and dynamics.

In aerobic soil, nitrate is the main available source of N. The uptake of NO_3^- ions by plant roots occurs through two systems: the Low Affinity Transport System (LATS) and the High Affinity Transport System (HATS). The LATS is a nonsaturating transport system mainly involved in nitrate transport at external nitrate availability higher than 0.5 mM while HATS is a saturable transport system involved when availability is lower than 0.5 mM (Glass et al., 1992; Crawford, 1995; Forde, 2000, Orsel et al., 2002). Both systems are further composed of constitutive (cHATS, cLATS) and nitrate-inducible components (iHATS, iLATS). Both high-affinity systems, cHATS, and iHATS, are upregulated in response to nitrate. In barley and white spruce, cHATS provide a high affinity, the low-capacity pathway for nitrate in uninduced plants. Although constitutively expressed, cHATS activity was also upregulated by exposure to NO_3^- by three-fold in white spruce and wheat while the fully induced iHATS flux was almost thirty times than that resulting from the cHATS in barley (Aslam et al., 1992; Kronzucker et al., 1995; Pang et al., 2015). iHATS induction, locally stimulated by the presence of NO_3^-, is transient, and long exposure to nitrate may repress NO_3^- uptake. Both in *Populus tremuloides* and in *Triticum aestivum* an inducible iLATS system was reported (Min et al., 2000; Pang et al., 2015) although its dynamics are poorly understood.

1.6 NPF nitrate transporters

Nitrate is absorbed by plants mainly through the action of membrane transporters belonging to the NPF and NRT2 protein families and reduced to ammonium thanks to both nitrate reductase (NR) and nitrite

reductase (NIR). The NPF family (formerly NRT1/PTR family) is composed of 53 genes in *Arabidopsis thaliana* and up to 140 genes in higher plants and was divided into eight subfamilies based on its phylogenetic tree (Léran et al., 2014). This gene family display sequence homology with all kingdoms of life in which it is known as Proton-coupled Oligopeptide Transporter (POT), Peptide Transporter (PepT/PTR), or Solute Carrier 15 (SLC15). In *Arabidopsis* almost all *NPF* genes are involved in the low-affinity transport both in internal plant transport and in the root uptake with the exception of NPF6.3 (formerly NRT1.1/CHL1) which is the only dual-affinity NPF transporter and was the first NPF member identified in plants (Tsay et al., 1993). Its affinity is regulated by the phosphorylation of the T101 residue that can decouple its dimer form allowing a switch from the low- to the high- affinity mode (Liu et al., 2003). Only two NPF genes, the NPF2.7 (NRT1.2/NAXT1) and NPF4.6 (NAXT1) were shown to be involved in root nitrate uptake whereas most of the remaining NPF genes are associated with inner plant transport and root-to-shoot translocation of NO_3^- (O'Brien et al., 2016). The high number of NPF genes allows highly specific regulation of nitrate transport in particular tissues or times. For instance, AtNPF2.12 is induced after pollination in the vascular tissues of the silique to mediate the delivery of nitrate from maternal tissues to developing embryos (Almagro et al., 2008; Babst et al., 2019) whereas AtNPF5.11, AtNPF5.12 and AtNPF5.16 are localized in tonoplasts to modulate nitrate efflux from vacuoles (Wang et al., 2018).

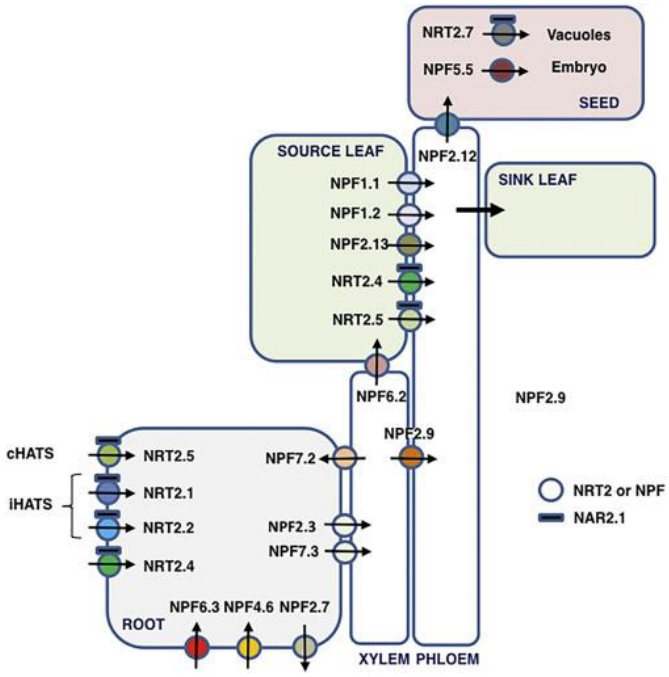

Figure 2 Localization and Function of the Arabidopsis Nitrate Transporters of the NRT2 and NPF Families. The functions depicted are root uptake (influx/efflux), loading/unloading of the xylem, loading/unloading of the phloem, accumulation in seed vacuoles, and transport into the embryo. At the cellular level, all proteins are localized at the plasma membrane, except NRT2.7 localized at the tonoplast. All NRT2 proteins are assumed to

interact with NAR2.1 to be functional, with the possible exception of NRT2.7. cHATS, constitutive high-affinity transport system; iHATS, inducible high-affinity transport system. (O'Brien et al., 2016)

Both nucleotide variations and variable transcription patterns were demonstrated to influence the N uptake ability of plants. In rice, the different nitrate-absorption rates between the two subspecies indica and japonica are attributable to a polymorphism of OsNPF6.5 (NRT1.1) gene (Hu et al., 2015) while a haplotype of OsNPF6.1 was responsible for the enhancement of nitrate uptake and grain yield (Tang et al., 2019).

1.7 NRT2 nitrate tranporters

The *NRT2* gene family was identified for the first time in *Aspergillus nidulans* (Brownlee and Arst, 1983) while the first higher plant member was identified in barley (Trueman et al., 1996). Unlike *NPF*, the *NRT2* gene family contains a much lower number of genes, ranging from one to eight in most plant species (Von Wittgensteine et al., 2014; Zhao et al., 2021). Despite their similar general structure, composed of eleven or twelve transmembrane domains, *NPF* and *NRT2* proteins show little to no sequence homology, underlying their functional difference. Most NRT2 proteins are unable to transport NO_3^- without the interaction with the NAR2.1 (NRT3.1) protein. In *Arabidopsis* AtNRT2.1 appears to be the main component of the iHATS and its knockout mutation results in the loss of almost the 75% NO_3^- influx (Orsel et al., 2002). The functional unit of the NRT2.1-NAR2.1 complex seems to be formed by a heterotetrameric protein complex involving a dimer of AtNAR2.1 and a dimer of AtNRT2.1 localized in the plasma membranes of roots (Kotur and Glass, 2015). Four out of the seven identified AtNRT2 genes are involved in root NO_3^- influx (AtNRT2.1, AtNRT2.2, AtNRT2.4, AtNRT2.5) while the role of AtNRT2.3 and AtNRT2.6 remain unclear. AtNRT2.1 and AtNRT2.2 are mainly involved in iHATS and in shoot-to-root nitrate transport whereas the AtNRT2.5 is deputy to the cHATS in N starvation conditions (Kotur and Glass, 2015). Both AtNRT2.4 and AtNRT2.5 were found also expressed in shoots and are also involved in the NO_3^- phloem loading (Lezhneva et al., 2014). The number, functions and regulation of NRT2 genes is highly variable depending on the plant species. In rice (*Oryza sativa*) four NRT2 and two NAR2 genes were characterized (Cai et al., 2008). Interestingly not all NAR2 members showed a direct interaction with NRT2 proteins. In barley three very similar NAR2 genes were characterized (HvNAR2.1-HvNAR2.3) but only one, the HvNAR2.3 were showed to form a functional unit with HvNRT2.1 (Feng et al., 2009; Tong et al. 2005). In rice, the same interaction between OsNAR2.1 and OsNRT genes (OsNRT2.1, OsNRT2.2 and OsNRT2.3) was highlighted (Yan et al., 2011) and transgenic plants with enhanced OsNRT2.1 expression showed higher grain yield and biomass accumulation (Chen et al., 2016) whereas the function of OsNAR2.2 seems to be unlinked from the interaction with NRT genes (Xu et al., 2020).

1.8 Nitrate signaling and NPF/NRT2 regulation

Soil nitrate concentration is highly influenced by numerous factors like seasonal rainfall changes or by factors influencing microbial activity like pH, oxygen concentrations, and temperature. These fluctuations demand highly fine sensing and signaling system by plants that allows the activation and modulation of genes encoding for NO_3^- transport and all the enzymes involved in its assimilation and relocation (Gojon et al., 2011).

Nitrate is a key signaling molecule involved in numerous signaling pathways that modulate gene expression as well as metabolic, physiologic, and development processes. It is involved in flowering induction, in seeds germination, in leaf expansion, and in the regulation of root development, growth and architecture (Krapp et al., 2014). Numerous transcriptome analysis in *Arabidopsis* highlighted that the expression of more than 2000 genes is influenced by NO_3^- (Gutiérrez et al., 2007). The first response to nitrate occurs within the first twenty minutes from N supply, does not involve new protein synthesis and is defined as Primary NO_3^- Response (PNR) (Krouk et al., 2010; Bouguyon et al., 2012; Kant, 2018). Pathways influenced by the PNR include ion transport, primary and secondary metabolisms, biosynthesis of nucleic acids, transcription and RNA processing, and hormone homeostasis (Ho et al., 2009; Rashid et al., 2018; Fredes et al., 2019). Many studies have reported that NPF6.3 may act as one of the main components of nitrate sensing and signaling. In detail, Riveras et al. (2015) detected a rapid increase in cytosolic Ca_2^+ levels in response to nitrate treatments, that were absent in NPF6.3 knockout lines. NPF6.3 has at least two independent signaling pathways, one calcium-dependent and one calcium-independent.

The calcium-dependent signaling pathway is mediated by the interaction with the phospholipase C (PLC), and results in the upregulation of numerous genes, including the Transcription Factor TGA1 and its target the NRT2.1 whereas in the calcium-independent pathway NPF6.3 interacts with the *Auxin Signaling F-box3* (AFB3). Further studies by Bouguyon et al. (2015) suggested a four-way downstream regulation system of NPF6.3 also depending on the post-translational modifications of the transporter. NPF6.3 is also involved in the feedback repression of NRT2.1 in the long-term response to high nitrate and both proteins have been reported to regulate lateral root development and architecture (Muños et al., 2004; Krouk et al., 2010).

Several transcription factors and protein kinases are involved in transporters and enzyme fine regulation to achieve a correct NO_3^- uptake and assimilation. Many of these belong to the Nodule Inception (NIN), the Calcium-dependent Protein Kinases (CPKs), and the Lateral organ boundaries domain (LBD) gene families and are often regulated by nitrate at the transcription level. Two Nodule Inception like proteins (NLP6 and NLP7), were found to have a central role in nitrate signaling in *Arabidopsis* being part of the so-called NPF6.3-Ca_2^+-NLP mediated nitrate signaling (Fig. 3). Both NLP6 and NLP7 are constitutively expressed and translocate to the nucleus where they interact with CPK10, CPK30 and CPK32. The phosphorylated proteins are retained in the nucleus where they bind to four gene loci: NRT2.1, NRT2.2, NIA1 and LBD37 (Marchive et al., 2013; Liu et al., 2017). Many other transcription factors are involved in the nitrate signal transduction like calcium sensors (e.g., CBL1/9), phosphatase 2C (ABI2), NAC4, TGAs (TGA1/4) and CIPKs (CIPK8/23).

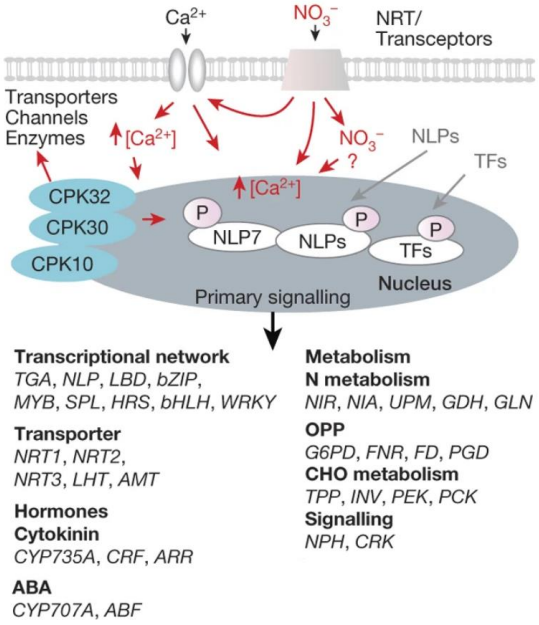

Figure 3 Nitrate–CPK–NLP signaling model. Modified from Liu et al., 2017

1.9 Nitrogen remobilization

In plants, N can be remobilized both in organic and inorganic forms. Organic remobilization consists of the breakdown of N-containing macromolecules into simpler molecules (e.g., amino acids, peptides) that can be easily translocated to various organs under nutrient starvation. The inorganic translocation involves the remobilization of nitrate through the xylem and phloem vessels and is carried out through short-distance and long-distance transportation (Han et al., 2016). After being taken up from the soil, in fact, nitrate can be assimilated directly in roots, or transported to shoots for assimilation or storage purposes. Under normal conditions, a significant part of nitrate assimilation takes place in shoots because of the reducing power needed deriving from photosynthesis (Wang et al., 2012). Numerous

nitrate transporters are in fact involved in the loading and unloading of NO_3^- from xylem and phloem and in the long-distance nitrate transport (Liang and Zhang, 2020). In *Arabidopsis* NPF7.3 (NRT1.5), expressed in pericycle cells surrounding the protoxylem, is a low-affinity bidirectional transporter involved in the transport from roots to aerial parts through NO_3^- xylem loading (Lin et al., 2008) whereas the low-affinity nitrate transporter NPF7.2 (NRT1.8) play an opposite role, unloading NO_3^- from xylem (Liang and Zhang, 2020). Furthermore, NPF1.1 and NPF1.2 are involved in the redistribution of root-derived nitrate from the xylem to the phloem in the petiole (Hsu et al. 2013). Another low-affinity transporter, the NPF2.13, is involved in the remobilization of stored nitrate from expanded leaves to smaller and younger leaves by loading it into the phloem (Fan et al., 2009). The interplay of these transporters ensures proper nitrate remobilization from source to sink tissues. Although the function and regulation of many of these genes have been characterized, the organic understanding of all their Spatio-temporal expression patterns and their interactions are far from being understood.

Another key mechanism for nitrate remobilization is the short-distance transport of NO_3^- from and to the vacuoles. When nitrate is sufficiently available vacuoles are used as temporary storage pools before its assimilation. Stored nitrate can be delivered to N-demanding tissues using phloem. Nitrate in the cytoplasm is rapidly assimilated and therefore the rate of cellular assimilation is highly determined by the vacuolar NO_3^-/H^+ exchange mediated by two CLC anion transporters genes, CLCa and CLCb, and their interaction with vacuolar ATPases (V-ATPase and V-Ppase) (Geelen et al., 2000; von der Fecht-Bartenbach et al., 2010). The combined activity of these vacuolar proton pumps creates an H^+ gradient across the tonoplast that allows the CLC mediated transport of NO_3^- (De Angeli et al., 2006).

1.10 Nitrate assimilation

Nitrate assimilation occurs mainly in the cytosol of leaves tissues although a smaller part of absorbed nitrate is assimilated directly in root tissues. The assimilation phase involves a set of biochemical reactions that converts nitrate into various forms that can be utilized by plants like amino acids. These metabolic steps are mediated by numerous enzymes namely, NO_3^- reductase (NR), nitrite reductase (NiR), glutamate synthase (GOGAT), and glutamine synthetase (GS) (Mokhele et al., 2012). NO_3^- is reduced in the cytosol by the NR to nitrite (NO_2^-). Nitrite is a highly reactive molecule that needs to be reduced rapidly. Plant cells immediately transport the NO_2^- from the cytosol into chloroplasts or plastids respectively in leaves or roots through an HPP transporter and reduced by the NiR into ammonium (Maeda et al., 2014). All inorganic N is reduced to ammonium as it is the only reduced nitrogen form available to plants for assimilation into amino acids (Ruiz et al. 2007). The last metabolic step of the nitrate assimilation is catalyzed by the GOGAT and GS enzymes. Both are involved in the conversion of glutamine and 2-oxoglutarate to two molecules of glutamate. GS is a key enzyme that catalyzes the ATP-dependent fixation of ammonium to the δ-carboxyl group of glutamate to form glutamine. The outcome of the GS–GOGAT cycle is the production of glutamate, which can then be used to form other

amino acids by aminotransferases and transaminases (Forde and Lea, 2007). Specific amino acids can subsequently become precursors for all nitrogen-containing molecules (e.g proteins, chlorophyll, and nucleic acids) (Bernard et al., 2009).

1.11 NPF and NRT2 transporters in bread wheat

The large and complex wheat genome has posed many challenges for the study of NPF and NRT2 genes, being less characterized in comparison to model plants also due to the difficulty of its genetic transformation (Paux et al. 2008). Some studies have focused on the responses of these transporters in wheat under N-deficient conditions, under drought stress, and in presence of Arbuscular mycorrhizal colonization (Buchner and Hawkesford 2014, Duan et al. 2016 Tian et al. 2017). Recently Li and colleagues (2020) reported that the transcription factor TaNAC2 directly regulates the expression of wheat nitrate transporter TaNRT2.5 and that the overexpression of either of the genes increases both grain nitrate concentrations and seed vigor. Transgenic tobacco plants overexpressing wheat transcription factors (ZFP593, bHLH1, and NBP1) had significant upregulation of nitrate transporters like NRT2.1 and NRT2.2 and it is reasonable to think that they may play a similar role in wheat (Li et al., 2021). To be able to deeply study NPF and NRT2 genetic variability in terms of both nucleotide variation and differential expression a full annotation on the genome of these gene families is necessary. Both the NPF and NRT2 gene families were annotated in the wheat genome for the first time in 2018 by Bajgain and colleagues (2018) and later by Li and colleagues (2021). This last study identified 331 NPF and 46 NRT2 genes in the entire genome. These numbers are way higher than those in other crops like rice (93 NPF and 4 NRT2 genes) and soybean (120 NPF and 5 NRT2 genes) or those in Arabidopsis (53 NPF and 7 NRT2 genes) (You et al., 2020). This may be attributable mainly to its hexaploidy, and to the high number of tandem and segmental duplication in the wheat genome. The IWGSC estimated an average of 23.6% of duplicated genes per chromosome suggesting tandem duplication caused by unequal crossing-over or replication-dependent chromosome breakage. According to the phylogenetic tree, the NPF gene family was divided into eight subfamilies in agreement with the NPF phylogeny built by Léran and colleagues (2014) used for the unified NPF nomenclature.

1.12 Nitrate uptake in durum wheat

The lack of a reference assembly, the large dimensions of the genome, and the high number of repeated elements have posed many difficulties to molecular studies on durum wheat, especially from an -omics point of view. This has been partially overcome by using the bread wheat's A and B genomes for reads mapping and PCR primers design or by assembling de novo transcriptomes (Vendramin et al., 2019; Vicente et al., 2019). Some studies have focused on characterizing the response to N starvation in durum wheat while others highlighted the effects of various types of stress on nitrogen-related genes (e.g. salt,

drought) (Habash et al., 2014; Kosová et al., 2016). Transcriptomic changes in various tissues (roots, leaves, spike) during chronic N-starvation were highlighted by Curci and colleagues (2017) using the cultivar Svevo. Numerous genes involved in nitrate, sugar, and peptide transport, as well as genes involved in carbon metabolism (TCA, photosynthesis, glycolysis) and in phosphorylation, were found differentially expressed between the control and the stressed treatments. Furthermore, more than 30 transcription factor families were involved in the N starvation response, with the MYB and bHLH being the most abundant. During water deficit, the down-regulation of the nitrate reductase (NR) together with the up-regulation of glutamate dehydrogenase (GDH), glutamate synthase (GOGAT) and glutamine synthetase (GS) suggest reduced assimilation of inorganic nitrogen in favor of the recycling of NH_3 generated by the GDH for nitrogen remobilization (Miflin et al., 2002; Habash et al., 2014). Recently Lupini and colleagues underlined the effect of both nitrogen and water limitations on ancient and modern durum wheat genotypes (Lupini et al., 2021). Results indicated a higher resistance to both water and N stresses in ancient varieties and a higher NUE under stress conditions. Furthermore, gene expression of both NRT2.1 and NPF6.3 was significantly higher in ancient varieties compared to modern ones.

Many breeding programs for durum wheat genetic improvements have had a significant impact on grain yield and quality over the last century (De Vita et al., 2007; Giunta et al., 2007; Subira et al., 2014). This has led to pure lines and varieties selection and to an improvement of quality traits and agronomic performances at the expense of reduced genetic variability and of an increased vulnerability to biotic and abiotic stresses (Keneni et al., 2012; Fu, 2015; Taranto et al., 2020). Notably, in rice, the elite allele OsNPF6.1HapB has been lost in 90.3% of rice varieties, probably due to the increased usage of nitrogen fertilizer over the past decades (Tang et al., 2019).

A deep understanding of the genetic targets for the selection of NUE efficient genotypes is essential and may assist in the correct use of the durum germplasm and for efficient breeding (De Vita and Taranto, 2019). The analysis of genetic variation at the nucleotide level can help highlight candidate regions for marker-assisted selection, and genome editing and improve our knowledge of genomic regions involved in NUE-related traits. Recently Zhang and colleagues (2019) performed a QTL mapping using Recombinant Inbred Lines (RILs) of bread wheat identifying 121 and 130 QTLs associated with multiple NUE-related traits like yield and biomass traits. Another study on durum wheat using 240 accessions focused on grain protein content and on its associated QTLs. The results highlighted seven QTLs associated with N-related candidate genes, including NRT2, NIR, NR, GOGAT, and GS (Nigro et al., 2019).

These methods however add limited information on the complex molecular interactions and regulatory mechanisms underlying nitrogen uptake and assimilation. Comparative transcriptomics approaches, using multiple cultivars of durum wheat, may help to investigate the mechanisms regulating nitrogen use efficiency and to select key genes involved in these processes.

Objectives

The excessive use of N fertilizer is leading to high environmental pollution with impacts on both ecosystems and human health. N inputs reduction is, therefore, one of the most important challenges to develop more sustainable agricultural systems. The selection of N-responsive genes determining high NUE in crops is, therefore, among the main goals in plant nutrition research. The two major objectives of this PhD thesis were: i) the identification of key genes involved in nitrate-related pathways responsible for differences in nitrogen use efficiency; ii) the characterization of transcriptional patterns underlying nitrate uptake, remobilization, and assimilation dynamics and their regulatory network in durum wheat.

In order to achieve these goals, we performed four separate experiments:

1. Selection of NUE contrasting genotypes through two agronomic experiments using ^{15}N and variable N supply to evaluate both NUpE and NUtE of durum wheat varieties (Chapter 2)
2. Characterization of the two nitrate transporter gene families (NPF and NRT2) in the durum wheat genome (Chapter 3)
3. RNA-seq of durum wheat under salt-stress colonized by AM Fungi (AMF) to select candidate genes involved in stress tolerance enhancement (Chapter 4)
4. High-depth comparative RNA-seq of the NUE contrasting genotypes (selected in Chapter 2) grown under high and low nitrate concentrations in a time-course design (Chapter 5)

Chapter 2: Variation in nitrogen use efficiency among wheat varieties released from 1915 to 2013

2.1 NUpE evaluation and root structure characterization

2.1.1 Introduction

Public awareness about the importance of protecting the environment and health is currently calling for the identification of sustainable cropping systems capable of ensuring adequate yields while minimizing the impact of production processes on the environment. Particular attention has been paid to the use of nitrogen (N) fertilizers, as their misuse in mode, timing, and form can lead to the release of N into the environment, causing global warming through nitrous oxide emissions (Bouwman et al., 2002); pollution of water by nitrate emissions (Wang et al., 2019); and soil acidification, eutrophication, and loss of biodiversity of natural ecosystems when N is returned to the surface by deposition in the form of NH_3 (Beusen et al., 2008).

In cereal systems, an often-substantial proportion of N fertilizers is not intercepted by crops (Raun et al., 1999; Sylvester-Bradley and Kindred, 2009). In a study performed in Spain on durum wheat (*Triticum turgidum* L. subsp. *durum* (Desf.) Husn.), López- Bellido et al. (2006) reported values for labeled ^{15}N fertilizer recovery ranging from 12.7% to 41.6% depending on the distribution method. Values in that range have also been reported for the species in other researches (Sanaa et al., 1992; Pilbeam et al., 1997; Giambalvo et al., 2010; Ruisi et al., 2014; Ruisi et al., 2016). This shows the need to identify solutions able to improve the ability of crops to absorb N and reduce N loss potential; in this context, the choice of variety may be essential.

Nitrogen use efficiency (NUE) is generally defined as the grain yield produced per unit of N available from the soil and fertilizer (Moll et al., 1982); it is the product of two physiological factors: (1) N uptake efficiency (NUpE, defined as the amount of N taken up by the crop per unit of N available to the crop) and (2) N utilization efficiency (NUtE, defined as the grain yield per unit of N taken up by the crop). A certain genetic variability for NUE has been detected in wheat (Fageria et al., 2008). Differences in NUE among genotypes do not seem clearly related to the year of release of the variety. For example, some studies have found that NUpE has increased with the introduction of improved varieties (Le Gouis et al., 2000; Brancourt-Hulmel et al., 2003; Guarda et al., 2004; Guttieri et al., 2017). In contrast, other studies have found that modern wheat varieties are less efficient at recovering soil N than older varieties when no N fertilizer is applied and are more efficient only when N is applied profusely (Foulkes et al., 1998). The limited progress of breeding in improving NUE under conditions of low available N in the soil may be due to the fact that plant selection is routinely carried out with sufficient to excess N, orienting selections only toward genotypes capable of responding to non-limiting N levels in the soil. NUE is a quantitative trait subject to large genotype-environment agricultural management interactions, and the current understanding of the plant traits and mechanisms that influence and regulate it is very

limited. There are still many gaps in our knowledge, in particular around the role of root traits. This is mainly because basic knowledge of root biology in the soil context is limited due to the difficulties of characterizing root morphology and functionality in the field (Garnett et al., 2009). The ability of a plant to use N efficiently depends on a variety of factors, including root traits (depth, length, density, speed of growth) and root N transport and metabolism (Garnett et al., 2009).

Thus, the objectives of the present study were to determine whether differences exist among genotypes of durum wheat in (1) N uptake when the plants are grown in conditions of low N availability, (2) the amount and rapidity of N use as it becomes available and (3) morphological or physiological root traits. We hypothesized that (1) in conditions of low N availability, older varieties would have more efficient N uptake compared to modern ones and that this superiority would be associated with greater root length and root length density, and (2) modern varieties would be more able and quicker than older ones to intercept N when it became available after fertilization.

To this end, we studied nine genotypes chosen for their large variability in terms of plant growth habits, grain yield potential, and year of release. The isotopic tracer ^{15}N was used to measure the fertilizer NUpE. The information obtained could help identifying wheat varieties (and developing new lines) able to use N efficiently and therefore suitable for low-input systems or organic systems (i.e., those less reliant or not at all reliant on the use of chemical fertilizers).

2.1.2 Materials and Methods

The experiment was conducted outdoors in a wire house under a transparent plastic roof (pots were protected from the rain) with open sides at the Pietranera farm (S. Stefano Quisquina, Sicily, Italy; 37◦53′ N, 13◦51′ E; 162 m a.s.l.). Nine genotypes of durum wheat that varied greatly in their year of release, morpho-phenological characteristics, and productive traits (Table 1).

Table 1. Year of release, pedigree, plant height, and earliness of the nine genotypes of durum wheat used in the experiment.

Genotype	Acronym	Year of release	Pedigree	Plant height	Heading
Cappelli	Capp	1915	Selection from Tunisian population	very tall	late
Capeiti 8	Cape	1955	EITI 6/Cappelli	tall	early
Trinakria	Tri	1970	B-14/Capeiti-8	tall	early
Creso	Cre	1974	YT-54/N10B//2*CPP-63/3/3*TC60/4/CP-B144	short	late
Appio	App	1982	Capelli//Gaviota/Yuma	medium-short	medium-late
Simeto	Sim	1988	Capeiti-8/Valnova	medium-short	medium-early
Svevo	Sve	1996	Cimmyt selection/Zenit	medium	early
Orizzonte	Ori	2011	Rusticano/Simeto	short	early
Antalis	Ant	2013	Unknown	medium-short	medium

Plants were grown in 4 L pots (diameter = 8 cm, height = 80 cm) filled with artificial substrate. There were 12 pots for each genotype, for a total of 108 pots. The growth substrate was composed of a mixture

of 80% silica sand (Gras Calce, Trezzo sull'Adda, Italy) and 20% w/w agricultural soil; we used a high percentage of silica sand both to have a substrate poor in N and to easily extract all the roots. Both substrates were sieved through a 2 mm mesh and characterized separately. Sand total N (Kjeldahl) and available phosphorous (P; Olsen P) were 0.11 g kg^{-1} and 7.44 mg kg^{-1}, respectively. The soil was collected from the first 30 cm of a well-structured clay soil classified as Vertic Haploxerept with the following characteristics: 267 g kg^{-1} clay, 247 g kg^{-1} silt, and 486 g kg^{-1} sand; pH 8.0; 10.8 g kg^{-1} total carbon (C; Walkley-Black); 0.86 g kg^{-1} total N (Kjeldahl); 40.1 mg kg^{-1} available P (Olsen P); 598 mg kg^{-1} total P; 26 cmol kg^{-1} cation exchange capacity; 1.70 dS m^{-1} electrical conductivity (saturated paste at 25 ◦C); 27.9% water content at field capacity; and 18.9% water content at the permanent wilting point. Therefore, the resulting mixture was poor in N and sufficiently supplied with P.

Sowing was performed on 22 January 2019. Four seeds per pot were distributed; all pots were arranged in a completely randomized design. Ten days after emergence, plants were thinned to two plants per pot. The soil water holding capacity of the substrate was determined with the gravimetric method (Dobriyal et al., 2012). Briefly, 10 perforated crucibles were filled with 100 g soil and placed in a basin with water up to half of the height of the crucibles. The crucibles were allowed to absorb water by capillarity until each pot was saturated. Excess water was allowed to drain, and the crucibles were weighed and oven-dried at 105 ◦C to a constant weight. The difference in weight between the crucibles before and after the drying process represented the soil water content at field capacity. The plants were kept in optimal conditions in terms of water supply throughout the experiment; watering was pot specific. Pots were weighed every 2 days to determine whether irrigation was needed. When the soil water content reached approximately 70% of the available water capacity threshold, a volume of water sufficient to bring the substrate back to field capacity was added. Variation in weight was attributed to evapotranspiration. Then 90 days after emergence, 0.19 g fertilizer per pot (10% ^{15}N-enriched ammonium sulphate) was applied.

During the experiment measurements were taken at the following three times: 90 days after emergence (just before the application of fertilizer; T1), 7 days after the application of fertilizer (T2), and 35 days after the application of fertilizer (T3). At each time, measurements were carried out on four pots per genotype (36 pots total). At each time (T1, T2, and T3), shoots from each pot were removed, separated into botanical fractions (leaves, stems, ears, dry and senescent tissue), and weighed. A fresh sample of the leaf fraction was used to determine the leaf area with an area meter (LI-3100C; LiCOR, Lincoln, NE, USA). Each fraction was oven-dried to a constant weight to determine the dry matter content. The aboveground dry matter was then reunited, finely ground using a Qiagen TissueLyser II, and analyzed for total N content by the Dumas method (flash combustion with an automatic N analyzer; DuMaster D-480; Büchi Labortechnik, Flawil, Switzerland) and for ^{15}N content with an elemental analyzer (NA1500; Carlo Erba, Milan, Italy) paired with a mass spectrophotometer (Isoprime, Cheadle, UK).

The soil profile was sampled from top to bottom in 20 cm sections, and roots were extracted from each section by sieving and washing. Each of these sections was then oven-dried to determine the dry weight

and divided into two subsamples of equal weight. One subsample was used to measure length, mean diameter, and root surface with a Win-RhizoTM scanner-based system (version 2007; Regent Instruments, Quebec, QC, Canada). The other subsample of each fraction was reunited, finely ground with a TissueLyser II, and analyzed for total N content and the relative isotopic excess.

The amount of N taken up by the plants represents a valid index of their uptake efficiency (NUpE; defined as the amount of N taken up by the crop per unit of N available to the crop), given that it is reasonable to hypothesize that the N potentially available in the substrate did not vary among treatments, as the plants grew on the same substrate, the plants were managed in the same way, and no leaching was observed. The ^{15}N concentration was used to determine the amount (^{15}Nrec) and percentage (%^{15}Nrec) of N recovered from the fertilizer, respectively, with Equations (1) and (2):

$$^{15}Nrec = N_t \times \frac{atom\%\ ^{15}Nfp\ excess}{atom\%\ ^{15}Nfert\ excess} \quad (1)$$

$$\%^{15}Nrec = \frac{^{15}Nrec}{f} \times 100 \quad (2)$$

where N_t is N content (g pot^{-1}) in the biomass at T2 or T3, atom% ^{15}Nfp excess is the ^{15}N isotopic excess (atom% ^{15}N-0.3663) in the fertilized plant, atom% ^{15}Nfert is the ^{15}N isotopic excess in the fertilizer and f is the amount of fertilizer (g pot^{-1}).

The specific uptake ratio of N was calculated according to the following equations:

$$SNupR1 = \frac{N_tT1}{RT1} \quad (3)$$

$$SNupR2 = \frac{(N_tT2 - N_tT1)}{RT1} \quad (4)$$

$$SNupR3 = \frac{(N_tT3 - N_tT1)}{RT1} \quad (5)$$

where N_tT1, N_tT2, and N_tT3 are N content (g pot^{-1}) in the biomass at T1, T2, and T3, respectively, and RT1 is root dry weight (g pot^{-1}) or root length (m pot^{-1}) at T1. SNupR1 represents the amount of N taken up by the plant per gram or meter of root at T1. SNupR2 and SNupR3 represent the amount of N taken up by the plant on the 7th and 35th day following fertilization, respectively (calculated as the difference between the amounts of N at T2 and T3 compared to T1, respectively), per gram or meter of root at T1. Therefore, SNupR2 and SNRupR3 give, respectively, an estimate of the speed and capacity of use of the N fertilizer by each variety as a function of both the weight and length of roots at the fertilization time. The data collected at each time point were analyzed in accordance with the experimental design (a completely randomized design with four replicates). Means were compared with Fisher's least significant differences test at the 5% probability level. All analyses were performed in the R environment (R Core Team 2021). Furthermore, the data were analyzed in relation to the year of release of the genotype; significant results ($p < 0.05$) are shown in the figures.

2.1.3 Results

The shoot biomass at T1 (90 days after emergence) ranged from 1.49 g pot^{-1} (Creso) to 2.22 g pot^{-1} (Simeto and Capeiti; Table 2); overall, the observed differences are attributable to the different phenology of the accessions, as the earlier heading ones had more shoot biomass. In the later heading genotypes (Cappelli and Creso), the percentage of leaves on the shoots (on a dry weight basis) was significantly higher (more than 50%). The leaf area ranged from 136 to 196 cm2 (Trinakria and Cappelli, respectively; Table 2).

Table 2. Shoot and root biomass, leaf area, and root traits for the nine studied genotypes at 90 days after emergence (Time 1).

Genotypes	Shoots	Roots	Leaf Area	RMD	Root:Shoot Ratio	RLD	SRL
	g DM pot^{-1}	g DM pot^{-1}	cm^2 pot^{-1}	mm		cm cm^{-3}	m g^{-1} Root
Cappelli	1.83	1.92	196	0.23	1.06	5.01	105
Capeiti	2.22	1.57	172	0.24	0.71	3.67	94
Trinakria	1.78	1.66	137	0.26	0.95	4.07	98
Creso	1.49	1.57	154	0.23	1.06	4.24	108
Appio	1.61	1.56	155	0.24	0.97	4.08	105
Simeto	2.22	1.56	165	0.26	0.71	4.30	110
Svevo	1.96	1.57	162	0.24	0.82	4.02	103
Orizzonte	2.11	1.38	152	0.23	0.66	3.83	111
Antalis	1.71	1.58	146	0.23	0.96	4.44	112
p	0.007	0.011	0.006	0.156	<0.001	0.006	0.056
$LSD_{0.05}$	0.407	0.227	6.3	–	0.169	0.599	11.6

DM, dry matter; RMD = root mean diameter; RLD = root length density (root length per unit of soil volume); SRL = specific root length (root length per unit of biomass).

The total root biomass (Table 2) ranged from 1.92 g pot^{-1} (Cappelli) to 1.37 g pot^{-1} (Orizzonte); the differences among genotypes were highly significant in statistical analyses. A highly significant negative relationship emerged between root biomass and the year of release of the variety (R2 = 0.71; data not shown). No significant relationships between shoot and root biomass were observed. Moreover, appreciable differences emerged among the genotypes in the distribution of roots in the soil profile; overall, greater uniformity in the distribution of roots along the soil profile was observed in Cappelli and Creso, whereas the less uniform varieties were Orizzonte, Capeiti, and Simeto.

No appreciable differences were observed among the studied genotypes in mean root diameter (Table 2), which ranged from 0.230 mm (Creso and Orizzonte) to 0.256 mm (Simeto and Trinakria). Conversely, substantial variation was observed in root length density, which ranged from 3.67 to 5.01 cm cm^{-3} in Capeiti and Cappelli, respectively.

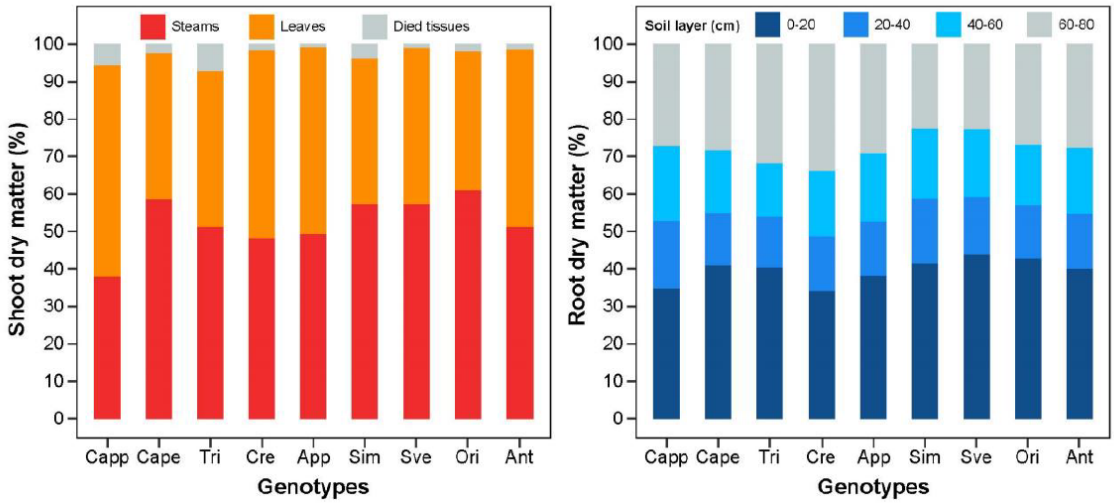

Figure 1. Shoot dry matter by botanic fraction (in percent of total shoot dry matter; left) and root dry matter by soil layer (in percent of total root dry matter; right) for the nine studied genotypes at 90 days after emergence (T1).

Cappelli showed the lowest total N in the shoot tissue (27.6 mg pot^{-1}); this is attributable mainly to the low N concentration in the shoot biomass (just 1.52%). The same variety showed the highest N accumulated in the root biomass (11.8 mg pot^{-1}). In contrast, Orizzonte showed the highest N uptake in the shoot biomass and the lowest in the roots (40.7 and 7.8 mg pot^{-1}, respectively). Therefore, a large difference emerged among the genotypes in the distribution of this element between the different organs of the plant (shoot and root tissue) rather than in total N uptake. The data revealed negative relationships between root biomass and total N uptake and between root length density and total N uptake (r = 0.71 and 0.79, respectively). Overall, a weak, albeit significant, positive relationship emerged between shoot N uptake and the year of release of the variety (Figure 2a), whereas an opposite trend was observed between root N uptake and the year of release of the variety (Figure 2b)

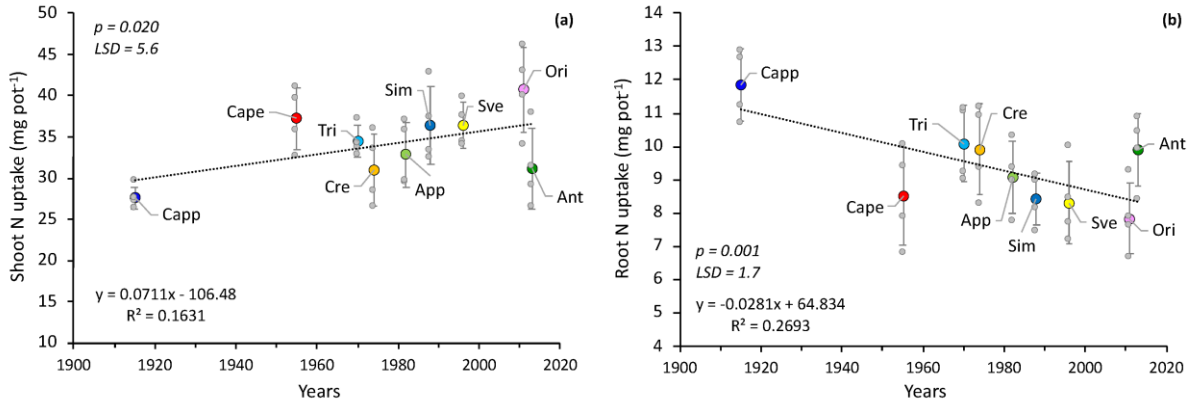

Figure 2. Relationships between shoot N uptake (a) and root N uptake (b) and the year of release of the nine studied genotypes at 90 days after emergence (Time 1). For each trait the p-value and the LSD (Fisher's LSD test,

p = 0.05) are reported. All genotype data are plotted with the mean depicted as a colored circle ± standard deviation (n = 4) represented by the end of the vertical black line. N, nitrogen; LSD, least significant difference.

Seven days after the application of fertilizer (T2), large and significant differences in growth emerged among the studied genotypes. Orizzonte showed the highest shoot growth (1.25 g pot^{-1}), whereas Simeto showed the lowest (0.57 g pot^{-1}; Figure 3a). Root growth ranged from 0.07 to 0.41 g pot^{-1}, respectively, in Trinakria and Capeiti (Figure 3b). It is interesting that Cappelli showed low shoot growth (0.67 g pot^{-1}, statistically not dissimilar to the worst variety) and high root growth (0.40 g pot^{-1}, statistically similar to the best variety); in contrast, Trinakria showed high growth of both shoots and roots (in both cases with values statistically not dissimilar to the best variety). The differences observed in shoot and root growth among the genotypes did not appear to be related to the year of their release (Figure 3a, 3b).

Large differences were observed among the genotypes in the quantity of total N taken up in the 7 days following fertilizer distribution (from 14.92 to 34.26 mg pot^{-1}, respectively, for Capeiti and Cappelli; Figure 3c). No relationship emerged between growth rate and N uptake 7 days after fertilizer distribution (r = 0.319). Seven days after the application of fertilizer, Cappelli had already intercepted more than 50% of the N applied (calculated using the ^{15}N isotope as a tracer); whereas Capeiti and Simeto intercepted N most slowly (34% and 35%, respectively; Figure 3d). No significant relationships emerged between N uptake and year of release or between ^{15}N fertilizer recovery and year of release (Figure 3c, 3d).

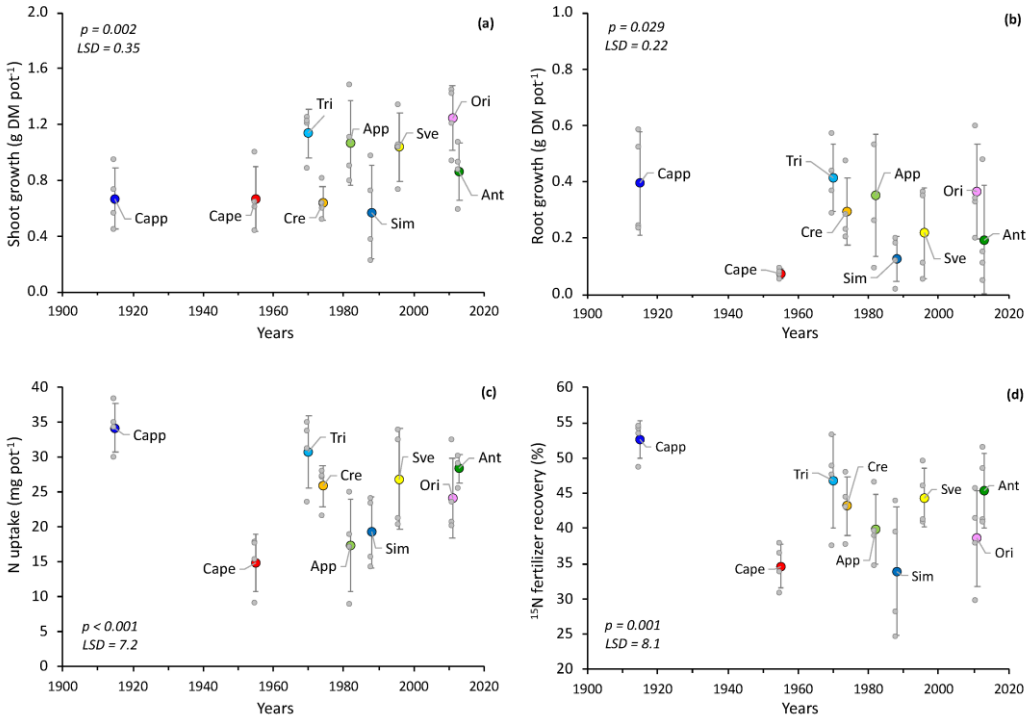

Figure 3. Relationships between shoot growth (a), root growth (b), N uptake (c) and ^{15}N fertilizer recovery (d) 7 days after the application of N fertilizer (Time 2) and the year of release of the nine studied genotypes. For each trait the p value and LSD (Fisher's LSD test, p = 0.05) are reported. All genotype data are plotted with the mean depicted as a colored circle ± standard deviation (n = 4) represented by the end of the vertical black line. N, nitrogen; LSD, least significant difference; DM, dry matter.

The growth of both shoots and roots in the 35 days following the application of fertilizer varied by genotype; shoot growth ranged from 5.7 g pot^{-1} (Capeiti) to 7.4 g pot^{-1} (Cappelli; Figure 4a), whereas root growth ranged from 0.77 g pot^{-1} (Orizzonte) to 1.65 g pot^{-1} (Creso; Figure 4b). The amount of N accumulated in the phytomass, both shoot and root, during the same interval was significantly higher in Cappelli (77 mg pot^{-1}) than in any other genotype (from 43 to 57 mg pot^{-1}, respectively, in Capeiti and Creso; Figure 4c). Furthermore, as regards N fertilizer recovery, the highest value was observed in Cappelli (about 95%), whereas in the other genotype values ranged from 69% to 76%. The differences observed among the genotypes in N uptake and ^{15}N fertilizer recovery appeared, to some extent, negatively related to their year of release.

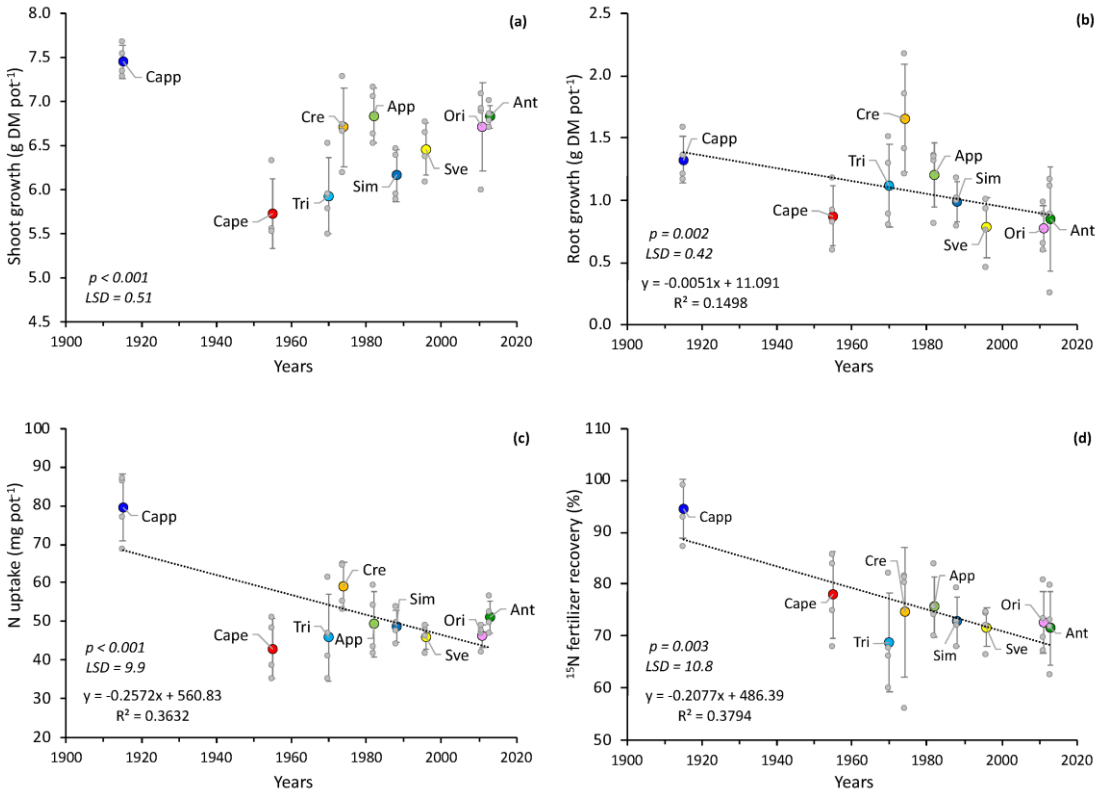

Figure 4. Relationships between shoot growth (a), root growth (b), N uptake (c), and ^{15}N fertilizer recovery (d) 35 days after the application of N fertilizer (Time 3) and the year of release of the nine studied genotypes. For each trait the p-value and LSD (Fisher's LSD test, p = 0.05) are reported. All genotype data are plotted with the mean depicted as a colored circle

± standard deviation (n = 4) represented by the end of the vertical black line. N, nitrogen; LSD, least significant difference; DM, dry matter.

The SNupR1 index (Table 3), which represents the amount of N taken up by the plants per gram or per meter of root at T1, varied widely among the genotypes, being highest in Orizzonte (35.0 mg N g^{-1} root and 0.32 mg N m^{-1} root) and lowest in Cappelli (20.6 mg N g^{-1} root and 0.20 mg N m^{-1} root). Large differences were also observed among the genotypes in the efficiency of recovery of the N applied with the fertilizer (both as gram or meter of roots); the SnupR2 index (calculated 7 days after N fertilization) was between 9.5 (Capeiti) and 18.5 (Trinakria) mg N per gram of root, whereas the SnupR3 index (calculated 35 days after N fertilization) was between 27.4 (Capeiti) and 41.5 (Cappelli) mg N per gram of root.

Table 3. Specific N uptake ratios in the nine genotypes.

Genotypes	*SNupR*1		*SNupR*2		*SNupR*3	
	mg N g^{-1} Root	mg N m^{-1} Root	mg N g^{-1} Root	mg N m^{-1} Root	mg N g^{-1} Root	mg N m^{-1} Root
Cappelli	20.6	0.20	17.9	0.17	41.5	0.40
Capeiti	29.2	0.31	9.5	0.10	27.4	0.29
Trinakria	27.0	0.27	18.5	0.19	27.6	0.28
Creso	26.0	0.24	16.5	0.15	37.6	0.35
Appio	27.1	0.26	11.2	0.11	31.6	0.30
Simeto	28.7	0.26	12.4	0.11	31.1	0.28
Svevo	28.8	0.28	17.2	0.17	29.3	0.29
Orizzonte	35.0	0.32	17.5	0.16	33.4	0.30
Antalis	26.1	0.23	18.0	0.16	32.3	0.29
p	<0.001	<0.001	0.006	0.007	0.008	0.041
$LSD_{0.05}$	3.94	0.042	5.19	0.049	7.32	0.072

*SNupR*1 represents the amount of N taken up by the plants per gram or meter of root at Time 1; *SNupR*2 and *SNupR*3 represent the amount of N taken up by plants in the 7 and 35 days following fertilization, respectively (calculated as the difference between the amounts of N at Time 2 and Time 3 compared to Time 1, respectively), per gram or meter of root at Time 1.

The differences observed among the genotypes in rapidity and ability to intercept the N applied with fertilizer were, to an appreciable extent, correlated with both root length and leaf area, as is clearly shown by the relationships shown in Figure 5.

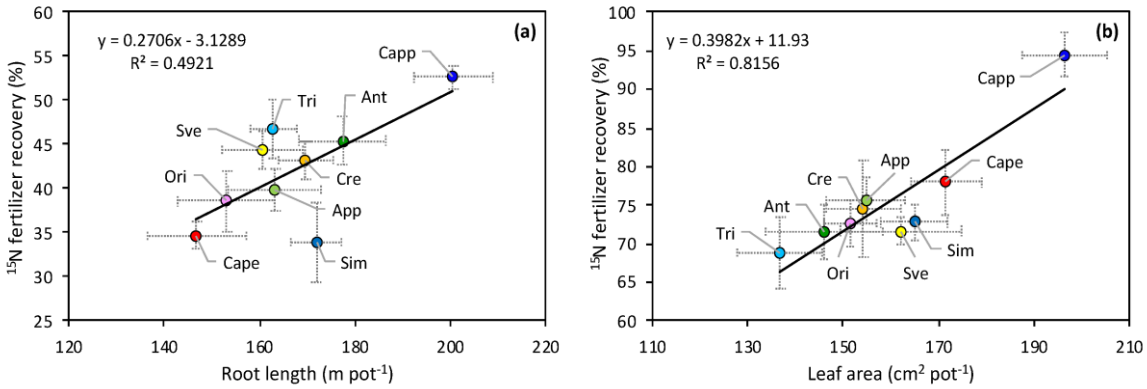

Figure 5. Relationships between root length (measured 90 days after emergence; Time 1) and the percentage of ^{15}N recovered from the fertilizer (%^{15}Nrec) 7 days after fertilization (a) and leaf area (measured at 90 days after emergence; Time 1) and the percentage of ^{15}N recovered from the fertilizer (%^{15}Nrec) 35 days after fertilization (b).

2.4 Discussion

This research highlights great variability among the nine studied genotypes in terms of root traits and N uptake when grown in conditions of low N availability and of rapidity and type of response when N has been made available. However, in contrast to our hypothesis, the results did not show a clear relationship between the year of release of the variety and N uptake efficiency when plants were grown under conditions of low N availability. The new varieties, in contrast to what we had hypothesized, were less able than the old ones to intercept N when it became available after fertilization. In fact, after fertilization, and with more available N, the N uptake and ^{15}N fertilizer recovery of the varieties appeared to be (albeit weakly) negatively related to their year of release. Therefore, it seems that breeding, which has led to a progressive increase in yield and grain quality (De Vita et al., 2007), has not had univocal effects on root traits and on the efficiency of the root system.

We observed large differences among the studied genotypes in root weight and length (greater in the older variety Cappelli) as well as the distribution of roots along the soil profile. Overall, the later heading genotypes (Cappelli and Creso, which reach heading on average 2–3 weeks after the earlier heading genotypes) had a more uniform distribution of the root system compared to the earlier heading genotypes (Orizzonte, Capeiti, Simeto), which had more of the root system in the top layers. These results, even if obtained from a pot experiment, are of interest, as information about variability in root development within the species is limited. In this study, when the genotypes were grown in a shortage of N, a negative relationship emerged between the year of release of the genotype and root biomass but not shoot biomass. This is in line with Zhang et al. (2009), who observed in *Triticum aestivum* that total root length decreased slightly from earlier cultivars to recently released ones; the authors stated that wheat breeding to reduce plant height also reduced root size (in particular in the upper soil layers), resulting in a smaller root-to-shoot ratio. In this experiment, a significant negative relationship was observed between the year of release and root-to-shoot ratio (values ranging from 0.417 to 0.633 depending on the time of measurement; data not shown), which highlights how breeding has influenced the belowground plant organs more than the aboveground ones.

Large differences among the genotypes were also seen in N uptake values in the first 90 days of growth in which the plants were grown in conditions of marked N deficiency. As mentioned, weak relationships, with opposite trends, emerged between both shoot and root N uptake and year of release of the variety; so altogether, no relationship between total N uptake and year of release emerged, which suggests that breeding has had little influence on this important trait. Indeed, Foulkes et al. (2009) found

that when N fertilizer was applied at optimal rates, modern varieties were more efficient than older ones, whereas the opposite was true when N was a limiting factor. Other authors (Brancourt-Hulmel et al., 1992; Ortiz-Monasterio et al., 1997; Sylvester-Bradley and Kindred, 2009) have found that N uptake is greater among newly released varieties compared to older ones, which indicates that N uptake ability has increased through breeding, regardless of the amount of N fertilizer applied. Moreover, other authors have found no relationship between N uptake and the year of release of the variety (Slafer et al., 1990; Calderini et al., 1995; Motzo et al., 2004; Ruisi et al., 2017). They have ascribed the general increase in NUE resulting from wheat breeding mainly to the improved ability of new genotypes to use the assimilated N to increase grain yield rather than to any improvement in their capacity to extract N from the soil. However, it should be highlighted how the discrepancy in results may be partly due to different methodologies to assess NUE and its components. In this research, negative relationships unexpectedly emerged between some characteristics of the root system (root biomass and root length density) and the amount of N taken up when the genotypes were grown in conditions of N deficiency (in the first 90 days). Therefore, the differences in N uptake capacity among the genotypes seem to be attributable to different levels of efficiency in N uptake capacity per unit of root length and root weight rather than to morphological differences in the root system. Aziz et al. (2017) showed that the selection for wheat productivity carried out in Australia between 1958 and 2007 reduced the total root length and at the same time increased N uptake by increasing the efficiency of the root system for capturing N; this is partially in agreement with the results of the present study. Liu et al. (2017) compared two wheat lines and found that the line with the lower root biomass absorbed more N than the other. This was associated with differential expression of nitrate and ammonium transporter genes. Therefore, it would seem that to improve the N uptake efficiency of wheat it would be more advantageous to select for high NO_3^- and NH_4^+ affinity rather than for a vigorous root system. However, other research has associated a more developed root system with improved N uptake (Palta, et al., 2011; Palta et al., 2014; Pang et al., 2014; Pang et al., 2015). Liao et al. (2004) also highlighted how N harvesting efficiency appears to be strongly correlated with early vigorous root and shoot growth, underlining how these characteristics should be considered in wheat breeding programs to improve N efficiency. According to Foulkes et al. (2009), the selection for deep rooting could represent an unexploited approach to increasing NUE given that through a deeper root system can improve N uptake from the subsoil, with positive effects on production, cropping system management, and the environment. In fact, many researchers have highlighted how subsoil can contribute in an important way to plant nutrition, especially when topsoil is dry or depleted of nutrients (Kirkegaard et al., 2007; Kautz et al., 2013). Severini et al. (2020) found a stronger correlation between root depth and yield than between root depth and shoot biomass, which suggests that a deeper root system may offer advantages during the late phase of the crop cycle, providing nutrients and water to support transpiration during grain filling. Others have shown that rooting depth is an important factor in N uptake from the deep layers of the soil (Kristensen et al., 2004; Kristensen et al., 2004; Thorup-Kristensen et al., 2009; Rasmussen et al., 2015); this certainly has

important environmental implications, as more deeply rooted plants will be able to utilize some N that would otherwise be lost into the environment through leaching, causing surface water and groundwater pollution. The discrepancies in these results could be explained by differences in genotypes, experimental conditions (pot or field), crop management (e.g., the timing and method of N fertilizer application), or climate and soil conditions (i.e., available water, soil fertility, and available N), as well as differences in the timing of measurement, as varieties, may have different N uptake patterns in different phenological stages.

After fertilization, with more available N, the N uptake and ^{15}N fertilizer recovery of the varieties appeared (albeit weakly) negatively related to their year of release. These relationships are partly attributable to the Cappelli variety, selected by the geneticist Strampelli in 1915, which differed greatly from the other accessions not only in morphological characteristics of both above- and belowground organs but also in its greater ability and rapidity of intercepting N when it became available. We hypothesize that this capacity of Cappelli (a much later heading variety than the others) is partly due to the perfect synchrony between the increase in available N induced by the application of fertilizer and the demand for N by the crop (with the maximum coinciding with the stem elongation stage). Moreover, in this research, the differences observed among the studied genotypes in terms of capacity and rapidity to intercept the N supplied were related to both the length of the root system and the photosynthesizing area. It would therefore seem that differences in N fertilizer recovery are attributable in part to the development of the root system (in particular in the deeper layers), which certainly increases the possibility of intercepting N supplied with the fertilizer, and in part to the increased demand for N by genotypes. In fact, it is easy to argue that greater leaf expansion favors growth and consequently increases the need for N to support the growth itself. This last result would seem to confirm the findings of other experiments on wheat and other species that have shown close relationships between the overall N accumulated in the canopy and the leaf area (Grindlay et al., 1997; Gastal et al., 2002). Furthermore, other studies have highlighted significant relationships between root traits (length, distribution, and density in the different soil layers), grain yield, nutrient uptake capacity, and water use efficiency (Zhang et al., 2009; Chen et al., 2003; Wang et al., 2014; Kamiji et al., 2014; Guo et al., 2019; Lamichhane et al., 2021)

In conclusion, this research shows that breeding activity in durum wheat has not had univocal effects on the characteristics of the root system (weight, length, specific root length, etc.) or N uptake capacity. The differences in N uptake observed among the studied genotypes varied with N availability. When plants were grown in conditions of low N availability, plant N uptake appeared to be related more to differences in uptake efficiency per unit of weight and length of the root system than to differences in morphological root traits. Conversely, the speed and ability to exploit the increase in N availability due to fertilization appeared, to a certain extent, to be related to root length and leaf area. Therefore, breeding to improve N utilization efficiency must aim to select for both a vigorous root system and high efficiency of N capture per unit of root length and root weight.

Furthermore, identifying genotypes with a root system able to better explore the substrate (i.e., with a greater length per unit of soil volume and a greater depth) would increase opportunities not only to intercept resources available in the substrate (water, nutrients) but also to activate symbiotic and associative relationships with soil microorganisms (mycorrhiza, plant growth-promoting rhizobacteria, etc.), with positive effects in terms of adaptability to difficult environments and resilience to climate change. To do this, experts must identify new solutions and techniques that allow for evaluations of the conformation and functionality of root systems in open field conditions. Finally, the present research, although performed among a limited number of genotypes, highlights certain variability in the development and distribution of the root system of this species, which suggests that there may be sufficient room for improving this trait within the species.

2.2 NUE, NutE, and Nitrogen remobilization evaluation

2.2.1 Introduction

Global population growth requires an increase in food supply with a lower environmental footprint. Through the use of synthetic N fertilizer and the selection of modern crop varieties, crop yields grew steadily in the 20th century, supporting population growth.

The application of nitrate fertilizers greatly improves crop yield and quality, especially for cereal crops. Both the increase in N fertilizer consumption and the increased production of legumes have boosted the amount of reactive N in the environment, having significant environmental effects (Lu et al., 2017; Swarbreck et al., 2019). In addition, because of its high mobility, nitrogen greatly contributes to agriculture-related pollution through leaching, volatilization, and denitrification. Furthermore, the production of fertilizers and their excessive usage increase greenhouse gas, like N2O, emissions.

The modern wheat cultivars require the use of mineral fertilizers and chemical herbicides and fungicides to maximize their production. Moreover, crops are able to recover only a fraction of the N fertilizer applied (about 20-40%), and this fraction decreases as the N fertilizer rate increases (Foulkes et al., 1998). One way to minimize N inputs and maximize production is the use of high NUE crop varieties. The identification of genotypes with high NUE is undoubtedly one of the crucial aspects for improving crop systems' environmental, energetic and economic sustainability.

This work was mainly aimed at evaluating NUE, NUtE, and the remobilization efficiency of durum wheat genotypes grown under two different conditions of nitrogen availability.

To this end, in a highly representative environment of arable land of inner Sicily, a field experiment was conducted using nine varieties widely differentiated by year of release, phenological, morphological, and productive characteristics (Senatore Cappelli, Capeiti, Trinakria, Creso Appio, Simeto, Svevo, Orizzonte and Antalis) grown both in the absence of nitrogen fertilization (N0) and in conditions of good availability of the element obtained supplying 120 kg N ha^{-1} (N120).

2.2.2 Materials and methods

Site characteristics

The field experiment was performed during the growing season 2018-2019 at the Pietranera farm, which is located about 30 km north of Agrigento, Sicily, Italy (3730′N, 1331′E; 178m a.s.l.), on a deep, well-structured soil classified as a Chromic Haploxerert (Vertisol) evolved on recent alluvial deposits. The soil is deep, with a sandy-clay texture and a very low OM content; it has a granular structure, good drainage, and a sub-alkaline reaction. Soil characteristics (measured at the beginning of the experiment and referring to the 0–0.40 m layer) were as follows: 52.5% clay, 21.6% silt, 25.9% sand, pH 8.1 (1:2.5 H_2O), 1.40% total C (Walkley Black), 1.29g kg^{-1} total N (Kjeldahl), 36 mg kg^{-1} available P (Olsen), 340 mg $kg^{-1}K_2O$ (exchangeable potassium), cation exchange capacity 35 $cmol_+ kg^{-1}$,

0.38cm^3cm^{-3}water content at field capacity (pF 2.5), and 0.16 cm^3 cm^{-3} permanent wilting point (pF 4.5).

Experimental design

The experiment was set with a split plot design with four replicates with plots of $9m^2$ (6m long and 18,75 wide) using the same 9 genotypes described in the 2.1 paragraph (Table 1). Cultivation was performed with commercial farm equipment. The total amount of N fertilizer was always split applied, with 50% applied at crop emergence and 50% applied at the end of tillering. Seeds were planted (for all genotypes and for all N concentrations) at 350 viable seeds m^{-2} in the second decade of December. Plants were grown in two different N availability conditions: N0, no N fertilizer applied; N120, applying 120 kg N ha^{-1}.

Calculations and statistical analysis

The leaf surface was determined with the leaf surface method using the Area Meter (LI-3100C Area Meter, LICOR GmbH, Germany) and the SPAD index for each genotype from heading start to maturity. The 10 flag leaves were then finely ground and used for the determination of the nitrogen content by the Dumas method (flash combustion with automatic N analyzer; DuMaster D-480, Büchi Labortechnik AG, Flawil, Switzerland). Furthermore, both in coincidence with the early heading phase and in coincidence with the maturation phase, the aboveground biomass of a micro-area of 1 m^2 was removed and divided into its botanical fractions: leaves, stalks, spikes, dry and senescent material (survey carried out in coincidence with the heading start phase); leaves, stalks, kernels and chaff (survey carried out in the maturation phase). Subsequently, each individual portion was placed in the oven until reaching a constant weight. Dry matter weight was evaluated, together with leaf surface using the Area Meter. Subsequently, each individual fraction was finely ground and used for the determination of its nitrogen content by the Dumas method.

At anthesis the following surveys were conducted: composition of the aboveground plant material; nitrogen content in the botanical fractions; the surface of flag leaves; dry weight and N content of aboveground biomass; Leaf Area Index (LAI). Upon maturation, the following surveys were carried out: lodging (plot surface containing bent plants); aboveground biomass; N content in the botanical fractions of aboveground biomass; grain production.

Nitrogen efficiency parameters were calculated according to Moll et al. (1982) and Huggins and Pan (1993). Nitrogen use efficiency (NUE) was defined as the ratio of grain produced (G_w, kg/ha) to N supply (N_s, kg N per ha), where N_s was estimated as the amount of applied N (f) plus aboveground plant N (N_t, kg N per ha) plus residual post-harvest N in the soil (N_{sph}, kg N per ha), both determined from control plots (no applied N). N uptake efficiency (NUpE) was calculated as N_t/N_s; N utilization efficiency (NUtE) was determined as G_w/N_t.

Furthermore, the following parameters related to N accumulation and remobilization were calculated according to Cox et al. (1986) and Arduini et al. (2006):

- postheading N accumulation (kg N ha^{-1}), as the difference between the amount of N uptake (kg N ha^{-1}) in the aboveground biomass at heading and at maturity; - N remobilization (kg N ha^{-1}), as the amount of N uptake (kg N ha^{-1}) in the aboveground biomass at heading minus the difference between the amount of N uptake (kg N ha^{-1}) in the aboveground biomass and the grain N yield (kg N ha^{-1}) at maturity; - N remobilization efficiency, as the ratio of the amount of N remobilization (kg N ha^{-1}) to the amount of N uptake (kg N ha^{-1}) in the aboveground biomass at heading; - contribution of N remobilization to grain N yield (CNRG), as the percentage ratio of N remobilization (kg N ha^{-1}) to grain N yield (kg N ha^{-1}). Means were compared with the Tukey test and with the least significant differences (LSD) test at the 5% probability level. Genotypes, N level, and their resultant interactions were tested using ANOVA for all measured parameters using a SAS 9.2.

Rainfall and temperature during the growing season

The climate of the experimental site is semiarid Mediterranean, with a mean annual rainfall of 581mm, mostly in autumn-winter (74%) and in spring (18%). The dry period is from May to September. The average minimum and maximum annual temperatures are 8.2°C and 23.4°C, respectively. The weather data were collected from a weather station located within 500 m of the site.

In 2018-2019, the overall rainfall was 647 mm in the September-June period, which was higher than the average of the trial environment (587 mm) (Fig. 1). However, the distribution of rainfall was irregular, with a strong concentration in autumn (330 mm compared to an average of 200 mm) and with dry periods in both winter and spring. The temperatures were significantly higher than in the long observation period (1981-2018); the average of the minimum and maximum temperatures was 1.6 ° C higher than the multi-year average: 9.8 vs 8.2 °C and 23.4 vs 21.8 °C, respectively.

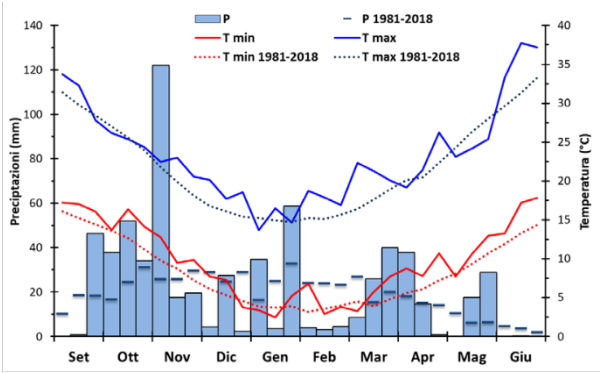

Figure 1. Rainfall and temperature distribution at Pietranera farm during the 2018-2019 period in a ten-day interval. Long-term average values are also shown as dotted lines (1981-2018). P = rainfall; T min = minimum temperature; T max = maximum temperature.

2.2.3 Results

As expected, the genotypes showed very different average height, varying between 56.1 cm (Simeto) and 124.0 cm (Senatore Cappelli). The Capeiti variety was the earliest, with about two weeks difference in heading time compared to the late variety (Sen. Cappelli). Interestingly, nitrogen supply did not significantly influence both plant size and heading time (Table 1).

Fertilization positively impacted tillering, with N120 plants having a higher average number of culms per m^2 compared to N0 (from 342 in N0 to 410 in N120). The highest tillering index was detected in Capeiti (465 stems per m^2) while Sen. Cappelli had the lowest index, with only 299 stems per m^2. Orizzonte showed the highest incidence of sterile stems (47%), on average 412 stems and 218 ears per m^2 while the Appio variety produced the highest number of stems and ears per m^2, (371 and 311 respectively).

Table 1. Heading time and morphological characters of the varieties, detected at the heading stage in both N0 and N120 treatments (mean andstandard error). Results of the statistical analysis (P-value and least significant differences for P = 0.05 of the main factors).

	Height *(cm)*				Heading (d 01/03)				Nr culms per m^2				Nr ears per m^2			
	N0		N120		N0		N120		N0		N120		N0		N120	
	$\bar{x}$	*es*	$\bar{x}$	*es*	$\bar{x}$	*es*	$\bar{x}$	*es*	$\bar{x}$	*es*	$\bar{x}$	*es*	$\bar{x}$	*es*	$\bar{x}$	*es*
Sen. Cappelli	124.0	10.8	129.6	2.4	29.3	0.7	30.0	0.3	296	20	302	20	259	5	210	11
Capeiti	71.0	6.0	81.4	1.3	15.7	0.7	16.2	0.4	445	29	484	12	276	56	271	34
Creso	67.2	2.6	71.3	1.2	27.3	0.3	27.4	0.2	401	37	479	41	351	28	368	26
Trinakria	104.8	4.7	101.9	1.1	20.3	0.7	21.6	0.2	324	10	318	13	281	6	254	18
Appio	64.5	1.3	65.7	1.2	23.7	0.3	24.2	0.4	336	25	405	33	293	15	328	27
Simeto	56.1	1.2	57.6	1.8	17.0	0.0	17.4	0.2	287	20	392	40	215	15	204	27
Svevo	63.3	1.4	63.5	1.8	17.3	0.3	17.8	0.2	306	7	437	26	235	28	263	29
Orizzonte	56.5	1.3	58.6	1.4	17.3	0.3	17.0	0.3	347	11	477	29	200	18	237	21
Antalis	68.2	1.4	72.2	2.6	22.7	0.3	23.0	0.4	336	29	393	17	266	8	250	24
Fertilization (Fe)	0.214				0.270				**0.018 (dms (51.6)**				0.958			
Cultivar (Cv)	**<0.001 (dms 6.46)**				**<0.001 (dms 0.68)**				**<0.001 (dms 54.1)**				**<0.001 (dms 50.8)**			
Fe × Cv	0.742				0.639				0.162				0.712			

Fertilization had a highly marked effect on the leaf area. We measured a Leaf Area Index (LAI) of 2.45 in N0 and 3.60 in N120 with an increase of 47% between conditions. Creso and Senatore Cappelli had the highest leaf area (on average 3.8 LAI), while Simeto and Svevo showed the lowest LAI values (on average 2.7). The aboveground biomass detected at the heading stage was not statistically influenced by fertilization, although the values observed for all genotypes were always slightly higher in N120 than in N0 (Figure 2). Moreover, Senatore Cappelli produced a much higher biomass per unit area than all the other genotypes tested.

The aboveground biomass at heading was split in its botanical fractions (stems, leaves, ears, dry and senescent material; Table 2).

Table 2. Weight incidence of the different fractions of the epigeic phytomass of the cultivars under test, detected at the heading stage in both N0 and N120 treatments (mean andstandard error). Results of the statistical analysis (P-value and least significant differences for P = 0.05 of the main factors).

	Culms (%)				Blades (%)				Ears (%)				Dry (%)			
	N0		N120		N0		N120		N0		N120		N0		N120	
	$\bar{x}$	es	$\bar{x}$	es	$\bar{x}$	es	$\bar{x}$	es	$\bar{x}$	es	$\bar{x}$	es	$\bar{x}$	es	$\bar{x}$	es
Sen. Cappelli	65.0	0.84	61.9	0.65	17.2	0.66	21.5	0.20	12.9	0.48	11.7	0.21	4.8	0.57	4.9	0.47
Capeiti	63.4	0.33	60.7	0.31	21.7	0.86	25.3	0.81	10.2	1.47	10.0	0.34	4.8	0.85	4.0	0.56
Creso	58.6	1.79	51.3	0.27	19.3	1.40	25.4	0.36	15.1	0.34	16.0	0.14	7.0	1.00	7.2	0.32
Trinakria	63.9	0.47	62.1	0.40	18.7	0.41	23.7	0.51	12.5	0.41	11.2	0.46	4.9	0.29	3.0	0.29
Appio	56.9	0.38	52.3	1.38	19.8	0.41	25.1	0.65	17.9	0.61	17.1	0.75	5.4	0.90	5.5	0.53
Simeto	60.9	0.72	55.5	0.46	21.4	0.08	27.8	0.78	13.6	0.18	13.5	0.78	4.0	0.59	3.2	0.36
Svevo	58.2	0.39	53.4	0.68	21.7	0.18	27.2	0.69	15.6	0.73	14.1	0.21	4.5	0.85	5.4	0.35
Orizzonte	59.6	0.41	53.7	0.40	23.1	0.64	28.6	0.36	13.1	0.76	14.5	0.27	4.2	0.40	3.2	0.24
Antalis	61.0	0.76	56.4	0.83	19.8	0.98	25.9	0.65	15.8	0.03	15.5	0.74	3.4	0.33	2.1	0.44
Fertilization (Fe)	**<0.001 (dms 0.64)**				**<0.001 (dms 0.92)**				0.474				0.071			
Cultivar (Cv)	**<0.001 (dms 1.53)**				**<0.001 (dms 1.28)**				**<0.001 (dms 1.01)**				**<0.001 (dms 1.03)**			
Fe × Cv	**0.033**				0.495				0.084				0.262			

The impact of each fraction on the total weight was evaluated. Fertilization negatively impacted Stem incidence and leaf fraction while it did not cause significant changes in the incidence of the ears. In Creso and Orizzonte, nitrogen fertilization had the greatest influence on these characters, while Trinakria and Capeiti showed no significant change with increased nitrogen availability.

The aboveground biomass measured at maturity did not show significant differences between plants grown with or without fertilization (Figure 2). Simeto, Svevo, and Orizzonte had a lower production of biomass at maturity, while the old varieties Sen. Cappelli and Trinakria and the modern variety Antalis, had the greatest amount of aboveground biomass accumulated during the whole productive cycle.

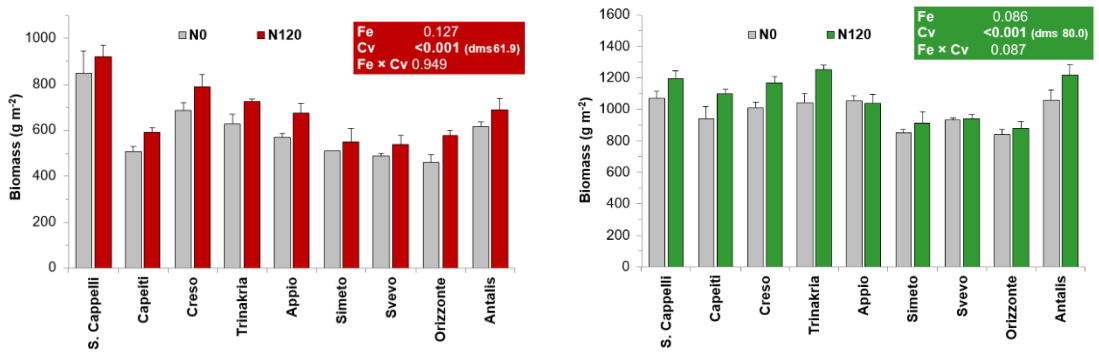

Figure 2. Aboveground dry biomass dat heading (left) and at maturity (right) of the nine genotypes (average value ± standard error). The two treatments, N0 and N120 are highlighted using red and green colors. (P-value and least significant differences for P = 0.05 of the main factors are shown). Fe = Fertilization; Cv = Cultivar.

Surprisingly, the greater N availability in the N120 condition did not determine significant variations in grain production compared to N0 treatment, although very different responses were detected among genotypes (Figure 3). In fact, fertilization caused a depressive effect in Appio, S. Cappelli, and Orizzonte (on average, -17% in N120 compared to N0), whereas fertilization increased the grain yield of Antalis (clearly the most productive) and Trinakria (on average, + 13%).

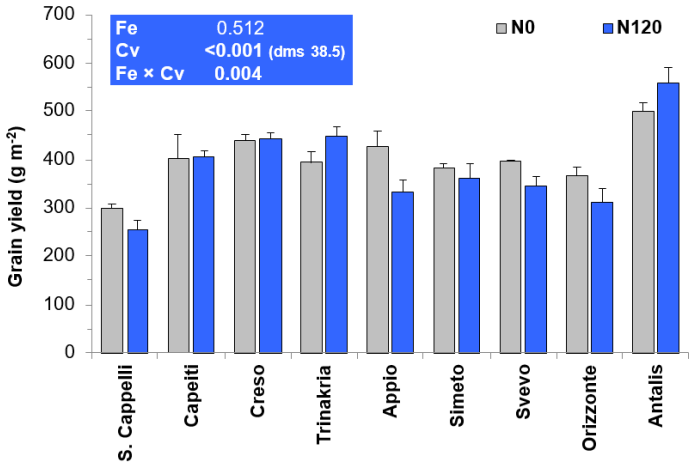

Figure 3. Grain yield (mean ± standard error) of the varieties both in unfertilized (N0) and fertilized (N120) treatments. (P-value and least significant differences for P = 0.05 of the main factors).

As expected, the older varieties Senatore Cappelli, Capeiti and Trinakria were susceptible to lodging: in N0, on average, a 34% of the surface was lodged and this percentage increased to 80% in the N120 treatment. No lodging was detected for all the other varieties (Table 3).

Fertilization significantly influenced the 1000-kernel weight: on average, in N0, a weight of 43.3 g was found, while in N120 the value decreased to 40.3 g. However, it should be noted that the genotypes responded in a rather diversified manner so that a decrease of only 1.4 g was observed for the Trinakria variety, while for the Orizzonte variety the reduction was equal to 10.3 g.

The greater availability of nitrogen also led to a reduction in the test weight (on average, from 85.8 kg in N0 to 83.5 in N120) ranging between 81.5 for Appio and 86.9 for Antalis.

Table 3. Lodging at maturity and some components of the grain yield of the nine genotypes both in unfertilized (N0) and fertilized (N120) treatments (mean and standard error) (P-value and least significant differences for P = 0.05 of the main factors).

	Lodging (%)				Nr ear per m²				1000-kernel weight(g)				Hectoliter weight (kg hl⁻¹)			
	N0		N120		N0		N120		N0		N120		N0		N120	
	x̄	es	x̄	es	x̄	es	x̄	es	x̄	es	x̄	es	x̄	es	x̄	es
Sen. Cappelli	40.0	23.1	88.0	2.0	256	19.4	226	8.8	43.8	1.6	41.1	1.0	85.8	1.2	83.6	0.7
Capeiti	20.0	10.0	82.0	5.8	303	8.9	384	24.0	42.1	1.9	39.0	0.6	87.2	1.7	86.3	0.5
Creso	0.0	0.0	0.0	0.0	318	14.0	404	20.1	47.7	0.9	39.9	0.2	86.4	0.6	84.9	0.4
Trinakria	43.3	18.6	73.0	9.2	282	31.5	282	16.9	49.0	0.7	47.6	0.9	86.4	1.0	85.5	0.4
Appio	0.0	0.0	0.0	0.0	358	10.7	382	15.4	42.0	1.2	33.8	0.9	82.5	1.1	80.5	0.8
Simeto	0.0	0.0	0.0	0.0	257	4.8	313	23.7	50.1	2.7	40.4	0.5	85.0	0.6	81.4	0.7
Svevo	0.0	0.0	0.0	0.0	329	13.3	372	12.7	42.4	0.5	34.6	0.7	85.0	1.6	81.9	0.3
Orizzonte	0.0	0.0	0.0	0.0	308	0.5	358	23.4	49.7	1.2	39.4	0.9	86.4	0.6	81.4	0.2
Antalis	0.0	0.0	0.0	0.0	326	44.8	359	39.0	50.3	1.3	47.0	1.6	87.6	0.6	86.1	1.0
Fertilization (Fe)	**0.015 (dms 11.2)**				0.084				**<0.001 (dms 1.38)**				**0.008 (dms 1.46)**			
Cultivar (Cv)	**<0.001 (dms 11.4)**				**<0.001 (dms 40.1)**				**<0.001 (dms 2.19)**				**<0.001 (dms 1.39)**			
Fe × Cv	**<0.001**				0.149				**0.001**				0.092			

The nitrogen content of the total aboveground biomass at heading was positively and significantly influenced by fertilization (Figure 4) in all genotypes. The two old varieties Capeiti and S. Cappelli had, respectively, the higher content of N in the biomass (on average 2.13%) and the lowest content (on average, 1.33%).

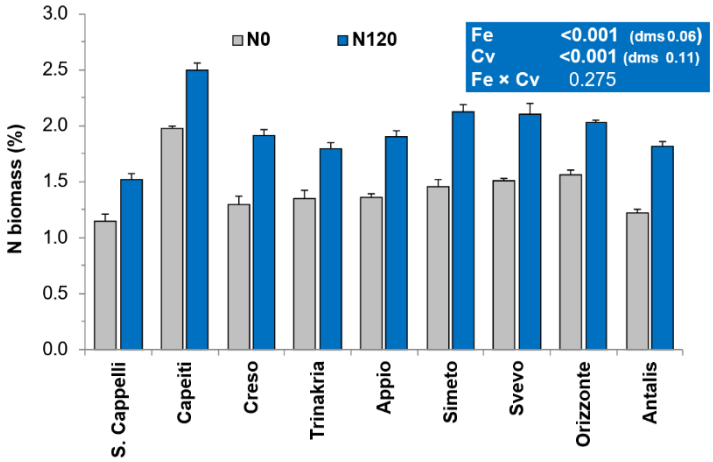

Figure 4. N content (% of dry weight) in the aboveground biomass at heading (mean ± standard error) (P value and minimum significant differences for P = 0.05 of the main factors)

A positive effect of nitrogen fertilization on the N content of the biomass was also detected at maturity (on average, 1.20% and 1.41% in N0 and N120 respectively; Figure 5). At maturity, the differences among genotypes appeared less marked than those observed at the heading stage, with a range between 1.11% (S. Cappelli) and 1.47% (Orizzonte).

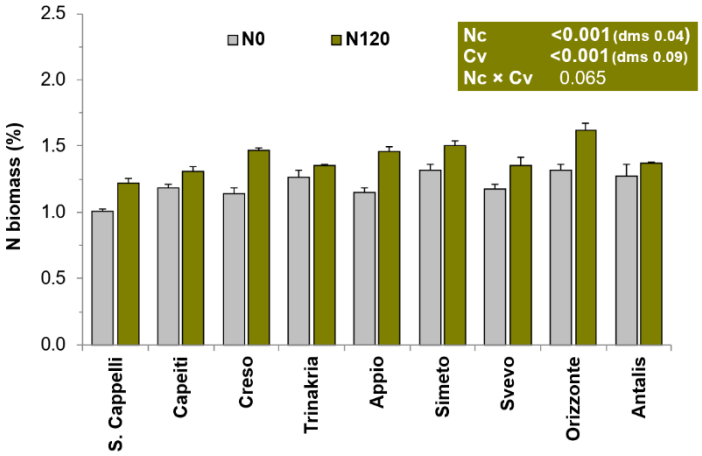

Figure 5. N content (% of dry weight) in the aboveground biomass at maturity (mean ± standard error) (P value and minimum significant differences for P = 0.05 of the main factors)

At maturity, the fertilization determined an increase in N content in all the botanical fractions (Table 4): + 40% in the stems and laminae and 54% in the ears. The increase detected in the kernels due to fertilization was on average about 5% (from 2.1 to 2.4%); some genotypes however showed a somewhat different behavior: Appio, Sen. Cappelli and Creso showed an increment of almost 26%, while for Antalis, Trinakria and Simeto the variation was just about 7%.

Table 4. N content of the different fractions of the epigeic phytomass of the cultivars under test, measured at maturity in both N0 and N120 treatments (mean andstandard error). Results of the statistical analysis (P-value and least significant differences for P = 0.05 of the main factors).

	Culms (%)				Blades (%)				Ears (%)				Kernels (%)			
	N0		N120		N0		N120		N0		N120		N0		N120	
	$\bar{x}$	es	$\bar{x}$	es	$\bar{x}$	es	$\bar{x}$	es	$\bar{x}$	es	$\bar{x}$	es	$\bar{x}$	es	$\bar{x}$	es
Sen. Cappelli	0.43	0.01	0.58	0.04	1.32	0.08	1.72	0.09	0.55	0.04	0.88	0.04	2.1	0.05	2.6	0.06
Capeiti	0.38	0.02	0.47	0.02	1.17	0.02	1.84	0.06	0.55	0.06	0.69	0.02	2.1	0.00	2.3	0.08
Creso	0.38	0.02	0.56	0.02	0.94	0.05	1.61	0.05	0.52	0.01	0.90	0.04	1.9	0.08	2.4	0.04
Trinakria	0.34	0.02	0.37	0.02	1.06	0.02	1.46	0.04	0.44	0.04	0.72	0.02	2.6	0.09	2.7	0.05
Appio	0.47	0.01	0.64	0.02	1.56	0.07	2.10	0.05	0.60	0.02	0.99	0.05	1.8	0.01	2.3	0.07
Simeto	0.42	0.01	0.61	0.02	1.55	0.04	2.17	0.07	0.56	0.05	0.86	0.02	2.2	0.11	2.3	0.06
Svevo	0.37	0.01	0.50	0.04	1.37	0.09	1.93	0.10	0.59	0.05	0.99	0.07	2.0	0.04	2.2	0.10
Orizzonte	0.43	0.04	0.75	0.07	1.43	0.09	2.13	0.09	0.61	0.03	1.04	0.09	2.2	0.07	2.6	0.08
Antalis	0.40	0.03	0.55	0.03	0.78	0.03	0.95	0.02	0.60	0.02	0.71	0.01	2.1	0.11	2.2	0.05
Fertilization (Fe)	**<0.001 (dms 0.032)**				**<0.001 (dms 0.106)**				0.474				**<0.001 (dms 0.08)**			
Cultivar (Cv)	**<0.001 (dms 0.071)**				**<0.001 (dms 0.134)**				**<0.001 (dms 1.01)**				**<0.001 (dms 0.14)**			
Fe × Cv	**0.041**				**0.006**				0.084				**0.024**			

In all genotypes the total N uptake at maturity increased greatly due to fertilization (+28% compared to N0; Figure 6). The higher increment was detected in the old varieties Trinakria and Creso and in the

modern Antalis with an average value of 15.1 g N m^{-2}, while the lowest was detected in Svevo (on average 11.8 g m^{-2}).

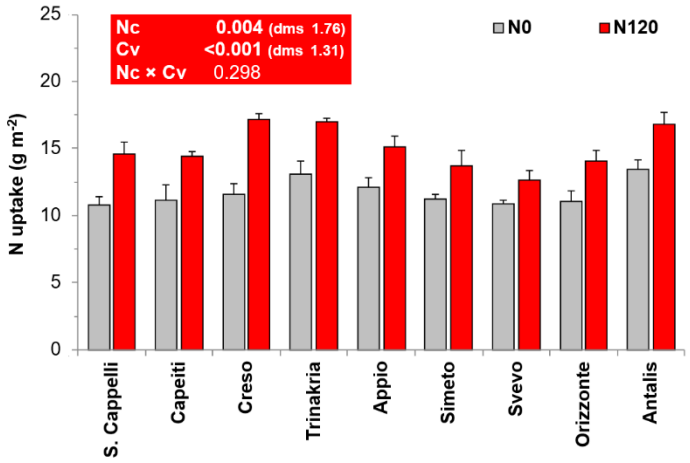

Figure 6. Nitrogen uptake (g m^{-2}) at maturity of the tested varieties (mean ± standard error) (P value and minimum significant differences for P = 0.05 of the main factors)

The amount of N accumulated in the aboveground biomass during the heading-maturation interval was markedly influenced by fertilization. We detected a reduction in N uptake during the heading-maturity interval determined by the nitrogen fertilization (Figure 7). On average, in the N0 treatment, the estimated quantity of nitrogen uptake was equal to 3.43 g m^{-2}, whereas in the N120 treatment the value decreased to 2,11 g m^{-2} (approximately -40%). The old varieties showed a lower N uptake during this phase of development with the exception of the Trinakria variety which, together with the modern variety Antalis had an average N uptake of 4.3 g m^{-2}.

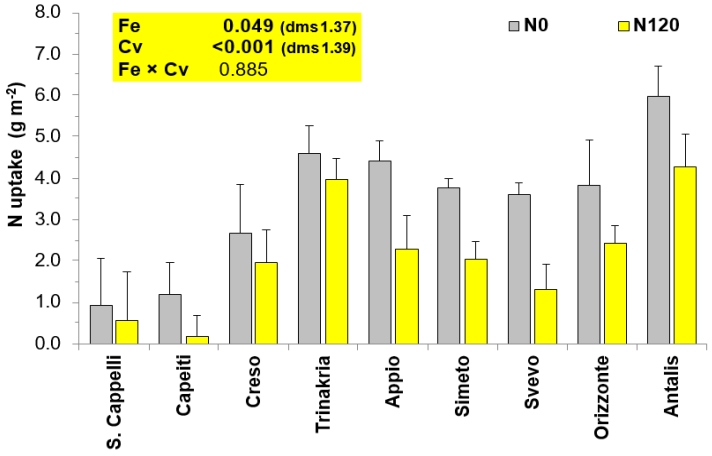

Figure 7. Nitrogen uptake (g m^{-2}) during the heading-maturity interval of the tested varieties as the dose of nitrogen fertilizer applied varies (mean ± standard error) (P value and minimum significant differences for P = 0.05 of the main factors)

Nitrogen fertilization determined an increase in flag leaf area for all the genotypes with an average increase of approximately 25%, ranging from 24.3 to 30.4 cm^2. The old variety Senatore Cappelli clearly differed from all the other genotypes tested showing an average value of 41.6 cm^2 (35.2 and 47.9 cm^2 respectively in N0 and in N120; Fig. 12). The Svevo variety, on the other hand, recorded the lowest average area of the flag leaf (21.5 and 26.6 cm^2 respectively in N0 and N120).
The nitrogen content in the flag leaf during the heading-ripening interval has been reported individually for each variety (Figure 8). A decrease in the amount of N in the flag leaf was observed for all the varieties during this interval. It is well known that the flag leaf "empties out" due to nitrogenous compounds being transferred to the reproductive organs and particularly towards the developing kernels. The nine genotypes showed large differences in the trend of this process. Antalis and Trinakria showed a high decrease rate, with an average of 25-30% of the nitrogen contained in the flag leaf at heading found in the same leaf at maturity. On the contrary, Appio and Simeto showed very low "emptying" rates, recording a reduction, during the same period, of -44% and -54%, respectively.

The addition of N fertilizer reduced NUE (Nitrogen use efficiency; kg kg^{-1}), as expected [on average, from 27.2 % (N0) to 20.8% (N120)]. The level of utilization efficiency varied greatly among the genotypes: Antalis and Creso were the most efficient (on average, NUE of 28.5 and 27.6%, respectively), while Senatore Cappelli and Appio were the less efficient (on average, NUE of 16.0 and 17.1%, respectively). Each genotype showed a different response to increasing nitrogen availability in the soil (highly significant variety × fertilization interaction): thus, for example, for the Trinakria variety the efficiency had a least reduction at varying of the N availability (from 24.5 in N0 to 22.9% in N120), whereas in Appio, Svevo and Orizzonte a strong reduction was observed (on average from 29.0 to 20.7%).

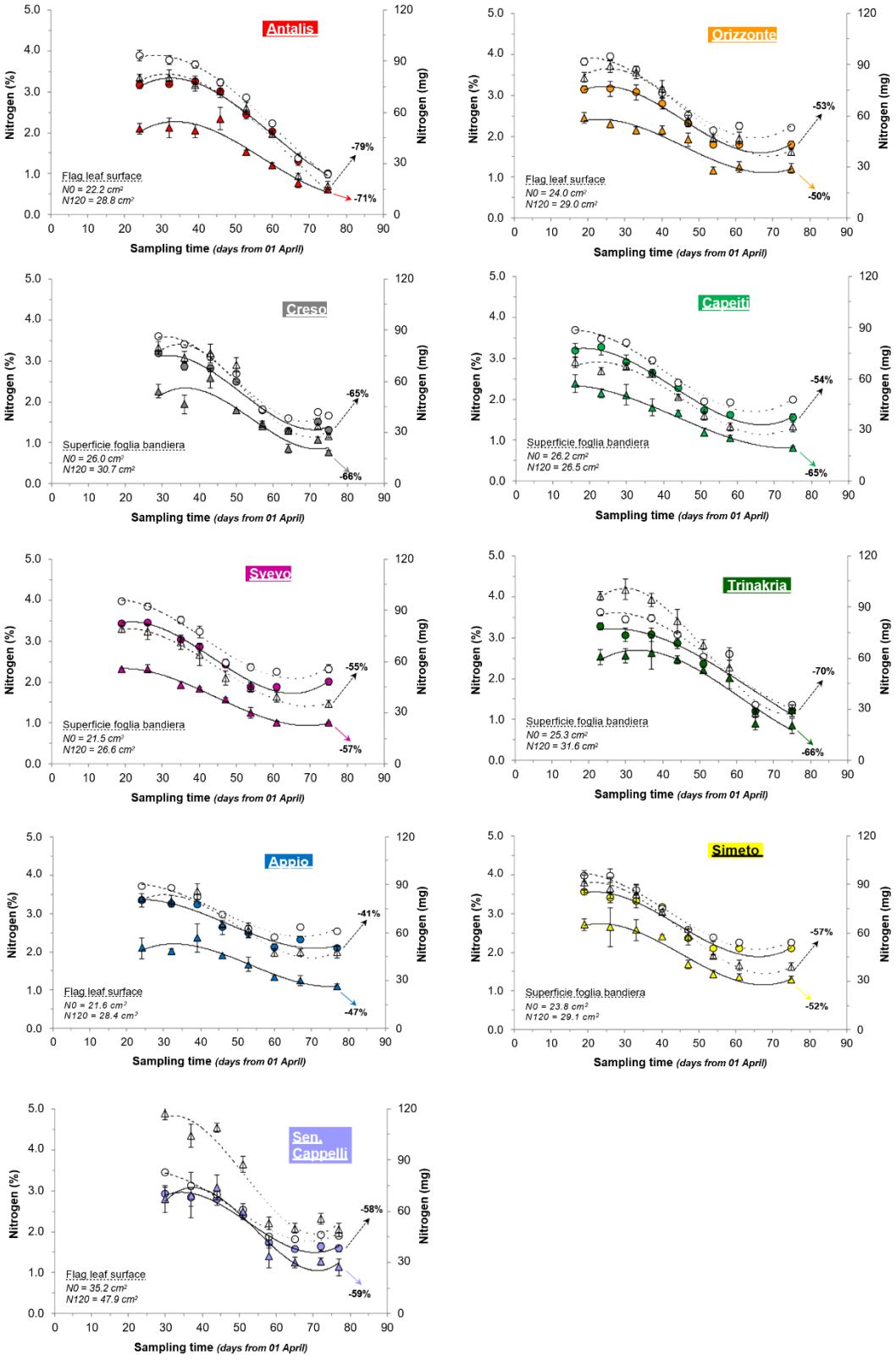

Figure 8 Trend of the nitrogen content [as a percentage of dry weight (circles) and in mg (triangles)] in the flag leaf of nine genotypes during the heading-ripening interval (average values ± standard error; N0: colored symbols; N120: empty symbols). The percentage values indicate the variation in the nitrogen content (in % and in mg) detected at maturation compared to that observed at anthesis.

Similar to what was observed for the NUE, the NUtE (the ratio between grain production and the total amount of nitrogen uptakenby the crop), decreased with the increased N availability (on average, from 34.2% in N0 to 25.4% in N120). Antalis and Sen. Cappelli were clearly distinct from every other variety: the first, in fact, had a mean NutE value of 35.2%, while for the second the mean value was just 22.7%. The interaction between fertilization and variety resulted highly significant also for this trait (P<0.001): The efficiency of nitrogen utilization in Appio, Creso, and Orizzonte varieties decreased, on average, from 28,1% in N0 to 19.6% in N120 while Trinakria and Antalis had a very modest reduction (from 27.4% in N0 to 24.7% in N120).

The remobilization of N from the vegetative organs to the grain in the heading-maturity period (Table 5), increased significantly, with the higher N availability in the fertilized condition (N120) for all the genotypes. The old variety Capeiti, probably also thanks to its marked earliness, showed the greatest translocation capacity during the heading-maturity period (on average, 8.5 g, corresponding to about 70% of the N present in the plant at heading). On the contrary, the variety Appio translocated only 4.2 g of N, corresponding to about 40% of N accumulated in the aboveground biomass at heading.

Table 5. Nitrogen Use Efficiency (NUE) and Nitrogen Utilization Efficiency (NUtE) indices of the genotypes under the two nitrogen fertilizer conditions (N0 and N120). (Mean and standard error) (P-value and least significant differences for P = 0.05 of the main factors).

	NUE				NUtE				N remobilization (g)				N remobilization (%)			
	N0		N120		N0		N120		N0		N120		N0		N120	
	$\bar{x}$	es	$\bar{x}$	es	$\bar{x}$	es	$\bar{x}$	es	$\bar{x}$	es	$\bar{x}$	es	$\bar{x}$	es	$\bar{x}$	es
Sen. Cappelli	21.7	0.46	16.0	1.18	27.8	0.89	17.5	0.92	5.3	1.32	6.1	1.06	52.1	5.69	42.6	4.31
Capeiti	28.1	1.46	25.1	0.76	35.7	1.14	28.2	1.15	7.2	0.44	9.8	0.46	71.4	2.12	66.3	1.76
Creso	30.1	0.89	25.1	0.78	38.1	1.58	25.8	0.67	5.9	0.72	8.7	0.92	65.8	3.03	56.9	2.35
Trinakria	24.5	0.27	22.9	1.07	30.1	0.68	26.3	0.86	5.6	1.01	8.3	0.50	64.3	3.98	63.2	1.66
Appio	28.1	0.83	17.1	1.24	35.0	0.64	22.0	1.04	3.2	0.28	5.3	0.90	41.0	1.73	40.5	4.96
Simeto	26.9	0.64	19.3	1.56	34.2	0.99	26.6	0.67	4.5	0.19	6.5	1.02	60.0	1.58	54.6	2.03
Svevo	28.5	0.33	18.5	1.11	36.4	0.61	27.1	1.41	4.2	0.32	6.1	0.89	56.7	2.42	52.6	2.90
Orizzonte	26.2	0.94	16.5	1.44	33.4	1.62	22.1	1.80	4.2	0.75	5.4	0.58	57.1	5.84	46.6	4.53
Antalis	30.4	1.00	26.5	1.55	37.2	1.46	33.2	0.55	4.6	0.12	8.1	0.92	61.4	2.51	63.8	3.31
Fertilization (Fe)	**0.002 (dms 2.88)**				**<0.001 (dms 1.66)**				**0.035 (dms 1.98)**				0.126			
Cultivar (Cv)	**<0.001 (dms 1.87)**				**<0.001 (dms 2.20)**				**<0.001 (dms 1.34)**				**<0.001 (dms 6.38)**			
Fe × Cv	**<0.001**				**0.001**				0.671				0.513			

2.2.4 Discussion

The aim of this research, conducted in a typical agricultural environment of inner Sicily, was to deepen our knowledge on the Nitrogen use efficiency of durum wheat genotypes, widely diversified by year of release and pheno-morphological and productive characteristics, grown in contrasting conditions of nitrogen availability.

The acquisition of such information is certainly useful for the identification of genotypes characterized by a greater capacity to use the available nitrogen and, more broadly, to the selection of the characteristics needed to enhance this capacity. Moreover, this acquisition enables the modulation of nitrogen supply to the crop and reduces the risk of soil loss to other environments (runoff waters, deep waters, river and marine systems, etc.). Hence, this research is part of a broader theme aimed at improving the sustainability of Mediterranean crop systems through the increase in the efficiency of use of the nitrogen available for the crop (native or supplied with fertilizers). This may highly reduce the risk of release of N into the environment (by volatilization, denitrification, etc.) and therefore the risk of contamination of the environment itself; at the same time, it can contribute to the reduction of the economic and energy costs of nitrogen fertilization.

The results of this study were obtained from a one-year field experiment that took place in climatic conditions outside of normal test conditions, so they must necessarily be considered preliminary. The rainfall was, in fact, overall higher than the multi-year average of the trial environment and, above all, with an irregular distribution. Very abundant rainfall occurred in autumn with long dry periods in winter and spring. Moreover, temperatures (both the maximum and the minimum) were significantly higher than the average throughout the crop cycle. This may have favored the mineralization processes of organic matter, making high quantities of nitrogen available even in the control without artificial inputs (N0). Furthermore, data relative to grain production showed, for many genotypes, a negative impact of nitrogen fertilization. Interestingly, this was not attributable to a lower ability to intercept the element, but probably to the water deficit during the spring period. Water deficit, especially during the heading stage can, in fact, highly impact grain production (Zhang et al., 1999; Hussain et al., 2004).

The research revealed great differences among the genotypes in their responses to changes in nitrogen availability. We found significant differences in the ability to uptake nitrogen from the soil and translocate it from the vegetative to reproductive tissues, as well as in the efficiency of nitrogen utilization. It is especially notable that only two out of the nine genotypes (Antalis and Trinakria) were capable of exploiting the high availability of nitrogen in the soil (N120) for grain production, but not for increasing grain nitrogen content. On the contrary, for other genotypes (in particular Senatore Cappelli, Creso, and Appio) the N fertilization did not cause significant variations in yield but increased the N content of the grain.

Nitrogen fertilization caused a decrease in nitrogen utilization efficiency (average values of NUE: 27.2% in N0 and 20.8% in N120), but not all varieties exhibited the same behavior. Antalis (by far the variety with the highest NUE) was able to use a relatively high fraction of the nitrogen available, in both conditions of N availability (NUE 30.4 and 26.5, respectively in N0 and N120) while the Appio variety drastically reduced its efficiency (NUE from 28.1 to 17.1).

Many works highlighted the main role of flag leaf (the last leaf emitted by the plant) in wheat, being the main photosynthetic organ contributing to 45–58% of photosynthetic performance during the grain-filling stage (Duncan 1971; Khaliq et al., 2008). Our analyses conducted on the flag leaf have shown

that the two varieties Antalis and Appio, although possessing similar quantities of N in the flag leaf, were able to transfer, respectively, 75 % and 44% of the element towards the reproductive organs.
The different capacities of nitrogen utilization of the varieties also appeared related to their different ability to translocate nitrogen towards the reproductive organs and in particular towards the grain.
Overall, therefore, the variety Antalis differentiated from all the other genotypes under test for high grain production, ability to intercept the N available in the soil both in conditions of high and low availability of the element, high ability to remobilize the N towards the reproductive organs and for high-efficiency indices (both NUE and NutE). On the contrary, the Appio variety showed a low ability to remobilize and translocate N from the flag leaf to the reproductive organs and a poor N use efficiency in conditions of high availability of the element for the plant. The old Senatore Cappelli variety was characterized by low productivity, scarce response to fertilization, and low ability to mobilize N from vegetative to reproductive organs with heavy negative repercussions on the efficiency indices (both NUE and NutE). For this latter variety, the results are in some way connected to its peculiar lateness which means that the reproductive phase falls into a period in which, in the trial environment, the climatic conditions become highly penalizing due to water and thermal stress.

2.3 Conclusions

The utilization of contrasting genotypes is a common strategy to identify key genetic features influencing a specific trait. The two agronomic experiments, evaluated nine durum wheat genotypes largely diversified for year of release morphological and phenological traits, and yield potential; this allowed us to identify both efficient and inefficient genotypes for NUE and for both NUpE and NUtE. Senatore Cappelli, the oldest variety, showed the most differentiated response among the genotypes with the highest N uptake and a greater ability and rapidity in intercepting N when available. This did not translate into a higher NUE, as expected from older varieties, being one of the less efficient in N utilization and in translocation from roots to shoot. Antalis, the most modern variety, was, by far, the most efficient both in NUE and in remobilization from flag leaves to the reproductive organs. Appio, instead, showed low values of N uptake, especially when N was in limiting concentrations, a slow response to nitrate fertilization, and the lowest remobilization from flag leaves to grain. Finally, Orizzonte was the most efficient in the uptake of N per gram of roots under limiting conditions with a highly efficient N translocation from root to shoot. These four genotypes (Sen. Cappelli, Antalis, Appio, and Orizzonte) were used for the RNA-Seq analysis performed in Chapter 5.

Chapter 3: Genome-wide characterization of the NPF and NRT2 gene families in durum wheat

3.1 Introduction

In plants, the nitrate transporter 1/peptide transporter (NPF) family represents a diverse array of membrane transport proteins found within multiple cell types and tissues. NPF family harbors a conserved structural arrangement consisting of twelve transmembrane domains I connected by short peptides and a central hydrophilic loop of about 90 amino acids between the sixth and the seventh TM (Wang et al., 2018). Previously, these proteins were named NRT (nitrate transporters) and/or PTR (peptide transporters), based on their first discovered substrates as. Later, Léran et al. (2014) suggested a unified nomenclature for the Nitrate transporter/Peptide transporter family (NPF). The phylogenetic analysis suggested their relationship with the proton-coupled oligopeptide transporters (POTs) and, accordingly, most NPFs operate as symporters in a proton-dependent transport.

NPFs are classified in eight subfamilies, from NPF1 to 8, with members of each subfamily assigned an increasing number resulting in a two-number code, based on a wide multi-species phylogenetic analysis. NPF family is often responsible for the low-affinity nitrate transport (LATS) although many members showed high affinity in many species like *ZmNPF6.6* in maize and *MtNPF6.8* in *Medicago truncatula* (Bagchi et al., 2012; Wen et al., 2017). The first gene member isolated in plants and one of the most studied is the *Arabidopsis thaliana* NPF6.3 (*AtNPF6.3*), previously known as *CHL1/AtNRT1.1*. It is a dual-affinity nitrate transporter contributing to root nitrate uptake and acting as nitrate sensor (Liu et al., 1999; Xuan et al., 2017). AtNPF6.3 can also act as chloride transporter when nitrate is absent and auxin transporter, a process negatively regulated by nitrate. The interaction between auxin and nitrate is associated with nitrate sensing, involved in the regulation of nitrate-dependent root development (Bouguyon et al., 2015). NPF proteins can transport a high number of different substrates other than nitrate, including phytohormones such as ABA and auxin, peptides, potassium and secondary metabolites (Chiba et al., 2015; Tal et al., 2016). Plant genomes contain a high number of NPF genes as opposed to bacteria, animals and algae, ranging from 20 in the moss *Physcomitrella patens* to 199 and 331 in *Brassica napus* and bread wheat respectively (Wen et al., 2020). In *Brassica napus*, the allopolyploidy greatly contributed to the expansion of the NPF family, and its high member number (Wen et al., 2020). A recent characterization of the NPF and NRT2 families in bread wheat showed a high number of members (331 and 46, respectively) mainly deriving from tandem and segmental duplication (Bajgain et al., 2018; Li et al., 2021). The retention of duplicated genes after duplication is often associated to the acquisition of new beneficial functions or the reduction of their total capacity, reaching the levels of the single-copy ancestral gene (Lynch and Conery, 2000). The high number of NPF and NRT2 genes in allopolyploid species suggests that these transporters may have evolved to play new essential non-overlapping roles in plants (Corratgé-Faillie et al., 2017; Longo et al., 2018).

The NRT2 family is much smaller, it is more specific to nitrate, with almost all the members involved in the high-affinity nitrate transport system (HATS). Seven members of this family were characterized in *Arabidopsis thaliana*, while five were detected in *Oryza sativa*. A higher number of NRT2 members are present in allopolyploid species as *Triticum aestivum* and *Brassica napus* with 47 and 17 genes, respectively (Tong et al., 2020; Li et al., 2021).

In wheat, almost all the studies focused on bread wheat with limited information on the regulatory pathways and functions of these gene families in durum wheat. Many reports focused on their expression levels under different abiotic and biotic stresses, such as drought, salt and N deficiency, in response to AMF, and several tissues and development stages (Buchner and Hawkesford, 2014; Duan et al., 2016; Tian et al., 2017 Bajgain et al., 2018; Choi et al., 2020). Recently, the *TaNRT2.5* overexpression, which localized on grain cell tonoplasts, was reported to increase grain nitrate uptake (Li et al., 2020). Many others studies highlighted improved crop yield, shoot biomass and N uptake when NPF or NRT2 genes were overexpressed (Hu et al. 2015; Fan et al. 2016; Sol et al., 2019; Wang et al., 2021).
Furthermore, the nucleotide variability in protein coding regions of the NPF genes seems to affect NUE related traits such as yield and shoot N content (Li et al., 2021). These findings suggest that further efforts in the detection and functional characterization of both gene families may greatly aid both the selection of N-use efficient cultivars. The high wheat genetic variability, the high number of duplicated genes and its economic relevance makes this plant a key species for the screening of potentially beneficial genes. Durum wheat is an important crop for many countries in the Mediterranean basin and the selection of key genes potentially involved in nitrate transport is a primary goal for NUE improvement, despite the limited knowledge compared to bread wheat. Thus, a detailed characterization and annotation of nitrate transporters is mandatory. Here, we identified both NPF and NRT2 genes in the durum wheat genome and performed a comprehensive analysis of their phylogenetic relationships, gene and protein structures and regulatory elements.

3.2 Materials and methods

NPF and NRT2 identification in durum wheat genome

To identify NPF and NRT2 genes in durum wheat genome, a sequence similarity approach and a machine learning approach (HMM) were adopted. Protein sequences of NPF and NRT2 genes of *Arabidopsis thaliana*, barley (*Hordeum vulgare*), maize (*Zea mays*), rice (*Oryza sativa*) and bread wheat (*Triticum aestivum*) were downloaded from Ensembl plants (http://plants.ensembl.org/). These sequences were used for a BLASTP search against the entire durum wheat proteome, also downloaded from Ensembl plants, using an e-value threshold of 1e-10 and a sequence identity of 50%. The durum wheat BLASTP best hits were then used as input for HMMER3 (Mistry et al., 2013), using the hmmscan

command and the 'Proton-dependent oligopeptide transporter family' (IPR000109) HMM profile with an e-value cut-off of 1e-5. Furthermore, Pfam (Bateman et al., 2004) was used to check that all the NPF protein sequences belonged to the PTR2 family (PF00854) and that all NRT2 protein sequences contained the NCBI conserved domain PLN00028. The final set of genes was then used to identify homologous groups. These were defined using a reciprocal BLASTN using nucleotide sequence identity >95% and chromosome location.

Motif discovery, collinearity, TF binding site and *CRE*s prediction and gene structure analysis

Gene structure of both TdNPF and TdNRT2 family members were analyzed using Webscipio2 (Hatje et al., 2011). The conserved motifs were identified using the Multiple Em for Motif Elicitation (MEME) suite (Bailey et al., 2015) with the classic mode algorithm using 6 and 100 for minimum and maximum motif width and a maximum number of 30 motifs per sequence. Through the NCBI protein domain search tool (https://www.ncbi.nlm.nih.gov/Structure/cdd/wrpsb.cgi) and the Conserved Domain Database (CDD), the conserved motifs were further investigated using an e-value threshold 0.01. Transmembrane helices and the protein localization were predicted by using the TMHMM2.0 tool (Krogh et al., 2001) and both WoLF PSORT (Horton et al., 2007) and PProwler1.2 (Hawkins et al., 2006), respectively. Chromosome location was extracted from the durum wheat genome annotation v1.0 and then displayed using the MG2C online tool (Chao et al., 2021). Significantly enriched chromosomal locations for both NPF and NRT2 were detected with ShinyGO (Ge et al., 2020) using a sliding window size of 6 and an FDR cutoff of 1e-05. The same tool was also used to perform a GO enrichment analysis of both TdNPF and TdNRT2 genes.

Transcription Factors (TFs) binding site prediction was performed on the promoter region using the binding site prediction tool of the Plant Transcription Factor Database (http://plantregmap.gao-lab.org/binding_site_prediction.php) using a p-value threshold of 1e-6 and the *Triticum aestivum* othologs. UniprotKB database (www.uniprot.org) was then used to extract protein domain information and annotation of the predicted TFs. Cis-regulatory Elements (*CRE*s) in upstream promoter regions (− 2000 bp) of *TdNPFs* and *TdNRT2s* were predicted by PlantCARE (Lescot et al., 2002)

The intraspecific collinearity was analyzed by using both TdNPF and TdNRT2 gene sets. A reciprocal BLASTP was performed using an e-value threshold of 1e-10. The output was fed to the MCScanX tool (Wang et al., 2012) to evaluate collinearity and duplication events using an e-value threshold of 1e-05 and a match score of 50.

Phylogenetic analyses

Phylogenetic trees including *Arabidopsis thaliana* and *Oryza sativa* NPF and NRT2 genes and those here identified on durum wheat were constructed. The final dataset included three hundred fifty-seven and 31 protein sequences for NPF and NRT2 families, respectively. Alignment was performed with the online tool CLUSTALW (Sievers et al., 2011) by setting up the default parameters. The unrooted

phylogenetic tree was generated through the Iqtree software v. 2.2 (http://www.iqtree.org/) with the maximum likelihood method, 1000 bootstrap replicates, and the JTT + G4 model for both NPF and NRT2 trees, selected by the Iqtree best-fit model selection. Another tree including the durum wheat nitrate transporters was developed using the same parameters. The dendrograms were visualized and analyzed through FigTree v. 1.4.4 (http://tree.bio.ed.ac.uk/software/figtree/).

3.3 Results

Durum wheat NPF and NRT2 identification

To identify NRT/NPF proteins in durum wheat, we carried out a BLASTP search against the genome using the full-length amino acid sequences from five different plant species. This step allowed us to select candidate NRT/NPF proteins based on the local alignment of highly similar portions of the proteins. The output of the BLAST search was further scanned using the machine learning-based HMMER3 tool that uses Hidden Markov Model (HMM) profiles to evaluate the probability that an amino acid sequence belongs to a protein family. Afterwards, using both BLASTP and HMMER searches with the 'Proton-dependent oligopeptide transporter family' profile (IPR000109) we were able to identify 211 and 20 NPF and NRT2 genes in durum wheat genome, respectively. These genes were further characterized using both sequence homology-based methods and several prediction softwares.
The TdNPF genes showed high variability in both gene length and aminoacids content. The nucleotide sequences of the 211 NPF genes showed a 3400 bp gene length mean and encoded proteins that ranged from 71 to 943 aminoacids, with a mean length of 583 aminoacids. The molecular weights varied from 7 to 105 kDa. Using TMHMM2, we predicted the number of transmembrane regions in both NPF and NRT2 protein sequences (Figure 1). About 80% of TdNPF proteins showed 12 predicted transmembrane domains, while the subcellular localization of almost the 95% of TdNPF proteins was on the plasma membrane. NRT2 is a smaller gene family with lower variability compared to the NPF family. Indeed, the 20 TdNRT2 had a 1600 bp mean gene length and encoded proteins that ranged from 113 to 573 aminoacids, with a mean length of 509 aminoacids. The molecular weights varied from 12 to 62 kDa. 75% of TdNRT2 proteins showed 12 predicted transmembrane domains, while the 90% were predicted to be localized on the plasma membrane (Table 1).

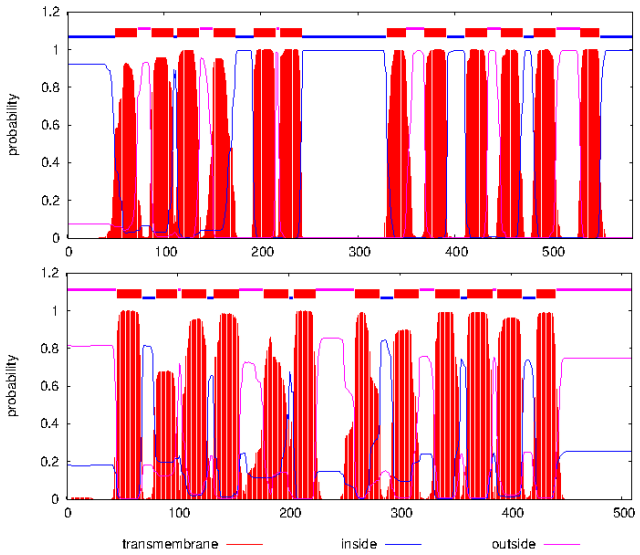

Figure 1. Prediction of transmembrane regions of TdNPF (top) and TdNRT2 (bottom) genes. The probability (y-axis) of each region being either transmembrane (red), outside (pink), or inside (blue) the plasma membrane was shown.

Table 1 TdNRT2 genes detected in the durum wheat genome.

name	Gene	Position	Nuc_length	AA_length	Chr	Subcellular_localization	TM
TdNRT2.1	TRITD6Bv1G009270	32873387-32873725	2342	510	2A	plasma membrane	12
TdNRT2.2	TRITD2Av1G017380	13607789-13616151	340	113	6A	plasma membrane	1
TdNRT2.3	TRITD6Av1G006050	13635920-13652904	1531	440	6A	plasma membrane	10
TdNRT2.4	TRITD6Bv1G008680	13657414-13658943	1531	439	6A	plasma membrane	10
TdNRT2.5	TRITD6Av1G006000	13885430-13886956	8364	567	6A	plasma membrane	12
TdNRT2.6	TRITD6Bv1G008710	14764657-14776088	1699	566	6A	plasma membrane	12
TdNRT2.7	TRITD6Bv1G008700	14787789-14789318	27855	299	6A	chloroplast	7
TdNRT2.8	TRITD6Bv1G008690	14816329-14817858	9608	508	6A	plasma membrane	12
TdNRT2.9	TRITD6Av1G006030	14838756-14840183	16986	509	6A	plasma membrane	12
TdNRT2.10	TRITD6Av1G006520	23537868-23539397	11433	573	6B	plasma membrane	12
TdNRT2.11	TRITD6Av1G006540	23543555-23553161	1531	510	6B	plasma membrane	12
TdNRT2.12	TRITD6Bv1G009290	23551638-23579491	1531	510	6B	plasma membrane	12
TdNRT2.13	TRITD6Av1G006530	23567751-23569448	1531	510	6B	plasma membrane	12
TdNRT2.14	TRITD6Bv1G008890	24015838-24017364	1528	509	6B	plasma membrane	12
TdNRT2.15	TRITD6Av1G006170	24062993-24064519	1528	509	6B	plasma membrane	12
TdNRT2.16	TRITD6Bv1G008870	24780504-24782378	1528	509	6B	plasma membrane	12
TdNRT2.17	TRITD6Av1G006560	24811485-24813825	1429	476	6B	plasma membrane	12
TdNRT2.18	TRITD6Bv1G009240	24864160-24865689	1876	520	6B	plasma membrane	12
TdNRT2.19	TRITD7Bv1G180680	617261095-617263773	2571	228	7A	chloroplast	6
TdNRT2.20	TRITD7Av1G231010	568796851-568799420	2680	498	7B	plasma membrane	12

TdNPFs and *TdNRT2s* phylogenetic analysis

To explore the molecular evolution and the TdNPF gene family organization, we performed a phylogenetic analysis using protein sequences from 53 *AtNPFs* (*Arabidopsis thaliana*), 93 *OsNPFs*

(*Oryza sativa*), and 211 *TdNPFs* here identified in durum wheat for a total of 357 *NPFs*. The Multiple Sequence Alignment (MSA) performed by CLUSTALW was fed to iqtree for both the model selection and the maximum-likelihood tree evaluation. The phylogenetic tree showed a separation between the known eight NPF families (Figure 2). All the key nodes between sub-families showed a bootstrap value higher than 98 and all the genes from *Arabidopsis* and rice belonging to the same sub-family clustered together. These results ensured the accuracy and reliability of the tree construction, suggesting a higher sequence variability between sub-families compared to the interspecific variability inside each sub-family. *TdNPFs* were assigned to the eight sub-families and named *TdNPF1-8* following the tree topology and the classification of two previously characterized species. The sub-families TdNPF5 and TdNPF8 included the highest numbers of members (63 and 52, respectively), while TdNPF1 and TdNPF3 were the smaller sub-families with four and 8 genes, respectively (Table 2). TdNPF4, TdNPF5 and TdNPF6 were the only monophyletic groups, while the sub-families TdNPF1, TdNPF2, TdNPF3 and TdNPF7, TdNPF8 formed two distinct clusters with TdNPF1 clustering inside the TdNPF2 branch. This feature has been observed in other species such as *Brassica napus* and often led to the definition of more than eight sub-families classification. Interestingly, this was not detected in *Triticum aestivum* with a separation of the two clades.

Table 2. Distribution of the members of the NPF gene family in six species.

	NPF1	**NPF2**	**NPF3**	**NPF4**	**NPF5**	**NPF6**	**NPF7**	**NPF8**	**Total**
Arabidopsis thaliana	3	14	1	7	16	4	3	5	53
Oryza sativa	3	6	5	12	29	6	11	21	93
Brassica napus	11	43	7	20	73	13	10	22	199
Zea mays	4	4	6	12	17	8	12	16	79
Triticum aestivum	6	41	15	32	94	22	40	81	331
Triticum durum	4	27	8	21	63	17	19	52	211

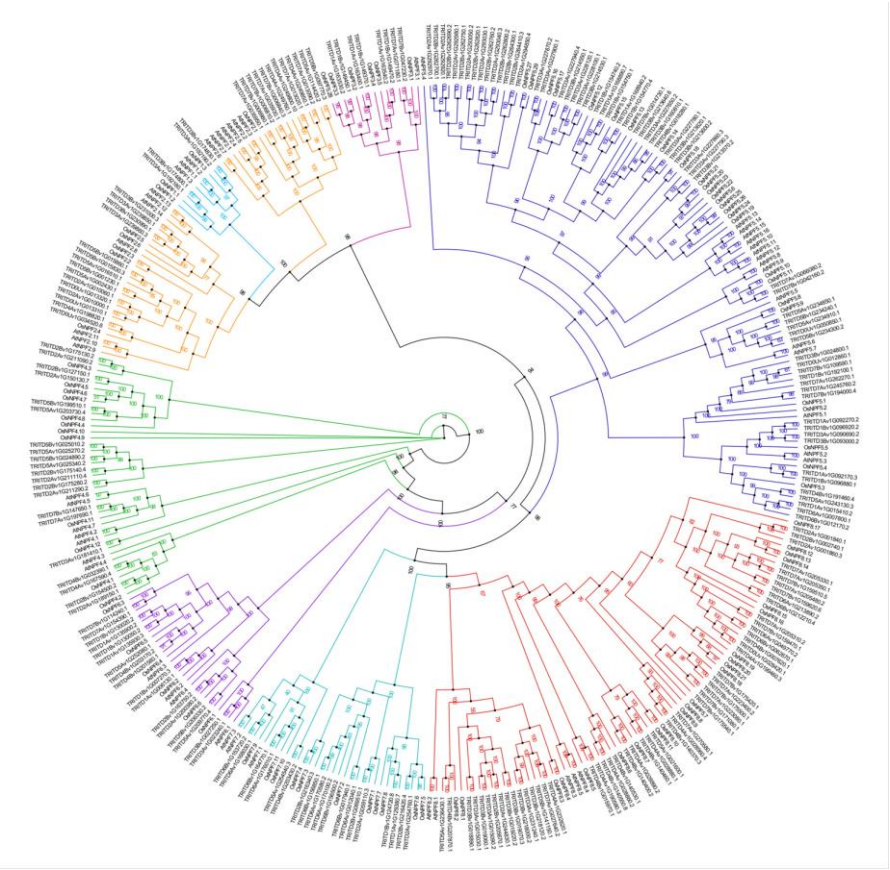

Figure 2. Phylogenetic tree of TdNPF, AtNPF, and OsNPF full-length protein sequences. The eight NPF sub-families are highlighted using branch colors: 1:Blue – 2:Orange – 3:Pink – 4:Green – 5:Turquoise – 6:Violet – 7:Cyan – 8:Red. Bootstrap values (1000 replicates) are shown for each node. The Maximum likelihood tree was constructed using iqtree2.2, visualized, and modified using Figtree.

The NRT2 gene family was analyzed using a similar approach used for *NPFs*. The maximum-likelihood phylogenetic tree was constructed using the same three species (*Arabidopsis*, rice and durum wheat), including 7 *AtNRT2s*, 4 *OsNRT2s*, and 20 *TdNRT2s* for 31 NRT2 total protein sequences. The phylogenetic tree showed lower similarity between NRT2 proteins from durum wheat and the other species with only a TdNRT2 protein (TdNRT2.2) that clustered with OsNRT2.1 and 2.2 (Figure 3). Interestingly, *TdNRT2.19* and *TdNRT2.20* showed a high sequence diversity from all the other genes, forming an independent branch, while all the *AtNRT2s* clustered together in three branches. All the nodes distinguishing genes from different species showed high bootstrap value (100), while the others exhibited lower bootstrap values, probably due to the highly conserved protein sequences inside a species. By contrast, the NRT2 tree highlighted high divergence between the three species, despite the interspecific variability.

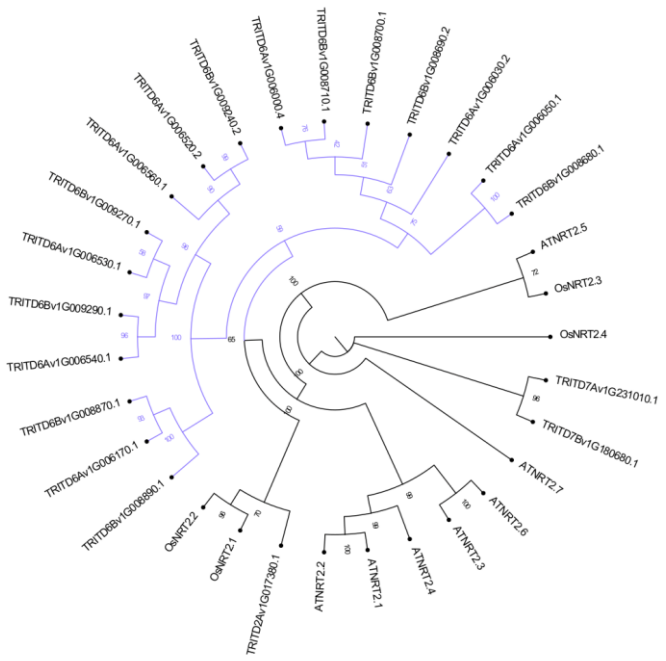

Figure 3. Phylogenetic tree of TdNRT2, AtNRT2 and OsNRT2 full length protein sequences. The colored branch shows the main TdNRT2 branch with 17 out of the 20 NRT2 proteins. Bootstrap values (1000 replicates) are shown for each node. The Maximum likelihood tree was constructed using iqtree2.2, visualized, and modified using Figtree.

Chromosome location

TdNPFs were evenly distributed in the genome (Chi-square), in addition, no significant difference between the two genomes was observed (Figure 4). We performed a hypergeometric test (FDR < 1e-05) using a sliding window approach to identify significantly overrepresented regions in each chromosome. Four regions in chromosomes 2B, 3A, 3B, and 4B were enriched in NPF genes ranging from 5 to 7 genes per window (6MB). These genes were mainly positioned in the R2b region of chromosomes which included the most abundant gene number while the central chromosomal regions showed a lower number of genes on average.

The *TdNRT2s* were unevenly distributed along the genome, with chromosome 6 in both genomes (A and B) significantly enriched with 9 and 8 genes in 6B and 6A chromosomes, respectively. Interestingly, all the *TdNRT2s* on chromosome 6 were located in the R1 region of the chromosome in a significantly overrepresented window in both genomes while only two genes were found in the R2b region.

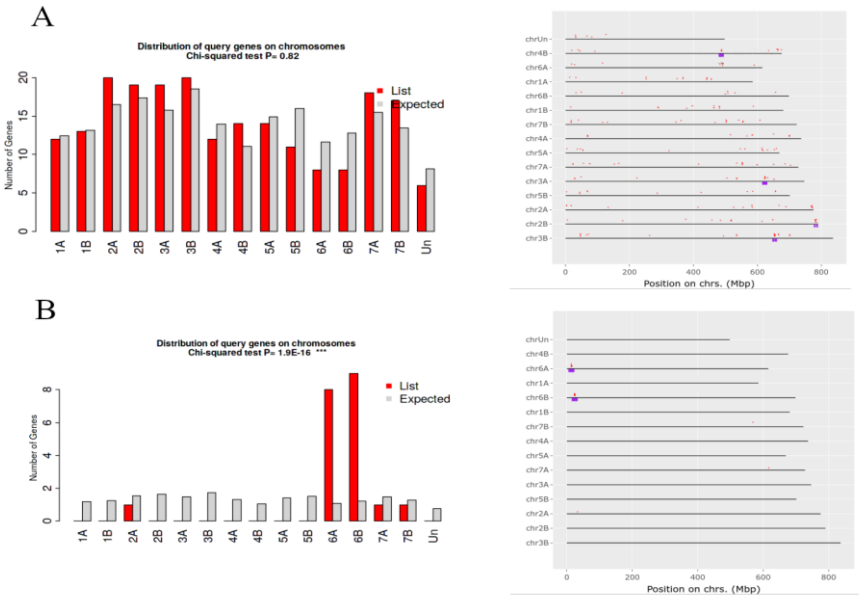

Figure 4. Left: Distribution of TdNPF (A) and TdNRT2 (B) genes on the 14 chromosomes of the durum wheat genome. **Right:** Hypergeometric test (FDR < 1e-05) on a sliding window scanning approach with a sliding window size set to 6MB for both TdNPF (A) and TdNRT2 (B) genes.

Gene structure, motif discovery, transcription factor binding site, and *CREs* prediction

Using the BioMart tool on the Ensembl plants database, we extracted both the gene structure and isoforms composition from the genome annotation (Figure 5). The gene structure of both families showed a significant difference in the number of exons and in the number of transcript isoforms. Most of the 211 *TdNPFs* exhibited more than two exons with the 85% of genes ranging from 3 to 6. The number of transcript isoforms was also significantly different from the genome distribution with an average number of 3 transcripts per gene. The *TdNRT2s* showed lower exons number with 9 out of 20 genes with one exon and a lower number of transcripts per gene with more than 50% of genes with one transcript.

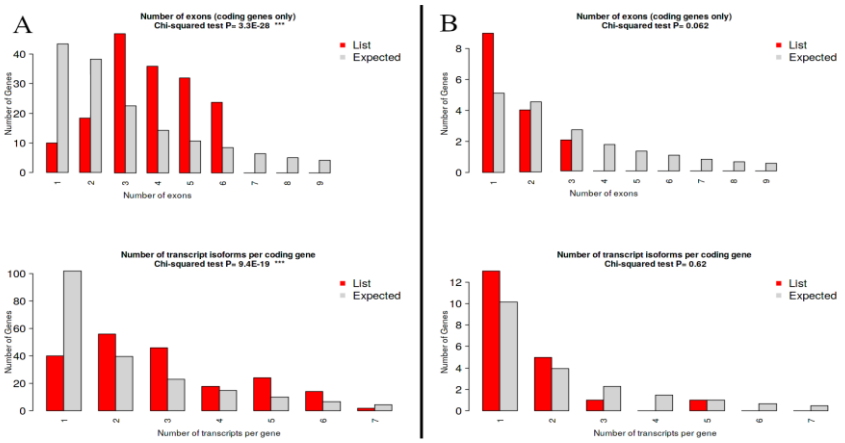

Figure 5. Number of exons (Top) and transcripts (bottom) of the 211 TdNPF (A) and TdNRT2 (B) genes. Chi-squared test was used to test if query genes significantly differ in terms of exons and transcripts abundance compared to all the background genes in the genome.

Intraspecific collinearity was analyzed through a reciprocal BLASTP of all the TdNPF and TdNRT2 genes using MCScanX able to identify homologous genes, tandem and segmental duplications. The TdNPF gene family was characterized by 44% of collinear pairs. The relevant number of duplication events explained the expansion of this gene family. In detail, 77 segmental and 94 tandem duplications, as well as fewer dispersed (30) and proximal duplication (10) were detected; 42% of *TdNPFs* formed tandem blocks, with 11 blocks including three or more genes.

The TdNRT2 gene family, as previously highlighted, is mainly located in two enriched regions on chromosomes 6A and 6B. These formed 5 tandem blocks, 3 and 2 on 6B and 6A chromosomes, respectively. Furthermore, 14 tandems and none segmental duplications were detected.

Protein motif analysis was carried out using the MEME tool to highlight conserved motifs and to analyze their distribution among sub-families. All TdNPF proteins showed highly conserved motifs patterns (Figure 6). Instead, the spatial organization and distance between conserved motifs were highly variable. The intra motif variability was very high, with only few positions conserved in almost all the protein sequences (Figure 7). The high intra motif variability may play a key role in the fine-tuning of each transporter substrate affinity or in their localization and regulation.

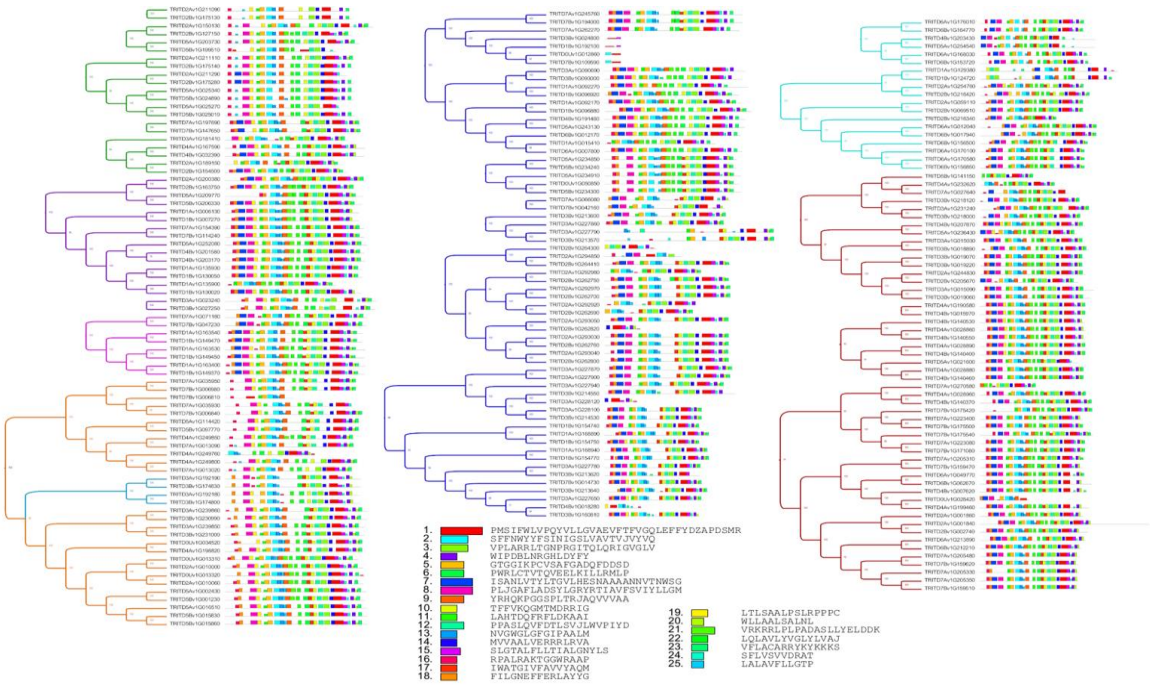

Figure 6. Conserved motifs detected in TdNPF protein sequences. NPF sub-families are highlighted using the same color coding as figure 14. The most represented motif for each of the 25 motifs is shown. The phylogenetic tree based only on TdNPF protein sequences is shown.

Figure 7. Sequence logos of the two most conserved motifs (Motif1 and Motif2) of both TdNPF and TdNRT2 identified using the MEME tool. The dimension of the letters represents the position-specific degree of conservation of the amino acid.

To better characterize these sequences, we extracted the more represented motif for each of the 25 conserved motifs for an NCBI protein domain search to highlight their function (Figure 8). Fourteen motifs were assigned to the Major Facilitator Superfamily (MFS), the remaining (11) were not assigned to any known protein domain, suggesting a highly specific function for these peptides (putatively species specific).

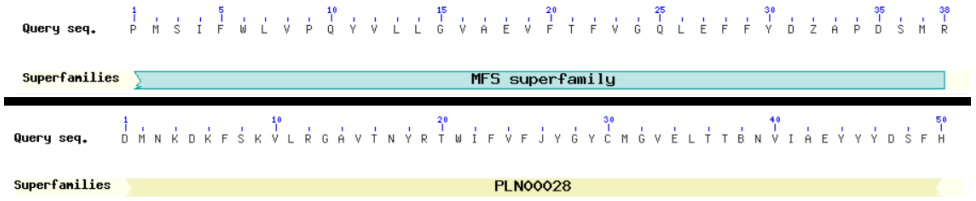

Figure 8. Output of the protein domain search on the Motif1 of TdNPF (top) and TdNRT2 (bottom) protein sequence performed using NCBI's protein domain search engine.

Motif1 was detected in all the 211 proteins, Motif19 and Motif21, the less conserved, were found only in 98 and 99 proteins, respectively. The conserved motifs are highly present in all the NPF sub-families but the sequence variability inside each motif appears high. Furthermore, Motif18 (FILGN**EFFER**LAYYG), shared by 147 TdNPFs, contains the highly conserved ExxER/K peptide, suggested its involvement in the proton binding. Among these sequences, both glutamic acids (E) were conserved in 80% of sequences, while the arginine residue (R) is less conserved. Occasional motif variants are found such as ExxDR and ExxEE. Interestingly, 11 proteins showed the variant ExxES identified by Longo et al., (2018) only in monocots and related to nitrate uptake not dependent on proton transport.

Fifteen conserved motifs were identified in the TdNRT2 gene family (Figure 9). Nine out of 15 are assigned to the nitrate transmembrane transporter superfamily (PLN00028). Moreover, the distribution and position of the motifs showed regular patterns and lower sequence variability compared to TdNPF family. Almost all NRT2 shared many conserved motifs, except four highly variable genes (TRITD7Av1G231010, TRITD7Bv1G180680, TRITD2Av1G017380, TRITD6Bv1G008700).

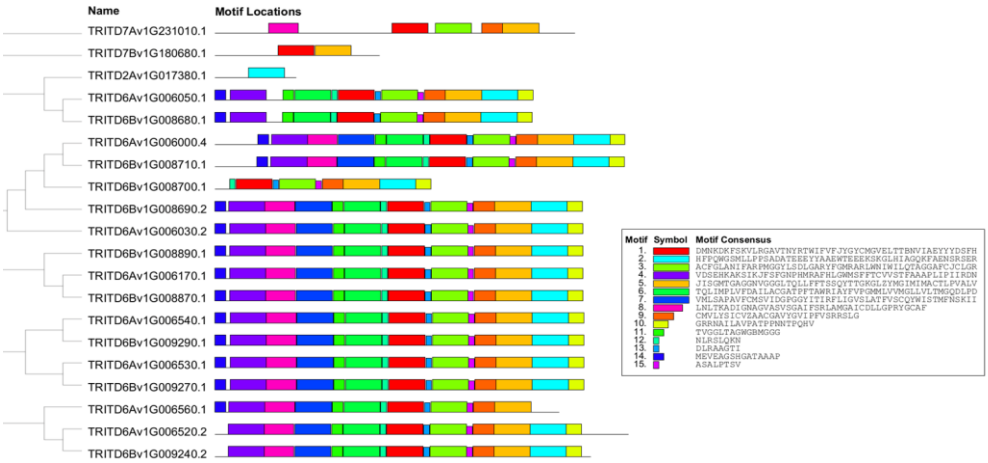

Figure 9. Conserved motifs detected in TdNRT2 protein sequences. The most represented motif for each of the 15 motifs is shown.

Transcription Factors (TFs) are essential for modulating gene transcription levels and many TFs were shown to directly regulate the expression of NPF and NRT2 genes (Marchive et al., 2013; Liu et al., 2017). Here, we predicted the TF binding sites in promoter regions (3000 bp upstream of gene sites) of TdNPFs and TdNRT2 using the Binding Site Prediction tool of the PlantTFDB, more than four thousand (4072) binding sites for 163 TFs were identified in the promoter regions of 197 *TdNPFs*. The most abundant TFs belonged to MYB, AP2, and NAC families (Figure 10). Two hundred twenty binding sites for 53 TFs were detected in the promoter region of 19 *TdNRT2s*, with the AP2 family the most represented. Interestingly, 51 out of 53 were shared with the TFs predicted to bind the NPF genes promoter region.

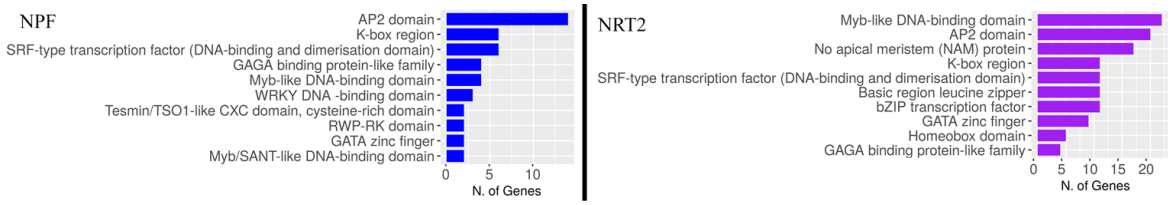

Figure 10. Domains of the Transcription Factors predicted to bind to the promoter regions of TdNPF and TdNRT2 genes.

The cis-regulatory elements (CRE) are non-coding DNA regions also involved in the transcription regulation of neighboring genes (Bai et al., 2013). Here, we predicted *CRE*s in the promoter regions of both *TdNPFs* and *TdNRT2s* using PlantCARE. More than five thousand (5121) *CREs* in the 211 promoter regions of TdNPF were found, including 27 different types (Figure 11). The most abundant sites were the Aba responsive element (ABRE), DRE and MYB binding sites, as-1, and the stress

response element (STRE) accounting for 70% of all the *CRE*s. Other less abundant *CRE*s were involved in light-response (G-box), biotic and abiotic stress response (MYC), and the common TATA-box and CAAT-box.

More than one thousand five hundred (1518) *CRE*s were predicted in the promoter regions of *TdNRT2s*. They were highly enriched in MYB and MYC binding sites, with many genes showing more than 5 sites in their upstream sequence accounting for almost 40% of *CRE*s, in agreement with the previously described TF binding site prediction.

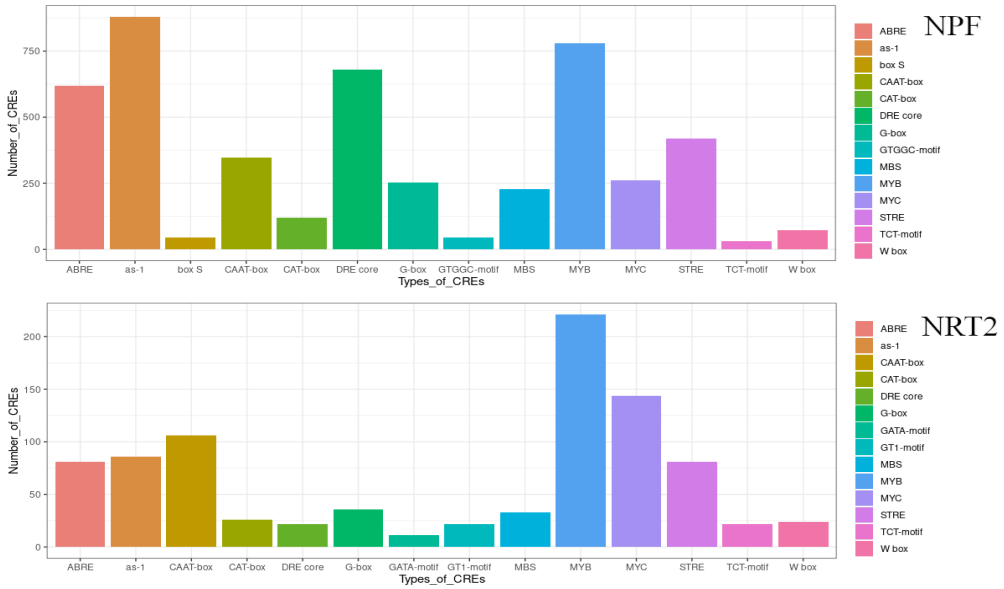

Figure 11. The number of Cis-Regulatory Elements (*CRE*s) detected in the promoter regions of TdNPF (top) and TdNRT2 (bottom) genes. The analysis was carried out using PlantCARE.

3.4 Discussion

The full characterization of NPF and NRT2 genes is a key to better understand the complex dynamics of nitrate uptake and utilization. In durum wheat, this characterization is even more important due to the high duplication level of gene families due to the allopolyploid genome. The high number of TdNPF and TdNRT2 genes could determine a system with higher modularity in terms of substrate affinity and specific gene expression.

In the present study, we identified 211 *TdNPFs* and 20 *TdNRT2s* from *Triticum turgidum* L. subsp. *durum* (Desf.) Husn. genome. The number of members was comparable to other allopolyploid species such as *Brassica napus* (199, 17), *Saccharum spontaneum* (178, 20), and *Triticum aestivum* (331, 46) and significantly higher than many diploid monocots and dicots such as *Arabidopsis* (53 and 7), rice (93, 4) and maize (79, 1). The NPF gene family expansion in plants seems to have arisen from neo- and sub-functionalization, as suggested by many works (Lynch and Conery 2000; O'Brien et al., 2016;

Jørgensen et al., 2017; Wang et al., 2019). In wheat, the huge number of genes in both gene families could be involved in highly differentiated responses to several substrates levels. In *Triticum aestivum*, the polymorphisms accumulation of both NPF and NRT2 gene family was mainly due to random drift. Nevertheless, this variation led to significant differences in the NUE of subpopulations clustered based on SNPs within the NPF and NRT2 genes (Li et al., 2021).

The phylogenetic analysis highlighted the high divergence among NRT2 genes from durum wheat, rice and Aarabidopsis with genes from different species clustering together in clearly separated groups. The best hit (BLASTP) of many *TdNRT2s* against the *Arabidopsis* NRT2 protein sequences is often attributable to *AtNRT2.1*, making difficult a full characterization of these transporters based on the sequence homology. This poses a major challenge in associating previous functional annotations from model species to the newly identified genes in durum wheat. Here, we focused on sequence and protein domains characterization, but further studies will be needed to fully characterize the *TdNRT2s*, mainly at the functional level. Instead of, the *TdNPFs* phylogenetic analysis yielded more informative result, with all the genes belonging to the same sub-family clustering together and allowing for a much more reliable annotation of the novel *TdNPFs*. Our results showed the clustering of *NPFs* from *Arabidopsis*, rice and durum wheat in the previously described sub-family structure. This result seems to confirm the hypothesis of NPF family divergence before the separation of monocots and dicots, as suggested by Wang et al. (2019).

The chromosome location of both families showed a non-random distribution inside the genome. Interestingly, *TdNRT2s* are highly concentrated on chromosomes 6 from both genomes (A and B), probably due to the tandem duplication events, as shown by the collinearity analysis. A similar enrichment on chromosome 6 of all three genomes (A, B and D) was found in bread wheat, also deriving from tandem duplication that was suggested due to unequal crossing-over events (Li et al., 2021). Although similar, the number of NRT2 genes in these genome regions is higher in bread wheat, suggesting that some of these duplication events should have happened after or during the hybridization of durum wheat with *Aegilops tauschii* (genome D). An alternative hypothesis referred to an ancient duplication of this region in the diploid wheat genome before the hybridization into the polyploidy wheat as suggested by Salse et al. (2008). Further studies on the intraspecific variability of these gene families on all the wheat species could be carried out to deeply understand how their expansions occurred and what type of mechanisms underlie their preservation after duplication.

In *Arabidopsis*, several putative NO_3^- response cis-regulatory elements (*CRE*s) in many promoters of N-related genes have been detected, despite limited information is available for other plant species (Konishi et al., 2010; Wang et al., 2010; Rolly et al., 2021). Here, a high number of *CRE*s related to ABA signaling and binding of Drought Responsive Element (DRE) and MYB TFs in the *TdNPFs* promoter regions were detected. Interestingly, the *TdNRT2s* upstream region was also highly enriched with MYB binding sites, as shown by both *CRE*s and TF binding site prediction. MYB TF are often involved in abiotic and biotic stress responses and plant development (root and flower development)

(Kaur et al., 2017), although their role in nitrate-related regulation have been reported (Todd et al., 2004; Wang et al., 2018; Zhang et al., 2021). Interestingly, both gene family promoters showed multiple putative MYB binding sites. The presence of multiple binding sites for the same TF has been already described and seems to be associated with a higher sensitivity of some genes to specific TFs (Howard and Davidson, 2004; Yáñez-Cuna et al., 2013; Brendolise et al., 2017).

The presence of many *CREs* and the partial overlap of their typology between the two gene families, suggests that a complex regulatory network is involved in modulating and fine-tuning these nitrate transporters gene expression, with common TFs regulating both families. These could be involved in the spatiotemporal- or tissue-specific activation of transporter genes or may take part in the signaling cascade in response to fluctuations of specific substrates concentration. Interestingly, the same analysis performed by Wen et al (2020) on the *NPFs* of *Brassica napus* yielded similar results on NPF genes, suggesting that the regulation of this gene family may involve the same categories of TFs and could be evolutionarily conserved.

The evidence that both tandem and segmental duplications had a similar role in the expansion of NPF genes found by Li et al., (2021) in bread wheat was here confirmed, with 37% and 44% of NPF genes derived from segmental and tandem duplication, respectively.

Overall, NPFs showed a much variable gene structure and sequence variability inside conserved motifs, compared to NRT2s. Interestingly, NRT2 genes have a much simpler gene structure, with only one or two exons and highly clustered genomic locations. Both gene structure and chromosome locations of this group seem to be highly conserved among many monocots such as *Brachypodium distachyon*, *Saccharum spontaneum*, and bread wheat with the NRT2 genes mainly distributed on two chromosomes and having mainly one or two exons (Wang et al., 2019; Wang et al., 2019; Li et al., 2021).

There are numerous limits to a purely bioinformatics approach to the full characterization of gene families that must be associated with RNA-Seq and genotyping experiments to better describe the complex regulatory mechanisms underlying NPF and NRT2 mediated transport. Tissue specific expression, environmental factors, response to biotic and abiotic stimuli are only a fraction of the elements playing a role in the modulation of these gene families. Furthermore, the high number of substrates, unclear transport mechanism and high inter-species variability of the NPF family makes further biochemical and structural studies of individual NPFs mandatory for a better understanding of the transport mechanisms and the different roles of each member. Nonetheless, the highly detailed characterization here produced will allow for a more precise investigation on NPF and NRT2 genes in durum wheat.

3.5 Conlcusions

The work here described allowed us to fully characterize both the NPF and NRT2 genes in the durum wheat genome. The manual annotation of these gene families is of great relevance for the study of

nitrate and nitrogen dynamics and their relationship with agronomic NUE. We identified for the first time 211 TdNPF and 20 TdNRT2 genes, providing a deep annotation of their protein sequences and conserved domains. We further predicted both Cis Regulatory Elements and Transcription Factors involved in their regulation and provided a detailed phylogenetic analysis of both gene families. The majority of genes were retained after small-scale duplication events, suggesting a neo- or sub-functionalization of many *TdNPFs* and *TdNRT2s*. These results suggest that the expansion of these families in wheat may be an important source of variability for the detection of NUE-related genes and potential candidates for transgenic plant development.

Chapter 4: Transcriptome changes induced by Arbuscular mycorrhizal symbiosis sustain higher salt tolerance in durum wheat

4.1 Introduction

Soil salinity is one of the most significant causes of abiotic stress in plants significantly limiting plant growth and crop production in cropping systems (Rengasamy et al., 2006). Approximately 20% of worldwide cultivated and almost 30% irrigated lands are affected by soil salinization (Shahid et al., 2018). High salt deposition in soil affects plants by inducing physiological, biochemical, and molecular modifications. High salt concentration in soil results in plant cellular osmotic stress, ionic and redox imbalances. Plants have evolved several mechanisms to avoid damages derived from salt stress mainly due to ion-homeostasis, solute accumulation, water and nutrient uptake regulation, and the detoxification of ROS through antioxidant enzymes and molecules (Munns et al., 2008; Ruiz-Lozano et al., 2012; Augé et al., 2014). The interactions between plants and microorganisms (plant-growth-promoting microorganisms and arbuscular mycorrhizal fungi) are also reported to play a key role in crop yield maintenance under stress environments (Singh et al., 2015; Vimal et al., 2017).

Arbuscular Mycorrhizal Fungi (AMF) are symbiotic with the roots of more than 80% of land plants, among the other several crop species (Smith et al., 2010). This symbiosis positively affects plant health and the ability to counter both biotic and abiotic stresses through various mechanisms. The improvement of the plant's ability to explore soil due to the fungal hyphae firstly determined higher water and nutrient (P, N, Mg, and Ca) acquisition. Further, AM symbiosis contributes to improve the root form and function, as well as the accumulation of osmolytes, the antioxidant defense system, the maintenance of ion homeostasis, and the photosynthetic efficiency (Pozo, et al., 2010; Bitterlich et al., 2018; Chandrasekaran et al., 2019; Evelin et al., 2019; Begum et al., 2019; Ingraffia et al., 2019&2020; Alaux et al., 2020). These positive effects are attributable to an increased expression of numerous genes involved in these pathways in mycorrhizal plants. Indeed, genes related to proline, trehalose, soluble sugars, and other osmolytes are often upregulated by AM inoculated plants to contrast the cell dehydration caused by the lower turgor (Evelin et al., 2013; Alqarawi et al., 2014). AM inoculation is also responsible for increased enzymatic and non-enzymatic oxidative stress responses due to the upregulation of peroxidases (POX), catalases (CAT), and superoxide dismutase (SOD) and higher synthesis of antioxidant molecules (Gill et al., 2010). A high concentration of Na^+ and Cl^- in the soil can also lead to harmful ionic imbalances. AM fungi have been shown to enhance ion homeostasis by influencing the concentration of organic acids and polyamines and by enhancing the expression of Na^+/K^+ and Na^+/H^+ transporters like HKT, NHX, and SOS to support Na^+ efflux from cytosol to apoplast or into the vacuole (Porcell et al., 2016). Furthermore, Nitrogen plays an important role in the amelioration of salt tolerance (Gómez et al., 1996; Mansour, 2000). The enhancement of root N uptake induced by AMF is one of the main mechanisms underlying salt tolerance in mycorrhizal plants (Wang et al., 2018). According to many gene expression analyses, salt can stimulate the expression of NO_3^-

transporters and increase NR activity (Popova et al., 2003; Nie et al., 2015; Fileccia et al., 2017, Evelin et al., 2019). The accumulation of N-containing metabolites is, in fact, an important strategy to counter both osmotic and oxidative stress (Shabala et al., 2013). These processes are often enhanced by the AMF colonization resulting in higher expression of host NRT transporters, and proton ATPases (Sa et al., 2019). All these mechanisms help mycorrhizal plants to cope with soil salinity resulting in improved plant growth compared to non-mycorrhizal plants.

Although the recent efforts in improving knowledge on the complex mechanisms underlying salt stress response in model plants (Porcel et al., 2015; Zhou et al., 2016), limited studies focused on transcriptional regulation in non-model organisms, including durum wheat. The agronomic, metabolomic and proteomic responses to salt stress in durum wheat have been already reported (Almansouri et al., 2001; Capriotti et al., 2014). Many other reports focused on the transcriptional profiling of stress-inducedced genes mainly in the bread wheat (*Triticum aestivum*) root (El-Amri et al., 2013; Talaat et al., 2014; Zhu et al., 2018), while limited information is available for durum wheat (Fileccia et al., 2017; Annunziata et al., 2017). Fileccia et al. (2017) detected a highly positive effect of AMF inoculation on the above ground and root biomass production, N uptake, and the plasma membranes stability in durum wheat grown under salt stress also highlighting a significant downregulation of drought-related genes in inoculated samples by q-PCR. Therefore, the study of expression profiles of non-model AM inoculated plants grown under salt stress could help to better understand the mechanisms involved in salinity stress tolerance attributable to AM symbiosis.

The aim of this work was to identify key genes involved in the improved response to salinity stress induced by AM fungi using RNA-Seq analysis on durum wheat. The transcriptomic profiling was conducted on green fully photosynthesizing leaves to determine the effects of AMF on yield and qualitative traits.

4.2 Materials and Methods

Plant material and experimental design

Durum wheat (*Triticum turgidum* L. subsp. *durum* (Desf.) Husn. cv. Anco Marzio) plants were grown outdoors in pots under salinity stress with and without AM fungi inoculation (namely 'AM+' and 'AM-', respectively). A complete randomized factorial design was adopted with seven replicates. Each pot (diameter 150 mm, height 130 mm) was filled with 2000 g of a quartz sand:soil mixture (1:1). Soil properties were as follows: 267 g kg^{-1} clay, 247 g kg^{-1} silt, and 486 g kg^{-1} sand; pH 8.0; 6.3 g kg^{-1} total carbon (C); 0.86 g kg^{-1} total N; 1.70 dS m^{-1} saturated electrical conductivity (EC) (25°C). Both soil and sand were sieved through a 2 mm mesh and autoclaved at 121°C for 20 min to completely impair soil biological (both fungal and bacterial) activity. The native bacterial microflora was extracted by suspending 500 g of fresh soil in 1.5 L distilled water. After shaking and decanting, the suspension was filtered (11 μm mesh) to discard the native AM fungal community. Each pot received 30 ml of soil

suspension filtrate to reintroduce the native microbial community before AM inoculation, performed by a commercial AM inoculum at 10 g per pot rate. This consisted of a spore mixture including *Rhizophagus irregularis* and *Funneliformis mosseae*, at 700 spores g^{-1} of inoculum rate for each. The commercial inoculum also contains 1 x 107 rhizosphere bacteria. To isolate the AM fungi effects, we extracted the bacterial community of the inoculum, using the same protocol used for the native soil microbial community reported above, and introduced it to the AM- treatment. The microbial inoculations were performed at the same time of sowing. The native microbiome and the bacterial community present in the inoculum (only for AM- treatment) were added in liquid form as reported above, while AM fungal inoculum was distributed just below the sowing bed. Each pot received 60 mg of N in the form of ammonium sulfate ($[NH_4]_2SO_4$).

Sixteen seeds, previously surface-sterilized with H_2O_2 at 4% for 3 minutes, were sown in each pot. Ten days after emergence, plants were thinned to six seedlings per pot. The plantlets were grown for 15 days before the application of salt to avoid its negative effect on the AM symbiosis establishment. Salt stress was determined by adding NaCl in the irrigation water (0 and 10 g L^{-1}). To prevent osmotic shock, salt was added gradually by distributing in total 1 L of NaCl solution in each pot in the 7 days from the beginning of the salinity treatment. This treatment led the EC of saturated soil extract to 13.00 dS m^{-1}. Afterward, plants were watered with tap water (0.58 dS m^{-1}) until harvest. Leaching was avoided by maintaining soil water always below field capacity. During the experiment, the irrigation was performed every two days and the amount of irrigation water consisted of the total replenishment of water lost through evapotranspiration for each pot.

All pots were harvested after 45 days from sowing. Plant aboveground biomass was immediately separated into stems, green leaves, and senescent and dry leaves, and the fresh weight of each fraction was recorded. Root biomass was extracted by carefully cutting the pots vertically and removing the substrate by washing. About 1 g of green leaves and 1 g of roots from each pot were immediately frozen in liquid N, stored at −80°C, and subsequently pulverized without thawing. At the same time, a sample of green full expanded leaves (about 400 mg) was taken from each pot to determine the membrane stability index (MSI). The leaf material was divided into two sets of 200 mg each. The first set was heated at 40 °C for 30 min in a water bath (10 cm^3); then the electrical conductivity bridge (C1) was measured. The second set was boiled at 100 °C for 10 min (in 10 cm^3 of water) before measuring the electrical conductivity bridge (C2). MSI was calculated according to Sairam et al. (1997).

A representative root sample (about 1 g) was taken from each pot to determine the overall colonization of roots by AM fungi. To this end, root samples were cleared in KOH and stained with trypan blue following the method described by Phillips et al. (1970). AM fungi root colonization was then measured with the grid intersect method (Giovannetti et al., 1980).

Plant N content was determined separately on dry material of each botanical fraction obtained as previously described using the combustion method of Dumas (DuMaster D-480, Büchi Labortechnik

AG, Flawil, Switzerland). For each pot, total N uptake was calculated as the sum of N accumulated in roots (root dry mass × root N concentration) and shoots (shoot dry mass ×shoot N concentration).

Statistical Analysis

All plant data were compared between the two groups (AM+ and AM-) using the package "dabestr" (Ho et al., 2019) to generate unpaired mean differences via a bias-corrected and accelerated bootstrapped 95% Confidence Intervals (CIs). Graphical data representations were generated using the "dabestr". All analyses were performed using R version 4.0.2 (R Core Team, 2021).

RNA-Seq library preparation & sequencing

RNA was extracted from leaves using the Spectrum Plant Total RNA kit (Sigma). RNA quantification was performed with the Nanodrop and its quality was assessed using gel electrophoresis by loading 1 µL for each sample on a 2% agarose gel. Quantitect Reverse Transcription Kit (Qiagen) was used to both perform the DNase treatment and the cDNA synthesis. Three biological replicates for each pot and both treatments were adopted. Each replicate included a pool of healthy fully expanded leaves taken from all the plants in the pot.

RNA-Seq libraries were made using the IlluminaTruSeq RNA-seq protocol (Illumina, CA, USA). Briefly, the mRNA was purified using poly-T-oligonucleotides bounded with magnetic beads and divided into small pieces following protocol instructions. Retrotranscription was performed using blunt ending plus "A" at the end. IlluminaTruSeq indexes were used to ligate the ends of the cDNA fragments. Amplifications were performed to selectively enrich those cDNA fragments with adapters at pair-ends. Samples were analyzed in a singular Illumina flow cell of the Illumina HiSeq 2000 (75 bp reads).

Reads pre-processing and mapping

The quality assessment of reads obtained from both AM inoculated and non-inoculated samples were performed using the FastQC tool v0.11.8 (Andrews, 2010). No sequence trimming was performed given the high sequencing quality with a median per base sequence quality of 36 (Phred Score) and the absence of adapter sequences (Figure 1).

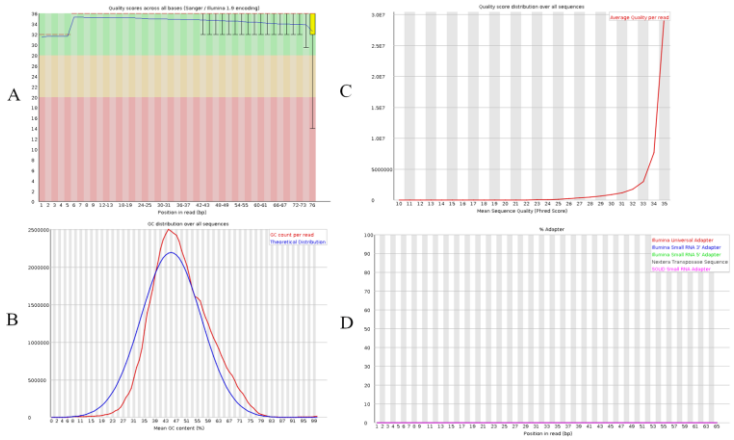

Figure 1. FastQC output. A) Boxplot of the phred-score for each position in all sequenced reads. B) GC content distribution. C) Read length distribution. D)Adapter content.

Reads were mapped to the newly released *Triticum turgidum* L. subsp. *durum* (Desf.) Husn. genome (Maccaferri et al., 2019) using STAR (Dobin et al., 2013) with default parameters and assigned to genomic features using featureCounts (Liao et al., 2014) with default parameters.

Differential expression analysis and annotation

Differentially expressed genes (DEGs) and long non-coding RNA (lncRNA) between treatments were obtained using the DESeq2 R package, using an adjusted p-value (padj) < 0.05 as threshold (Love et al., 2014). DEGs were annotated using the durum wheat genome annotation, the *Triticum aestivum* orthologues from the biomart plants database, and the online PANTHER functional classification (Thomas et al., 2003). DEGs were also assigned to specific metabolic pathways using the online functional annotator Mercator (Lohse et al., 2014) and visualized with MapMan (Thimm et al., 2004). Furthermore, differentially expressed (DE) lncRNA were annotated using the nhammer function of the online database RNAcentral (Williams et al., 2016).

GO enrichment and Co-expression network analysis

GO enrichment analysis was performed with PANTHER's overrepresentation test using the Fisher's exact test and a False Discovery Rate (FDR) threshold of 0.05, while KEGG analysis was conducted with g:Profiler (Raudvere et al., 2019). Enriched GO terms were then filtered with the REViGO tool (Supek et al., 2011) to reduce GO terms redundancy and visualized using R package ggplot2 (Wickham et al., 2007).

A Co-expression network analysis was performed by the CoExpNetViz tool (Tzfadia et al., 2016) using the 1st and 99th percentiles of the Pearson correlation coefficients distribution, as thresholds. Differentially expressed transcription factors (TFs) were used as bait genes while the entire set of DEGs was used as pool. The Network obtained was visualized and analyzed using Cytoscape (Shannon et al., 2003) using the network analyzer tool.

RNA-Seq analysis validation using qPCR

To validate the results from the RNAseq analyses, a set of five genes were randomly selected among DEGs (Table 1) and tested by qPCR, using the actin gene as reference (Kiarash et al. 2018). Primer 3.0 software (http://primer3.ut.ee/ (accessed on 16 October 2021), was utilized to design primer pair for each selected gene (Table 1). Total RNA was obtained from leaves of durum wheat plants belonging to an independent experiment performed following the same procedures described in "Plant material and experimental design" section. Reverse transcription was performed on 200 ng of total RNA extracted from AM- and AM+ samples, using iScript Reverse Transcription Supermix (Bio-Rad, Berkeley, CA,

USA), according to manufacturer's instructions. qPCR was performed as described in Puccio et al. (2022), starting from 20 ng of cDNA. Three biological and three technical replicates were analyzed for each sample (AM+ and AM-). Fragment amplification was verified by 1.5% w/v agarose gel electrophoresis and melting curve analysis. The relative expression ratio of each gene was calculated by the $2^{-\triangle\triangle CT}$ method (Livak and Schmittgen, 2001). Pearson correlation analysis between RNA-Seq and qPCR was also performed.

Table 1. List of randomly selected DEGs and primer pairs used in qPCR to validate the RNAseq result profiling.

Gene ID	Name	Primer	Sequence
TRITD7Av1G226260	*HKT*	F	TTCCATTGACTGCTCCCTCG
		R	TGTGTTCTGTGATGCCCCTC
TRITD4Bv1G187770	*LEA*	F	GGCGAGAAGAGTGAAGTTGTCA
		R	CGTAGCAGCACCCACCATAT
TRITD3Av1G286170	*MYB*	F	CTCCTTTGGAACGACGCCA
		R	AATCCGAGCAGCAGTAGTCC
TRITD6Bv1G164770	*NRT1*	F	TTCATGTACGTTGGGCAGCT
		R	GTAGTTCCCGAGCGAGATGG
TRITD7Bv1G180680	*NRT2.2*	F	AAAGGGGAGGGCTTCTGGAA
		R	CGCCACGTTCTCCATGATGA
GQ339780.1	*Actin*	F	CGTGTTGGATTCTGGTGATG
		R	AGCCACATATGCGAGCTTCT

4.3 Results

Effects of arbuscular mycorrhizal fungi on durum wheat plants grown under salinity stress

The mycorrhizal colonization of uninoculated plants was very negligible (always <1% of root length colonized), as expected. We detected typical structures of AMF in the inoculated plants (AM+) with levels of colonization >30%. AM plants showed higher aboveground and root biomass and total N uptake compared to the uninoculated (AM-) plants (+9.2%, +32.1%, and 21.5% respectively; Figure 2). Moreover, AM+ plants had a higher MSI value compared to the AM- plants (+12,5% on average).

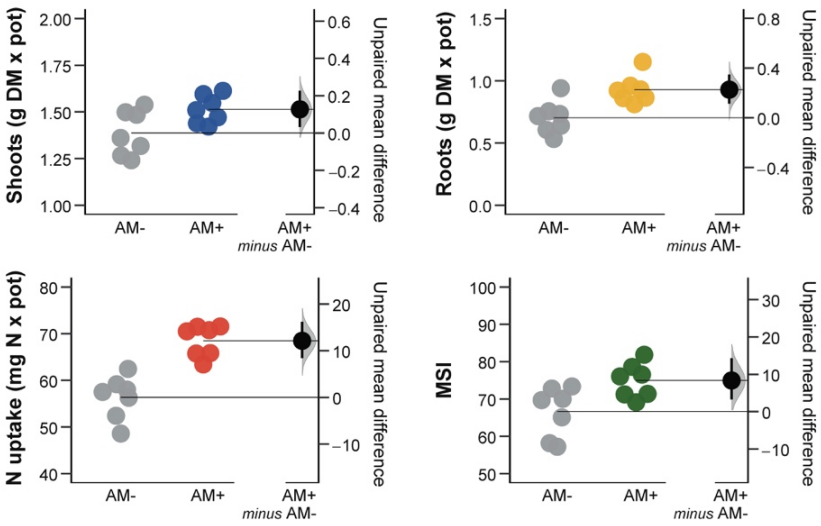

Figure 2. Shoot and root biomass in the above panels, and total N uptake and membrane stability index (MSI) in the below panels. Raw data of Control (AM-, grey dots) and arbuscular mycorrhizal treatment (AM+, coloured dots) are shown in the plot. The filled curve indicates the resampled distribution of unpaired mean difference, given the observed data. Horizontally aligned with the mean of the test group, unpaired mean difference is indicated by the black circle. The 95% confidence intervals are illustrated by the black vertical lines.

Differential gene expression analysis

RNA-Seq was performed on both Arbuscular Mycorrhizal fungi inoculated (AM+) and uninoculated durum wheat (cv. Anco Marzio) plants (AM-) grown under salt stress to identify key pathways involved in the AM induced salt tolerance in durum wheat.

A total of 311 million single-end reads were obtained from sequencing, with an average of 51 million reads per sample. Two hundred and seventy-eight million reads were mapped to the durum wheat genome with an average of 77% mapping reads per sample. Differential gene expression was assessed using DESeq2 to investigate the effect of AM inoculation under salt stress. Five hundred and sixty-three Differentially Expressed Genes (DEGs) were found between AM+ and AM- samples, of which 277 with a log2FC < -1 (downregulated by the AM inoculation) and 270 with a log2FC > 1 (upregulated by the AM inoculation) (Figure 3A and B). DEGs were identified on all the seven chromosomes of both sub-genomes A and B. DEGs chromosome abundance was correlated with chromosome length (Pearson correlation 0.83), while no significant differences were found between the two sub-genomes being 267 and 280 DEGs located on sub-genome A and B, respectively. The highest and lowest number of DEGs were found on chromosomes 3B (54) and 6A (21), respectively (Figure 3C).

LncRNA were also investigated by using the durum wheat genome ncRNA annotation. Five lncRNA were found DE between treatments, two resulted upregulated (STRG.778651, STRG.1311431) while three downregulated (STRG.234623, STRG.424631, STRG.1760891) by the AM inoculation.

Interestingly, all the DE lncRNA were located on the sub-genome B in chromosomes 1, 2, 3, 5, and 7 and were annotated using the RNAcentral sequence search tool.

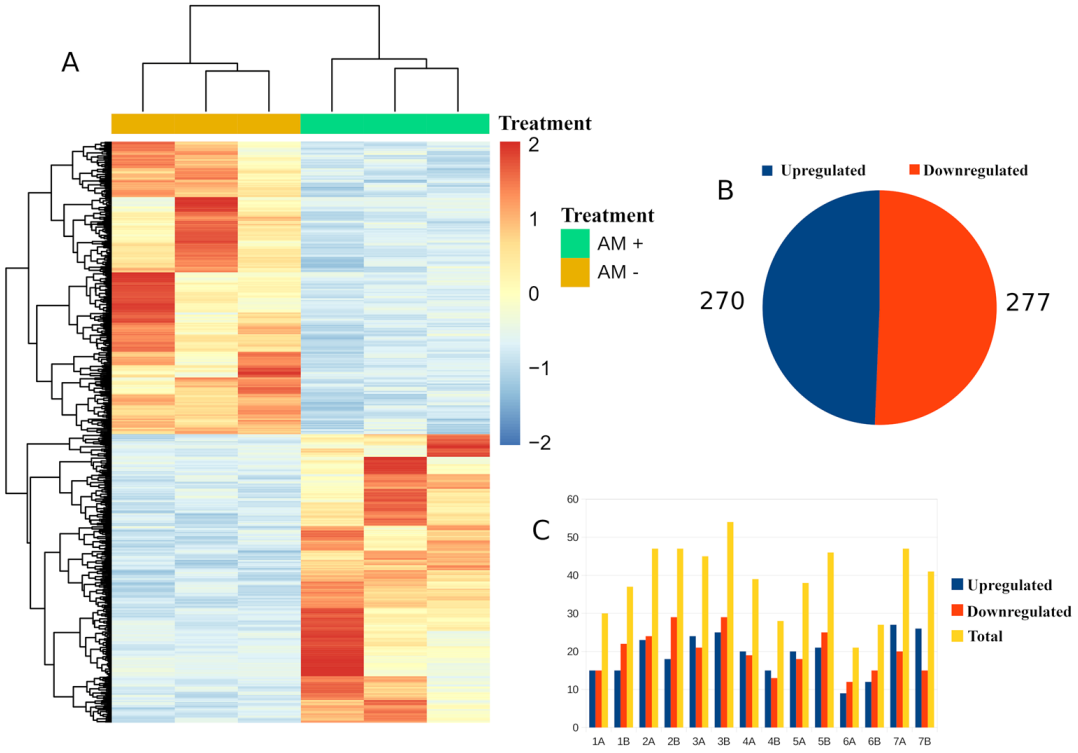

Figure 3 Overview of differential expression analysis performed with DESeq2. A Heatmap of the normalized expression levels of the 563 Differentially Expressed Genes (DEGs) between the AM+ and AM- conditions. B number of Differentially expressed genes in the two conditions. C Distribution of DEGs on the 7 chromosomes of the durum wheat genome.

Transcriptomic profile modification induced by AMF symbiosis

The analysis of DEGs between treatments revealed numerous genes involved in salt stress-related pathways like ion transport and binding, response to oxidative and abiotic stress, calcium signaling, and osmolytes accumulation. AM inoculation significantly increased the expression levels of many genes previously reported as related to AM-induced salt stress tolerance (Evelin et al., 2019). Concurrently a significant decrease in the expression of genes involved in the response to oxidative stress, GABA metabolism as well as ions and oligopeptides transport was observed (Table 2). In particular, two catalase (CAT), two Glutathione S-transferase (GST), and twelve Cytochrome P450 (CYP) genes, all belonging to the enzymatic antioxidative systems, were downregulated by the AM inoculation. Furthermore, several peroxidases (POX), also involved in the response to oxidative stress, were found DE (four upregulated and three downregulated).

Interestingly, AMF-induced modulation of genes involved in osmoregulation and osmolytes accumulation such as sugars, amino acids, and trehalose was also detected. The expression of three sugar efflux transporters (SWEET) and eight invertases (beta-fructofuranosidase) involved in the conversion of sucrose to fructose and glucose together with two ADP-glucose pyrophosphorylases and two polyamine oxidases (PAO) was significantly reduced in inoculated plants. At the same time, AM fungi inoculation significantly enhanced the expression of a trehalose-6-P synthase (TPS) and two trehalose-6-P phosphatases (TPP), both responsible for the biosynthesis of trehalose, while the trehalase (TRE), a trehalose degrading enzyme, was not found differentially expressed. Modulation of Transporters genes is a key process for regulating the accumulation and compartmentalization of both ions and solutes. Four amino acid transporters (ANT and LHT) (two up- and two down-regulated) and twelve lipid-transfer proteins (eight up- and four down-regulated) were found differentially expressed. AM fungi inoculation also enhanced the expression of a Tonoplast Intrinsic Protein (TIP) aquaporin while no plasma membrane aquaporin (PIP) was found differentially expressed.

Ten transporter genes, including two borate transporters (BOR) were upregulated in AM+ samples. By contrast, twenty-four transporters were significantly downregulated by the AM fungi inoculation. Many of these are involved in amino acids, oligopeptides, and sodium transport. Specifically, three anion transporters, two auxin transporters, (PIN, PILS), two sodium HKT, two ABC transporters, and two oligopeptide transporters (OPT).

Out of the 211 TdNPF characterized, 132 were expressed in leaves while only two NRT2 were detected. Of these, five NPF and one NRT2 gene involved in both low- and high-affinity nitrate transport were differentially expressed between treatments. Specifically, the TdNRT2.2 and three TdNPF5 were down-regulated while one TdNPF7 and one TdNPF8 gene were upregulated.

Genes involved in both calcium signaling and GABA were found downregulated by the AMF inoculation. Specifically, a GABA transaminase (GABA-T), a glutamate receptor, three calcium-dependent protein kinases, CIPK2, CIPK4, and CIPK21 as well as two glutamate decarboxylases (GAD), involved in GABA synthesis from glutamic acid. Calcium dependent transporters like Ca_2^+/cation exchanger (CCX) and Mitochondrial Ca_2^+ Uptake proteins (MICU) were dowregulated by the AMF inoculation while two P2B Ca_2^+ ATPase (ACA) were upregulated.

In addition, RAB GTPases, Late Embryogenesis Abundant (LEA) proteins, proline-rich proteins (PRP), and MAP kinases (MAP2K, MAP3K) were significantly upregulated in AM+ plants.

Transcription Factors modulated by AMF symbiosis

The expression profile of Transcription Factors (TFs) is a crucial step in RNA-Seq analysis. It allows to focus on the regulatory mechanism underlying the induction or repression of specific genes. Here thirty-six TFs were differentially expressed between treatments, 17 and 19 up- and down-regulated, respectively by the AM fungi inoculation (Figure 4A). Many of the TFs found upregulated were often involved in the response to abiotic and drought stress such as WRKY, Dehydration Responsive Element

Binding (DREB), Early Response to Dehydration 15 like (ERD15), and bHLH. Among the downregulated TFs, two MYB genes, MYB13 and MYB56, two NAC, and an Auxin Response Factor (ARF4) were identified.

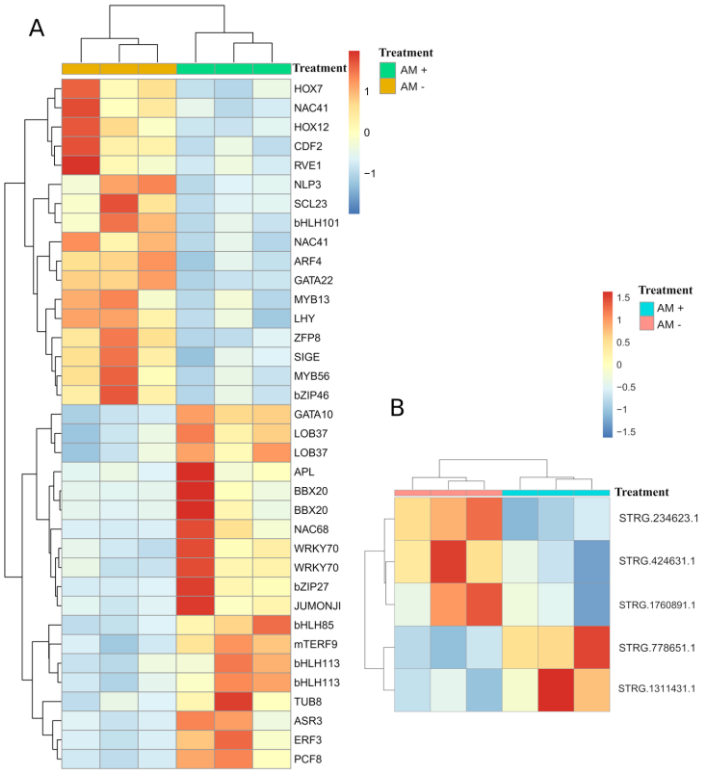

Figure 4 A) Expression patterns and hierarchical clustering of the 36 Transcription Factors identified comparing the AM+ (green) and AM- (yellow) conditions. B) Heatmap showing the lncRNA differentially expressed under salt stress in the AM+ (blue) and AM- (pink) conditions.

Table 2. Key genes involved in the response to salt stress found differentially expressed between AM+ and AM- samples. Log2 Fold Change (Log2FC), P-value, and Deseq2 adjusted P-value (Padj) are shown.

	Triticum durum Gene ID	Log2FC	P-value	Padj	Transcript description
Oxidoreduction	TRITD6Av1G007920	-2.2	3.9E-09	4.4E-06	Catalase
	TRITD6Bv1G012280	-2.1	9.3E-08	6.2E-05	Catalase
	TRITD3Av1G174080	-1.2	4.6E-05	7.4E-03	Glutathione S-transferase
	TRITD3Av1G263790	-1.7	6.2E-06	1.7E-03	Glutathione S-transferase
Osmoregulation	TRITD3Av1G171110	-1.7	1.1E-04	1.4E-02	Bidirectional sugar transporter SWEET
	TRITD3Bv1G149640	-1.6	7.7E-04	4.9E-02	Bidirectional sugar transporter SWEET
	TRITD7Bv1G019190	-2.1	4.0E-04	3.2E-02	Bidirectional sugar transporter SWEET
	TRITD1Bv1G219480	-2.1	1.3E-06	5.4E-04	Glucose-1-phosphate adenylyltransferase
	TRITD1Av1G222050	-2.2	2.0E-05	3.9E-03	Glucose-1-phosphate adenylyltransferase
	TRITD7Av1G204550	-2.8	3.9E-05	6.7E-03	Polyamine oxidase 1

	TRITD7Bv1G158080	-3.7	8.3E-09	8.2E-06	Polyamine oxidase
	TRITD4Bv1G194950	2.2	1.3E-05	2.8E-03	Aquaporin-like protein (TIP)
	TRITD3Av1G042320	-1.3	2.9E-04	2.6E-02	ABC transporter
	TRITD5Av1G221130	-1.5	4.2E-04	3.3E-02	ABC transporter
	TRITD6Bv1G179870	-1.3	1.5E-05	3.3E-03	Auxin efflux carrier component (PIN)
	TRITD5Bv1G152290	-2.5	1.3E-05	2.8E-03	Auxin efflux carrier family protein (PILS)
	TRITD5Av1G044900	1.4	1.0E-04	1.3E-02	Boron transporter
	TRITD5Bv1G042780	1.9	2.5E-04	2.3E-02	Boron transporter
Transporters	TRITD2Av1G215440	1.4	6.5E-04	4.4E-02	Mitochondrial Ca2+ Uptake protein (MICU)
	TRITD6Av1G057110	1	6.7E-04	4.5E-02	Calcium-transporting ATPase
	TRITD6Bv1G067420	1	4.7E-04	3.5E-02	Calcium-transporting ATPase
	TRITD2Av1G032000	-2.2	8.7E-07	3.9E-04	Cation calcium exchanger
	TRITD2Bv1G041270	-1.7	5.2E-05	7.9E-03	Cation calcium exchanger
	TRITD7Av1G226260	-1.2	4.5E-05	7.4E-03	HKT23 transporter
	TRITD7Bv1G172350	-1	6.8E-04	4.5E-02	HKT23 transporter
	TRITD1Bv1G205440	-1.7	2.1E-06	7.7E-04	Oligopeptide transporter
	TRITD1Bv1G205480	-1.6	9.3E-05	1.2E-02	Oligopeptide transporter
	TRITD2Av1G001860	-1.7	6.2E-05	9.0E-03	NPF transporter 8
	TRITD4Bv1G191460	-1.4	1.8E-05	3.7E-03	NPF transporter 5
NPF – NRT2	TRITD5Av1G243130	-1.8	1.7E-09	2.0E-06	NPF transporter 5
	TRITD6Bv1G164770	2.8	3.1E-04	2.7E-02	NPF transporter 7
	TRITD2Bv1G262700	1.1	1.0E-04	1.3E-02	NPF transporter 5
	TRITD7Bv1G180680	-1.9	1.6E-04	1.7E-02	NRT2.2
Glutamate metabolic pathway	TRITD2Av1G208370	1.6	6.6E-04	4.5E-02	Glutamate decarboxylase
	TRITD4Bv1G016030	0.9	6.2E-04	4.3E-02	Glutamate decarboxylase
	TRITD7Bv1G022320	-7.4	1.2E-07	7.4E-05	Glutamate receptor
Trehalose metabolic pathway	TRITD5Bv1G123710	2.8	7.0E-06	1.9E-03	Trehalose-6-phosphate synthase
	TRITD6Av1G158120	1.2	2.4E-04	2.3E-02	Trehalose 6-phosphate phosphatase
	TRITD6Bv1G144550	1.1	1.4E-04	1.5E-02	Trehalose 6-phosphate phosphatase
MAP Kinases	TRITD2Av1G270510	2	7.8E-06	2.0E-03	Protein kinase (MAP3K)
	TRITD6Bv1G202800	2.9	4.2E-06	1.3E-03	Protein kinase (MAPKK)
	TRITD2Av1G187690	1.2	5.5E-04	3.9E-02	Protein kinase (MAP3K)
Calcium signaling	TRITD5Bv1G079480	1.2	2.1E-04	2.1E-02	Calmodulin binding protein
	TRITD2Av1G044340	-1.6	3.4E-06	1.1E-03	CIPK21
	TRITD2Bv1G037460	-1.4	2.8E-07	1.4E-04	CIPK2
	TRITD5Bv1G024270	-2.8	1.5E-05	3.2E-03	CIPK4
Other	TRITD3Av1G219080	2.2	2.2E-04	2.2E-02	Early response to dehydration 15-like protein G
	TRITD3Bv1G211690	2.2	1.9E-04	2.0E-02	Early response to dehydration 15-like protein G
	TRITD7Bv1G038640	1.3	4.6E-04	3.5E-02	Late embryogenesis abundant protein

TRITD4Bv1G187750	1.5	8.4E-05	1.1E-02	Late embryogenesis abundant protein
TRITD4Bv1G187770	2.4	4.5E-10	7.7E-07	Late embryogenesis abundant protein
TRITD7Av1G099670	1.4	6.2E-05	9.0E-03	RAB GTPase
TRITD3Bv1G206370	1.3	5.1E-04	3.7E-02	RAB GTPase

Profile validation of DEGs via qPCR

RNA-seq results were validated by qPCR using a total of five randomly selected genes, two up- (LEA and NRT1), and three down-regulated (HKT, MYB, and NRT2.2), respectively. Their profiles were normalized to the expression of actin, used as a reference gene. The expression trend of selected genes in qPCR (Figure 5) was in agreement with the RNA-Seq expression levels. A Pearson's correlation analysis between RNA-seq and qPCR results showed high correlation and significance ($R=0.89$; $p < 0.0001$).

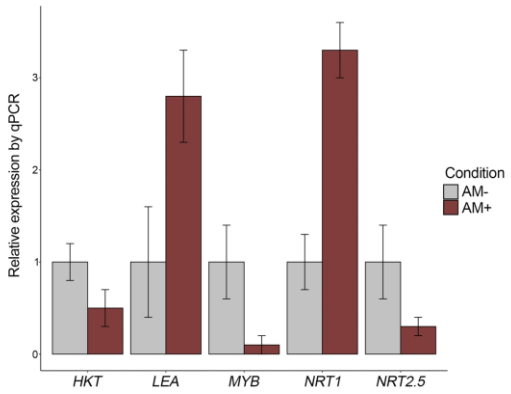

Figure 5 Expression levels of genes selected to validate RNAseq profiles

Gene Ontology (GO) and MapMan analysis

GO terms for each group, Biological Process (BP), Molecular Function (MF) and Cellular Component (CC), were assigned to all the 563 DEGs using PANTHER and an enrichment analysis was performed for both upregulated and downregulated genes.

In the BP category, no shared enriched GO terms were found between the two sets of DEGs (up- and down-regulated by the AMF inoculation). Many terms highly related to abiotic stress response such as "response to stress", "response to stimulus", "response to hydrogen peroxide", "oxidation−reduction process", "cell wall macromolecule catabolic process" and "lipid metabolic process" were found enriched in the downregulated genes set (Figure 6). By contrast, the upregulated genes were mainly enriched in the GO terms "macromolecule modification", "protein phosphorylation", "protein autoprocessing", "phosphorus metabolic process", "cellular macromolecule metabolic process" and "cell wall biogenesis"

In the MF category, only "molecular function" and "catalytic activity" terms were shared between the two sets of DEGs. In addition, the downregulated genes were enriched in "hydrolase activity" and

"oxidoreductase activity" terms, while three "purine binding" related terms, together with "ion binding", "anion binding" and "carbohydrate derivative binding" terms were found enriched in the upregulated genes.

Finally, in the CC category, the "protein−containing complex" term was enriched in both up- and down-regulated sets of DEGs being also the only term enriched in the downregulated set. In addition, other six terms were enriched in the upregulated genes set among which "cell wall", "cell periphery" and "external encapsulating structure" appeared the most representative.

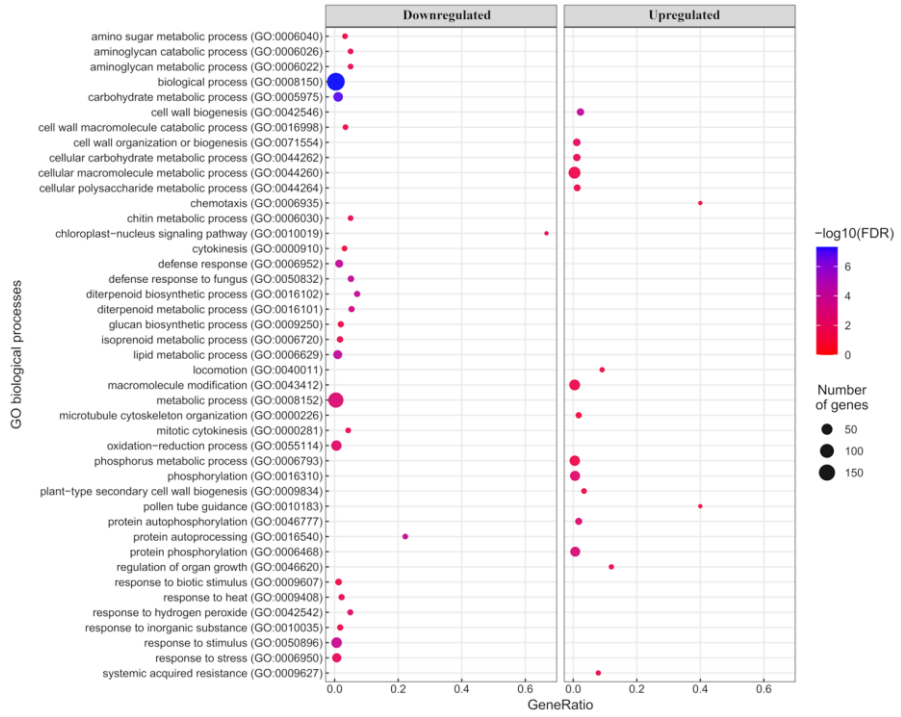

Figure 6 Biological Processes GO terms enrichment analysis for upregulated and downregulated genes. The dot plot shows enriched GO terms (FDR < 0.05) identified with PANTHER using the Fisher's exact test. The size of the dots represents the number of genes in each GO biological process while the GeneRatio (x-axis) is the ratio between the number of DEGs found and the number of genes in that category.

MapMan analysis highlighted the main metabolic pathways and functional groups involved in the response to salt stress in both treatments (Figure 7). Three hundred eighty-nine out of 563 DEGs were correctly assigned to known metabolic pathways. In detail, genes downregulated by AM inoculation were mainly involved in amino acids biosynthesis and degradation, lipid metabolism, redox homeostasis process, terpenoids biosynthesis, phytohormone transport and biosynthesis as well as carbohydrate metabolism. By contrast, genes induced in AM inoculated plants were mainly involved in RNA processing, vesicle trafficking, protein biosynthesis and cytoskeleton organization. Genes involved in solute transport, cell wall organization, RNA biosynthesis and external stimuli response were found in both up- and down-regulated genes sets.

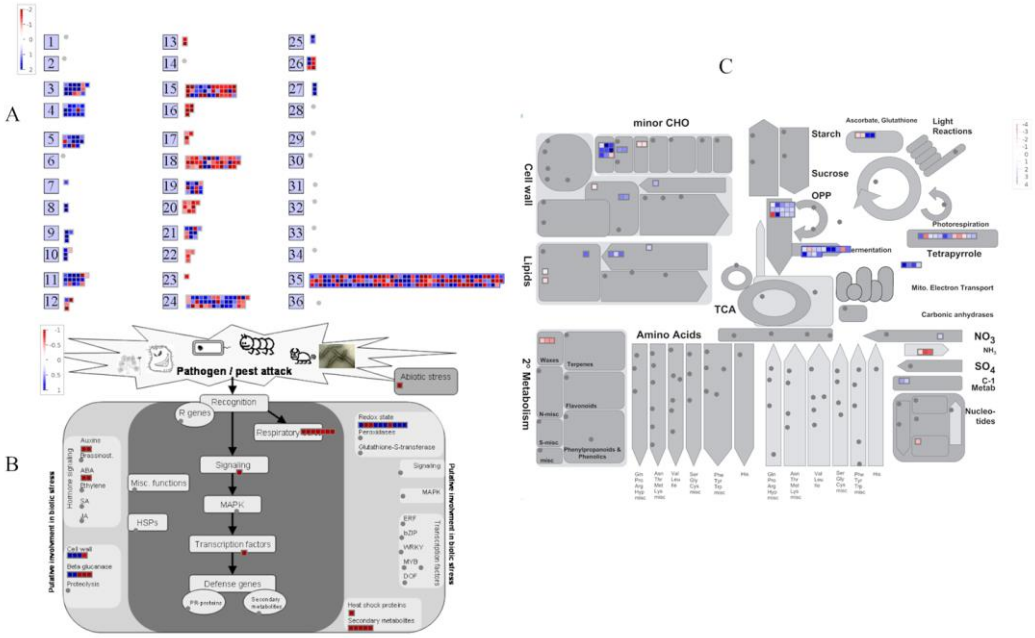

Figure 7 MapMan analysis graphical output. Each square represents a DEG while the color represents the log2FC (> 1 for AM-; < -1 for AM+). **A** An Overview of MapMan BINs. **B** Abiotic/Biotic stress response. **C** Metabolism overview.

Co-expression network analysis

The differentially expressed TFs panel was used for performing a co-expression network analysis to highlight specific interactions between TFs and putative target genes. Only the TFs with a sub-network of at least two genes were used for further analysis (six out of 36 were discarded). The network contains 206 co-expressed genes with a final set of 30 TFs defining a main sub-network complex that includes 122 genes and 11 TFs (4 and 7 up- and downregulated, respectively) and 8 smaller sub-networks (Figure 8). The main sub-network showed negative correlation between several TFs and their co-expressed genes, suggesting a TF repressive regulation. The zFP8 and GATA10 TFs showed the highest number of connections inside the main network (hub genes). More interestingly, many DEGs previously mentioned for their important role in the salt stress response were found co-expressed with some of the TFs utilized as baits. Both GATA TFs were linked to many of these genes such as one HKT, a PIN auxin transporter and a TPP gene. Both BBX20 like TFs were linked to the up-regulated ERDs and one TPP gene. zFP8 was connected with many OPTs, 5 Thaumatin-like proteins and the CIPK2 gene. Finally, an F-box (TRITD1Av1G225260) and a RING/U-box (TRITD4Av1G177780) genes, both involved in the ubiquitination process, were co-expressed with bZIP27.

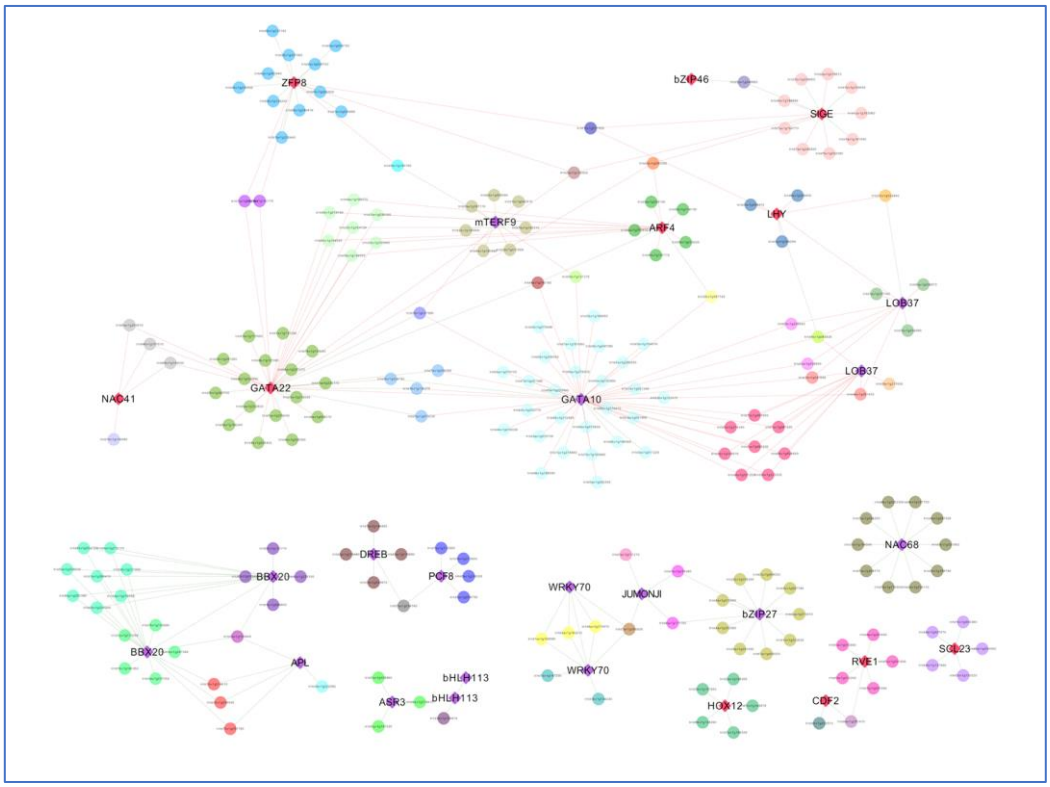

Figure 8 Co-expression network analyses of 30 Transcription Factors (TF) differentially expressed under salt stress as bait genes. The network was obtained with CoExpNetViz tool and visualized by Cytoscape. Bait TFs are represented as squared nodes. Colors represent downregulated TFs (red) and upregulated TFs (violet) while green and red lines denote positive correlation and negative correlation, respectively. Nine sub-networks are present, with the bigger one including 122 genes and 11 TFs.

4.4 Discussion

Soil salinity is a relevant abiotic stress that can drastically limit plant growth and development and crop yield. High salt concentration is known to induce osmotic and oxidative stress and nutrient deficiency. Indeed, salinity can alter cellular osmotic and ionic homeostasis through redox imbalances and the accumulation of toxic elements (i.e., Na+ and Cl–), photosynthesis, and the protein synthesis resulted inhibited and the cellular energy depleted.

Our data show that AM symbiosis can mitigate the negative effects of salt stress on plant growth. In particular, we found that AM symbiosis favored the acquisition of N, and the development of aboveground and root biomass under salt stress conditions, in agreement with previous findings, as reviewed by (Amagaya et al., 2020). Moreover, we detected a clear positive effect of AM symbiosis on the alleviation of the damaging effects of salinity on the stability of plasma membranes. Therefore, our data suggested that AMF symbiosis reduces the need to activate mechanisms of plant response to salt

stress. Thus, the AM+ plants appeared subjected to a lower level of stress caused by salinity compared to AM- plants.

Several studies underlined the ability of AMF symbiosis to enhance plant salt tolerance by genes transcription modulation in both root and shoot under different experimental conditions (Ruiz-Lozano et al., 2012; Porcel et al., 2016; Evelin et al., 2019). The protective effect of AM fungi under stress such as salinity, drought, and heat were already reported on both durum and bread wheat (Beltrano et al., 2008; Talaat et al., 2014; Cabral et al., 2016). Here, we described for the first time the differential gene expression profile of durum wheat leaves under salt stress with and without AM fungal inoculum. In the present study, RNA-Seq data were analyzed to describe the molecular mechanisms underlying the salt tolerance induced by AMF inoculum in durum wheat (Fileccia et al., 2017). Differentially expressed genes between treatments revealed important insights into the role of AM symbiosis in the plant response to salt stress.

High levels of salt in soil induce ROS formation and accumulation in both roots and shoot tissues resulting in oxidative damage of various cellular components. Plants react to ROS formation with both an enzymatic and non-enzymatic antioxidative system (Ahmad et al., 2010). The enzymatic system consists of superoxide dismutase (SOD), catalase (CAT), glutathione reductase, and S-transferases (GR, GST), as well as peroxidase (POX), while the non-enzymatic system involves the synthesis of antioxidant molecules such as ascorbate, carotenoids, and glutathione to aid counteract toxicity derived from ROS accumulation (Gill et al., 2010). In the present study, we found a higher number of enzymes involved in redox reactions such as CATs, CYPs, and GSTs significantly downregulated by AM inoculation. CATs are involved in the enzymatic response to ROS (Gondim et al., 2012), GSTs reduce oxidative stress by affecting glutathione pools (Qi et al., 2010; Chen et al., 2012), while CYP genes are known to provide tolerance to salinity and other abiotic stresses by influencing ROS scavenging and ABA levels (Pandian et al., 2020).

Nitrogenous compounds have been suggested to contribute to osmoprotective processes and mitigate oxidative stress by scavenging reactive oxygen species (Mansour, 2000). Here three NPF transporters and one NRT2 transporter were downregulated by the AM inoculation. This seems to confirm the ameliorating effect of the inoculation. Interestingly a recent study on *Solanum lycopersicum* under both drought and salt stress highlighted the upregulation of NRT2 genes under both stress conditions (Akbudak et al., 2022) while ectomycorrhizal fungi were shown to decrease the transcript levels of NRT2.1 in poplar (Sa et al., 2019). The inoculated plants, in fact, have an improved ability to intercept the element, as highlighted by the total N-uptake results. This may result in reduced expression of high-affinity transporters in leaves thanks to higher nitrate levels in the xylem. Interestingly, only two NRT2 were expressed (sufficiently for RNA-Seq detection), in the leaves, in agreement with many studies in *Arabidopsis*, tomato, and rapeseed that showed their main expression in roots (Orsel et al., 2002; Hildebrandt et al., 2002; Tong et al., 2020). This suggests that the expansion of the NRT2 gene family

did not translate into the alteration of its expression patterns and regulation, maintaining their main role in root uptake and translocation.

Furthermore, two HKT genes involved in the Na^+ transport from the photosynthetic tissues to the roots and Na^+ removal from the xylem appeared downregulated in the AM+ samples, in contrast with previous findings in which the AM symbiosis determined their upregulation (Porcel et al., 2016). The HKTs down-regulation may suggest a lower ionic imbalance in the AM inoculated plants in agreement with Estrada et al. (2013) which measured a higher K^+/Na^+ ratio in AM+ samples as well as a higher state of oxidative stress in AM- samples. This oxidative stress condition may be caused by less efficient water and ionic homeostasis also highlighted by many GO terms found enriched in downregulated genes such as "oxidation−reduction process" and "response to stress". The reduction of plant defense responses to salt stress in the oxidation-reduction reactions observed in the shoot of AM inoculated samples could be attributable to their healthier status compared to the non-inoculated samples.

To counter water potential, decrease due to soil salinity and high Na^+ and Cl^- levels, plants accumulate osmolytes such as proline, betaine, polyamines, sugars, organic acids, amino acids, and trehalose (Evelin et al., 2019), helping water flow from the soil into roots and then to leaves. Higher osmotic potential in AM inoculated compared to non-inoculated plants has been already reported (Navarro et al., 2014). In this study, we detected a high number of Proline-Rich Proteins (PRPs) up-regulated by the AMF inoculation that could be involved in the cell wall stress-induced fortification as confirmed by six cell wall-related GO terms enriched in the upregulated genes, including "cell wall biogenesis" and "cell wall organization". Proline is indeed an important osmoprotectant, accumulated under salt stress as free proline or in PRPs, especially in cell walls (Ueda et al., 2007; Stein et al., 2011). Trehalose is a non-reducing storage disaccharide that may serve as a source of energy and carbon but is also reported to be involved in both ROS scavenging and K+/Na+ ratio maintenance (Redillas et al., 2012). Garg and Pandey (Garg and Pandey, 2016) reported higher levels of trehalose in a legume crop under salt stress. In this study, a trehalose-6-P synthase (TPS) and two trehalose-6-P phosphatases (TPP), involved in the trehalose synthesis, resulted strongly upregulated by the AM inoculation.

Moreover, several genes involved in polyamines and carbohydrates metabolisms resulted downregulated by AM inoculum and in agreement, the GO term "carbohydrate metabolic process" was highly enriched in the downregulated genes set. Polyamines are reported to act as important regulators of cellular ROS homeostasis (Saha et al., 2015), while the accumulation of soluble carbohydrates was detected in the leaves of salt-treated Sorghum bicolor plants (de Lacerda et al., 2005).

Changes in cytosolic free Ca_2^+ concentration are known to be involved in message transduction and response to several external stimuli, biotic and abiotic stresses (Xiang et al., 2007; Batistič et al., 2012). During drought and salt stress, a high number of calcium-related genes involved in the $Ca2^+$ signaling pathway are induced. Here, a calmodulin-binding protein and two P2B Ca_2^+ATPase, both responsible for the active Ca_2^+ transport and homeostasis, were upregulated by AM inoculation, interestingly they were previously reported as involved in salt stress response in moss, soybean, and rice plants (Chung

et al., 2000; Qudeimat et al., 2008; Huda et al., 2013; Sun et al., 2016). Moreover, three MAPKs, which are involved in different signaling cascades including Ca_2^+, resulted also upregulated in the AM+ plants. The AM inoculation downregulated three CIPKs and two Ca_2^+/cation exchangers (CCX). Interestingly, CIPKs are known to be involved in Ca_2^+ signal transduction in abiotic stress responses in many crops (Sánchez-Barrena et al., 2005; Xiang et al., 2007; Hu et al., 2016), by contrast, the role of CCXs is still scarcely characterized. They localize to the vacuolar or plasma membrane and could be involved in Na^+/K^+ exchange and stress response having been found highly upregulated during both salt and drought stress in Arabidopsis, rice, and tomato, but until now, limited knowledge on their regulation and specific functions is available (Singh et al., 2014; Corso et al., 2018; Amagaya et al., 2020).

The aquaporins form a large protein family with a pivotal role in plant water use efficiency (WUE) and in water transport. A complex transcriptional pattern of aquaporins under salt stress has been described in several crops (Ouziad et al., 2006; Aroca et al., 2007; Jahromi et al., 2008). Both Tonoplastic Intrinsic Proteins (TIPs) and Protoplastic Intrinsic Proteins (PIPs), involved in the intracellular and transcellular water transport, respectively, were previously found to be modulated under salt stress by the AMF both in roots and leaves (Chen et al., 2017). Here, we identified a TIP gene upregulated by the AM fungi.

GABA is a non-protein amino acid known to cumulate in plants when subjected to different stresses (Kinnersley et al., 2000). Both GABA and glutamate metabolism and catabolism were reported to play a key role in the response to salt stress by controlling ROS accumulation and regulating redox balance (Wu et al., 2020). Indeed, genes involved in GABA biosynthesis were found to be induced during salt stress in Arabidopsis (Singh et al., 2017). Interestingly, we detected the AM-induced downregulation of two glutamate or Glutamic Acid Decarboxylase (GAD) enzymes involved in the synthesis of GABA from L-glutamate and of a GABA-T involved in the conversion of GABA to succinic semialdehyde (SSA), both reported to be induced by salt stress in Arabidopsis and maize (Renault et al., 2010; Wang et al., 2017) suggesting a lower state of ionic imbalance in the AM inoculated samples.

Many transcription factors belonging to DREB, NAC, MYB, bHLH, bZIP, ERF, BBX, and WRKY families have been reported to play a significant role in abiotic stress plant responses (Lindemose et al., 2013; Golldack et al., 2014). In this work, we identified 17 different transcription factors upregulated by the AM fungi inoculum among which two WRKY70 homologs, a DREB, a NAC68 homolog, and two bHLH. WRKY and DREB TFs are involved in abiotic but also biotic stress responses (Khan, 2011; Zhao et al., 2017). The transgenic expression of WRKY and DREB members from cotton and wheat were able to enhance abiotic and biotic stress responses in Arabidopsis and Nicotiana benthamiana (Huang et al., 2009; Shi et al., 2014; Qin et al., 2015), as well as the overexpression of SNAC1 and SNAC2 improved drought and salt stress tolerance in rice (Hu et al., 2006). In wheat, the overexpression of both NAC29 and bZIP15 has been recently reported to enhance salt stress response by reducing H_2O_2 accumulation (Xu et al., 2015; Bi et al., 2021). Furthermore, two BBX20 TFs were significantly upregulated by the AM inoculation in our experiment, in agreement with the higher expression of members of this family previously reported in several plants and more recently in Petunia under salt

and heat stress (Gangappa et al., 2014; Wen et al., 2020). MYB13 and MYB56 were identified among the downregulated TFs, and both members were reported to induce drought, salt, and cold stress tolerance in transgenic Arabidopsis plants by activating genes involved in the antioxidant system, allowing lower ROS accumulation (Zhang et al., 2012; Huang et al., 2018). The downregulation of these TFs in AM inoculated plants may, once again, suggest a lower oxidative stress level in these samples.

Interestingly, RAB-A, LEA, and ERD genes were identified in the upregulated DEGs induced by the AM inoculation. These are important stress response elements often highly expressed under several abiotic stresses. RAB-A GTPases are involved in membrane trafficking, and signal transduction and have been involved in the salt stress tolerance (Rehman et al., 2014; Khassanova et al., 2019). Members belonging to the LEA family enhanced salt and dehydration stress tolerance when overexpressed in transgenic plants such as tobacco, potato, and Arabidopsis (Kim et al., 2005; Brini et al., 2007; Muvunyi et al., 2018). LEA proteins have been reported to act as a molecular shield during abiotic stresses avoiding protein aggregation and preventing enzyme degradation (Chakrabortee et al., 2012).

Finally, long noncoding RNAs (lncRNAs) have been found frequently induced during abiotic stress responses in several plants (Qin et al., 2017; Deng et al., 2018; Zhang et al., 2019). Here we detected two lncRNAs up-regulated and three down-regulated by the AM inoculation under salt stress. Interestingly, the ortholog to a drought-responsive lncRNA (URS0000781584) identified in maize by Zhang et al. (2014) was, here, down-regulated.

The presence of GO terms such as “response to hydrogen peroxide” and “response to stress” and many other stress-related GO terms found enriched in downregulated genes, together with the presence of a stress-responsive lncRNA, the higher number of oxidoreduction, GABA, and transport-related genes in non-inoculated plants seems to suggest a higher oxidative stress condition induced by soil salinity and a reduced water absorption ability.

These findings are in agreement with the results obtained on durum wheat by Fileccia et al. (2017) and by Talaat and Shawky (2014) on bread wheat, supporting the hypothesis of lower salt stress levels in the AMF inoculated plants.

4.5 Conclusions

Using RNA-Seq, we analyzed the effects of mycorrhizal inoculation on durum wheat under salt stress observing a lower number of stress-related genes modulated by soil salinity in Arbuscular Mycorrhizae inoculated compared to non-inoculated samples. DEGs functional categories included the defensive genes against redox state (i.e., cytochrome P450, glutathione S-transferase, catalases) and genes involved in osmoregulation, osmolytes and ions transport. This work allowed us to define the pipelines and methods for RNA-Seq analysis on durum wheat, highlight key genes putatively involved in AMF-induced salt stress tolerance, and identify nitrate transporters expressed in durum wheat leaves and

putatively involved in stress response. Further studies will be necessary to narrow down the genes set here identified to isolate candidate major genes involved in AMF-mediated salt tolerance for further functional analyses. The adoption of different AMF species, salt concentrations, and times of exposure to stress may help to improve our knowledge on the interaction between plants and AMF.

Chapter 5: Transcriptome changes in response to variable N supply in four durum wheat genotypes with contrasting NUE

5.1 Introduction

Nitrogen (N), in particular nitrate (NO_3^-), is one of the most important nutrient components for plant growth, among the inorganic elements. Soil NO_3^- availability significantly impacts on plant establishment, yield, and quality. Nitrogen is acquired by plants *via* active uptake by nitrate transporters, which form large families including members of different functions (Dechorgnat et al., 2011).

In aerobic soil, NO_3^- is the main available source of N and its uptake by plant roots occurs mainly by and active mechanism through two systems: the Low Affinity Transport System (LATS) and the High Affinity Transport System (HATS). Both systems are further composed by constitutive (cHATS, cLATS) and nitrate-inducible components (iHATS, iLATS). Both systems are well known and described in *Arabidopsis*, but still limited details are available on the regulation of both systems in other plant species. The NPF family nitrate transporters showed a low nitrate affinity, mainly operating at high nitrate concentration, despite several dual-affinity transporters were also found such as *AtNPF6.3* (*Arabidopsis*), *OsNPF6.5* (rice) and *ZmNPF6.6* (maize) that are also able to operate at low N as high-affinity transporters (Liu et al., 2003; Morere-Le Paven et al., 2011; Bagchi et al., 2012; Hu et al., 2015). The expression patterns of these genes might greatly vary based on different N conditions and among species (Miller et al., 2007). In maize, both high affinity transporters NRT2.1 and 2.2 were inhibited by high nitrate concentrations and induced by low concentrations (Yu et al., 2014).

Nitrogen Use Efficiency (NUE) in plants included two components, Nitrogen Uptake Efficiency (NUpE) and Nitrogen Utilization Efficiency (NUtE), both characterized by high genetic differences as highlighted in several crop species (Muchow et al., 1998; Wang et al., 2014; Han et al., 2015; Hu et al., 2015; Stahl et al., 2019;). A deeper understanding on the genetic variability for N uptake, assimilation and remobilization should help the screening for high NUE genotypes, the breeding process by molecular assisted selection (MAS) and the utilization of candidate genes for genetic engineering. Comparative transcriptomics on genotypes with contrasting NUE has become frequent in plants for identifying candidate genes and metabolic pathways related to the complex trait (Hao et al., 2011; Zamboni et al., 2014; Quan et al., 2016; Wang et al., 2021; Zhang et al., 2021, Mauceri et al., 2021; 2022). Many of these studies were performed in low N conditions and in different tissues among which the root for identifying pathways involved in N uptake and genes related plant adaptation to low N. However, the mechanisms regulating NUE in both wheat species need to be further investigated.

A higher NUE genotype could derive from different physiological and molecular processes involved in the complex traits, such as N uptake from soil, nitrate assimilation, nitrate remobilization from roots to shoots/leaves or from leaves to seeds (Loussaert et al., 2018; Chen et al., 2020). Thus, the breakdown of each NUE component could provide a more precise tool to identify pathways and genes determining NUE differences.

Durum wheat is a relevant cereal crop for many Mediterranean countries, due to its employment in pasta, cuscus and bulgur making. In these regions, including southern Europe and northern Africa, low rainfall and critical problems such as drought, salinity and low organic matter, restricts the ability of crops to cope with N-limiting availability (Ryan et al., 2009). Genotypic differences in the N-use efficiency (both NUpE and NUtE) have been reported among durum wheat cultivars (Giambalvo et al., 2010; Ierna et al., 2016; Lupini et al., 2021).

In this study, transcriptomic changes in response to low and high nitrate supply in four durum wheat NUE-contrasting genotypes using an RNA-sequencing approach were investigated. The analysis on both root and shoot allowed us to identify the main genes and pathways involved in nitrate uptake, assimilation and remobilization. Using a weighted gene co-expression network analysis (WGCNA), we were able to cluster genes into co-expression modules and to characterize potential gene expression regulators (hub-genes), which may act as key regulators in response to nitrate. Furthermore, using the previously performed characterization of TdNPF and TdNRT2 gene families we were able to detect key nitrate transporters differentially expressed.

5.2 Materials and methods

Plant material and growth conditions

Seeds of four durum wheat genotypes (Senatore Cappelli, Orizzonte, Appio, and Antalis) were surface sterilized with sodium hypochlorite (0.5%, vol/vol) for 20 minutes, rinsed thoroughly in sterile water, and vernalized at 4 °C for two weeks.

After seed germination, seedlings were grown with lighting for 14 hours a day at 25 °C, 65% relative humidity, and a photoperiod of 14 h with 350 µmol m^2 s^{-1} light intensity in net pots containing six plants each.

After 7 days, seedlings selected by uniform size were transferred to hydroponic tanks (5 L, twelve seedlings for tank) filled with a first universal hydroponic growth solution.

The first hydroponic growth system was a nutrient solution containing 1.25 mM $Ca(NO_3)_2 * 4H_2O$, 0.75 mM K_2SO_4, 0.1 mM KH_2PO_4, 2 mM KCl, 0.65 mM $MgSO_4$ * 7H2O, 1.25 mM $CaSO_4$ * $2H_2O$ (to equalize ionic composition among each media application downstream) and 10 µM H_3BO_4, 1 µM $MnSO_4$, 1 µM $ZnSO_4$, 5 µM $CuSO_4$, 0.05 µM $[(NH_4)_6Mo_7]2{\cdot}4H_2O$, and 100 µM EDTA-Fe(III).

After 7 days, the hydroponically-grown seedlings were firstly deprived and starved from nitrogen (T0) for 7 days with the same nutrient solution without $Ca(NO_3)_2$ balanced by 2.5 mM $CaSO_4$.

Afterwards, seedlings were subjected to two nitrate concentrations (low and high). The low and high nitrate solutions were determined by adding 0.025 mM $Ca(NO_3)_2 * 4H_2O$ and 2.475 mM $CaSO_4 * 2H_2O$ and 2.5 mM $Ca(NO_3)_2 * 4H_2O$ and 0 mM $CaSO_4 * 2H_2O$ to the T0 solution. The nutrient solution was renewed every three days and pH was maintained at 6.0 with 0.1N H_2SO_4.

Root and shoot were harvested after at (T0) (14 days old), after 8 (T1) and 96 (T2) hours from low and high nitrate exposure (18 days old) collecting 120 samples (three independent biological replicates for each sample), immediately frozen in liquid nitrogen and stored at −80 °C for RNA extractions.

RNA extraction and illumine library preparation

Total RNA was isolated using a NucleoSpin RNA Plant (Macherey-Nagel GmbH & Co., KG, 52355 Düren, Germany) minikit for RNA extraction and treated with RNase-free DNase. Three biological replicates for each time point and treatment were used. RNA quality was assessed using an Agilent Bioanalyzer RNA nanochip (Agilent, Wilmington, DE, USA), and the Qubit using the RNA High Sensitivity (Thermo Fisher). All the RNA samples showed an RNA integrity number (RIN) > 8.0.

Sequence libraries were prepared using the Illumina Stranded mRNA library prep (Illumina, San Diego, CA, USA), according to the manufacturer's instructions. Both quality and insert size distribution were assessed using an Agilent Bioanalyzer DNA 1000 chip (Figure 1). All libraries harbor an average insert size of 340 bp and a concentration between 20 and 100 ng/ul. Sequence libraries were pooled in equimolar concentration and analyzed on Illumina Novaseq 6000 with a S4 flowcell generating 2 × 150 bp paired-end (PE) reads.

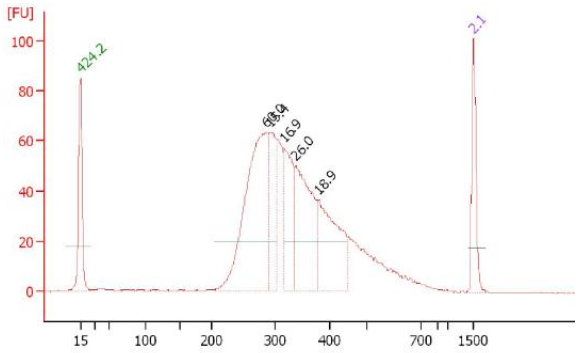

Figure 1 Agilent Bioanalyzer output for one library. Base pairs are on the x-axis while the absorbance is on the y-axis.

Quality check, reads trimming, and mapping

Raw reads from each sample were assessed for quality using the FastQC tool v0.11.8 (Andrews et al., 2010). Adapters were removed and the quality trimming was performed using Trimmomatic v0.38 (Bolger et al., 2014) using the parameters: LEADING:3 TRAILING:3 (removal of low-quality bases with Phred score < 3 from the beginning and end of a read) SLIDINGWINDOW:4:20 (removal of windows with Phred score < 20 in a 4 bp sliding window). Reads were filtered by length and only those longer than 36 bp were selected.

Reads were mapped to the *Triticum turgidum* L. *ssp. durum* reference genome (Maccaferri et al., 2019) using STAR (Dobin et al., 2013) with default parameters and assigned to genomic features using featureCounts (Liao et al., 2014) with default parameters.

Differentially expressed genes identification

Deseq2 (Love et al., 2014) R package was used for the raw counts normalization from feature counts, and the identification of Differentially Expressed Genes (DEGs). Before normalization, all genes with less than 10 reads in at least 6 samples were removed from the analysis, to ensure that only significantly represented genes are used. Normalization was performed using Deseq2 size factor normalization and then transformed using the variant stabilizing transform (VST). Pairwise comparisons were performed for each genotype using T0 as reference and among genotypes for each treatment. These comparisons allowed us to detect all the DEGs up- and down-regulated from T0 to T2 in each genotype for each treatment showing a significant difference between genotypes. An adjusted (Benjamini and Hochberg correction) p-value (Padj) < 0.001 was used as threshold. Principal Component Analysis (PCA) and sample-to-sample distance were also evaluated using Deseq2, while all heatmaps were drawn using Pheatmap (Kolde et al., 2015).

Weighted gene co-expression analysis, clustering, and GO enrichment

RNA-sequencing dataset was analyzed through a network biology approach to study their differential response to low and high nitrate supply by performing two independent analyses for root and shoot.

The weighted gene co-expression network analysis was performed using the WGCNA package (Langfelder et al., 2008). Briefly, the variance stabilized data of all the genes at least differentially expressed in one comparison were firstly used for the soft threshold selection using the scale-free topology criterion selecting a threshold of 7 and 9 for root and shoot analyses, respectively (Figure 2).

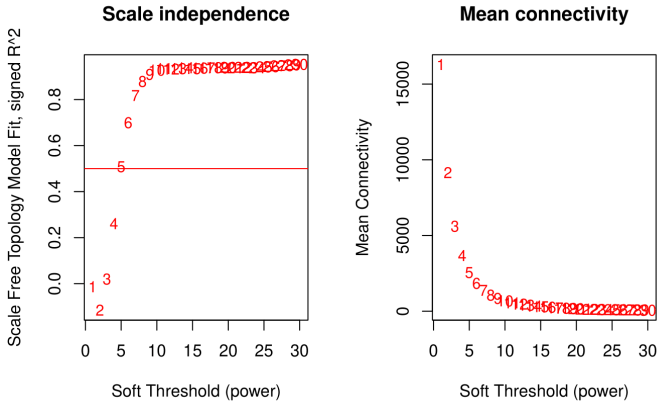

Figure 2 Scale-free topology index and mean connectivity for the shoot tissue.

The similarity matrices evaluated from expression data using Pearson correlation coefficients were transformed into adjacency matrices using a power function with the soft threshold as exponent. Connection strengths were transformed into a Topological Overlap Matrix (TOM). Finally, the TOM was used for a hierarchical clustering to produce the genes dendrogram. The branch cutting algorithm Dynamic Tree Cut was used to obtain the co-expression modules from both datasets. Modules including genes with similar expression profiles were further merged using the correlation coefficients between the eigengenes (the first principal component of the expression matrix) evaluated from each module using a threshold of 0.25. To visualize and analyze the network of each module the data were exported to Cytoscape (Shannon et al., 2003) using the exportNetworkToCytoscape function with an adjacency cutoff of 0.2. Furthermore, the clusterProfiler package (Yu et al., 2012) was used for the supervised clustering of NPF and NRT2 genes.

All the GO terms for each gene were obtained using the BioMart tool on the Ensembl plants database. The enrichment for each genes subset, and co-expression module was performed with ShinyGO (Ge et al., 2020) using the Fisher's exact test and a False Discovery Rate (FDR) threshold of 0.05.

5.3 Results

RNA-sequencing of durum wheat genotypes in response to nitrate treatments

To study the global transcriptomic changes to low and high nitrate availability of the four NUE-contrasting genotypes, RNA sequencing was performed on 120 different samples (4 genotypes, 2 tissues, 3 time-points, 2 N-treatments, 3 biological replicates). Overall, 10.25 billion raw paired-end reads were generated with an average of 83 million reads per sample. Read quality was fairly high with an average Phred score 36 per sample, removing only 0.5% average reads in the trimming phase. Clean reads were then mapped to the reference genome of *Triticum turgidum* L. subsp. d*urum* (Maccaferri et al., 2019) and assigned to genomic features with an average unique reads mapping of 85% and 75% of correctly assigned reads. Raw counts were extracted and fed to DESeq2 for differential expression identification.

Differentially Expressed Genes (DEGs) identification

Two independent analyses were performed for root and shoot. The count matrix was first pre-filtered to remove low count genes (at least 20 reads in at least 6 samples). Read counts were then normalized to allow between-sample comparisons and transformed using VST. A Principal Component Analysis was performed to assess variability among the samples (Figure 3). Biological replicates consistency was assessed using both the PCA and hierarchical clustering of the distance matrix. The analyses in both tissues showed a low inter-replicate variability, with the three biological replicates always clustering together. The PCA also highlighted a higher variability among treatments and time-points in root, compared to shoot. All the genotypes clustered along the x-axis (PC1) and all treatments clustered along

the y-axis (PC2). Furthermore, the effect of the two different N concentrations was lower than time sampling, with HN and LN treatments that clustered closely for each genotype.

Figure 3. Principal Component Analysis from root (left) and shoot (right). Biological replicates for each treatment clustered. Colors were used to highlight genotypes (orange: Antalis, green: Appio, blue: Cappelli, and pink: Orizzonte) and different shades of each color were used to highlight time sampling and N-treatments. On the x-axis and y-axis, the PC1 and PC2, respectively with the percentage of variance explained.

To identify Differentially Expressed Genes (DEGs), we performed pairwise comparisons between genotypes (inside each treatment and time sampling) and in a time course design inside each genotype (between T0 and all other treatments and time-points). We detected a total of 40 and 34 thousand DEGs, at least in one comparison, for root and shoot, respectively, representing 60% and 51% of all the durum wheat annotated genes. Venn diagrams were used to highlight the differences among genotypes in the time-course in both root and shoot (Figure 4). Interestingly, Cappelli and Appio shared a high number (8435) of DEGs in root, almost 21% of the total. The number of common DEGs between genotypes in root (7516, 18.5%) was lower compared to the shoot (11740, 34.5%), highlighting a much more complex genes regulation in root, as expected.

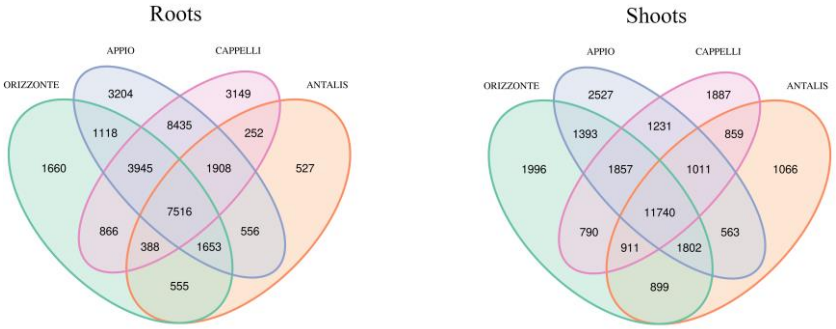

Figure 4. Venn diagrams showed overlap of Differentially Expressed Genes (DEGs) among genotypes identified in root (left) and shoot (right).

Weighted gene co-expression network analysis and module detection

The Weighted Gene Co-expression Network Analysis (WGCNA) is an unsupervised systematic biological method applied to the study of biological processes as effective for identifying co-expression modules (including many genes) with high biological significance for the trait under study. The high number of genes in the durum wheat genome (66 thousand) and genes involved in the response to N (estimated between 30% and 50% of total annotated genes) make the genes clustering crucial for grasping functional information on plant response to different N supply. Here, we used the WGCNA algorithm to cluster DEGs into co-expressed modules and to get insights on the differential behavior of the four genotypes in response to nitrate treatments. Two separate analyses were performed for root and shoot. After the hierarchical clustering based on TOM and the merging step, we identified a total of 28 and 21 modules in root and shoot, respectively (Figure 5).

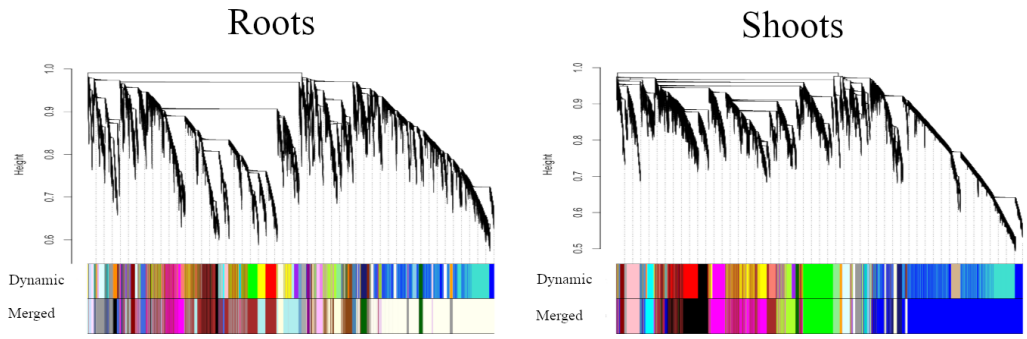

Figure 5 Modules detection by the WGCNA algorithm for root (left) and shoot (right). First, the Dynamic Tree Cut algorithm defines the modules dendrogram. Then, the eigengene of each module are used to evaluate module correlation for the merging step (second row of colors).

The number of genes for each module ranged from 102 to 11,112, with an average of 1,436. Eigengenes (the first Principal Component of each module) were evaluated for each module to summarize the module expression profile. These were used to evaluate the Pearson correlation coefficient between each module eigengene and N-treatment/time sampling for each tissue (Figure 6).

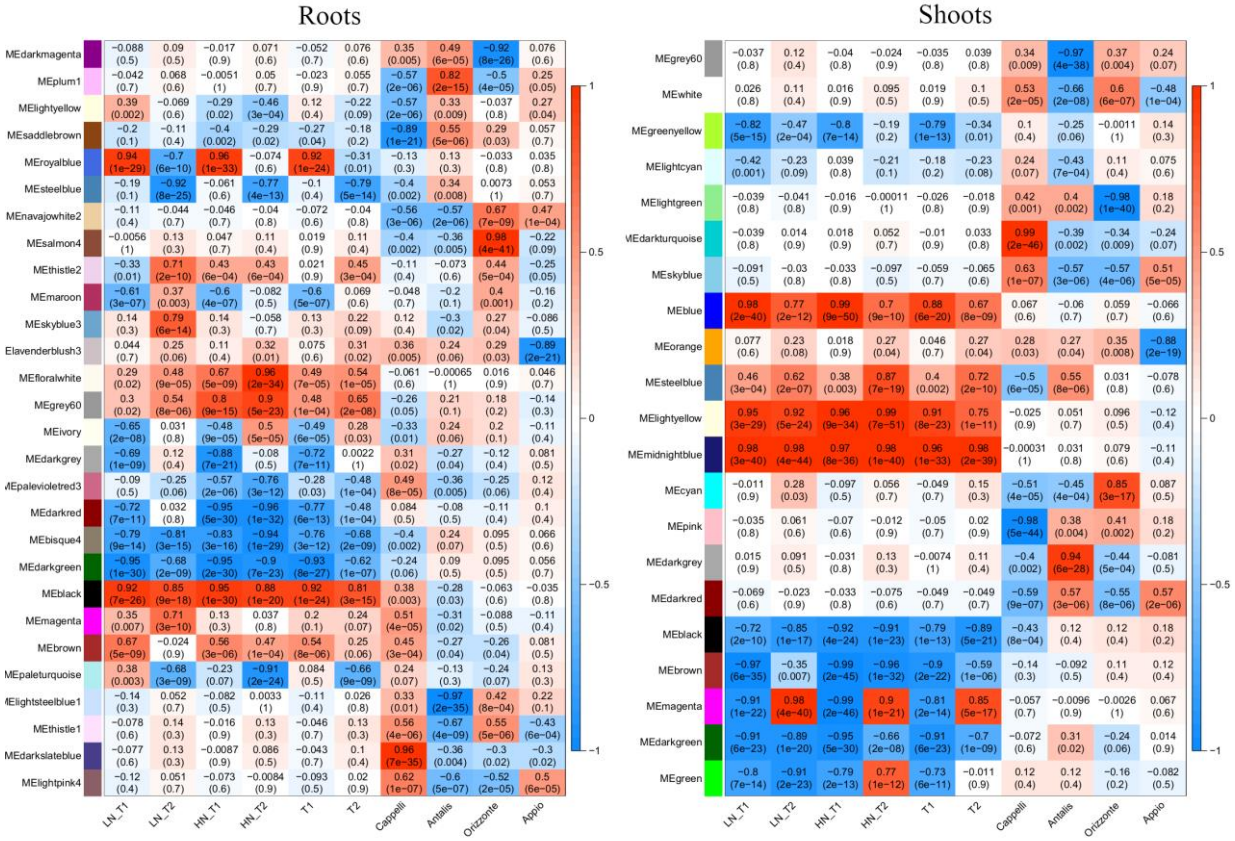

Figure 6. Correlation coefficients between module eigengenes and N-treatment/time sampling. Red and blue colors highlight positive and negative correlation with gene expression, respectively.

In root, six modules positively correlated with N treatments (upregulated) both at low and high N (p-value ≤ 0.05 and cor > 0.5) and 6 negatively correlated (downregulated) were detected. Furthermore, the royalblue module showed higher expression only at T1, both at LN and HN treatments, both ivory and darkgrey modules were downregulated at T1, while the floralwhite module was highly upregulated at T1 in HN condition. Interestingly, we also detected genotype specific modules, with expression levels often constitutively higher or lower in one genotype compared to the others.

In shoot, we identified four modules positively and 4 modules negatively correlated to N treatments. The degree of modulation between low and high N was lower compared to the root, with almost all the modules responding comparably to HN and LN. Remarkably, limited differences were detected between the time sampling. At T1, the magenta module was downregulated by N supply, while at T2 resulted highly upregulated both at LN and HN. In shoot, we also detected genotype specific modules, with high persistent expression differences in one genotype compared to the others.

A GO enrichment analysis was performed to highlight the Biological Processes (BP), Molecular Functions (MF), and Cellular Components (CC) of nitrate responsive modules. Interestingly, these modules were involved in highly diverse functions and metabolic processes (Table 1). The GO terms enriched in root N-responsive modules were often involved in amine, amino-acids and nucleotide biosynthesis, transmembrane transport, lipid metabolism, and small molecules metabolism. Otherwise, in shoots the most significantly enriched GO terms were related to photosynthesis, carbohydrates, peptides and terpenoids metabolisms, RNA processing, and translation. These results highlight both the functionality of co-expression modules in these tissues and the highly accurate clustering performed.

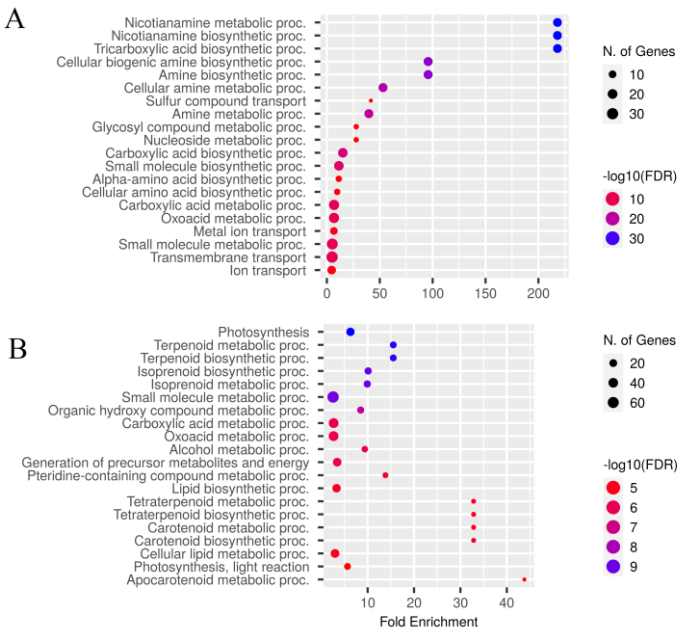

Figure 7 GO enrichment analysis performed on root floralwhite (A) and shoot midnight blue (B) modules. Both modules were highly upregulated by N supply. The enriched GO terms highlighted several specific metabolic pathways activated in both tissues.

Furthermore, using the Topological Overlap Matrix, the co-expression networks were drawn for each module to highlight the relationships between genes and to detect putative regulators (hub-genes), such as transcription factors and protein kinases, in significant nitrate responsive modules (Figure 8).

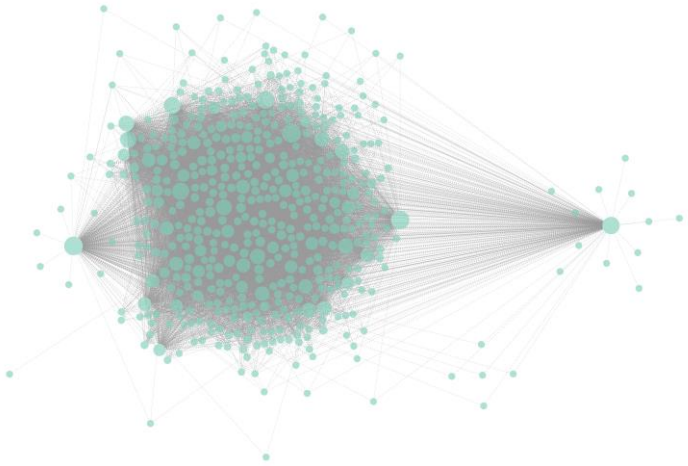

Figure 8. Network constructed using the Topological Overmap Matrix of the darkgreen module (root). The dimension is proportional to the degree (number of edges) of the node. The networks were visualized by using Cytoscape software.

Table 1. Top 4 GO terms found enriched in root and shoot co-expression modules. The three Biological Process, Cellular Component and Molecular Function are shown. The enrichment was performed by using a Fisher's exact test and a False Discovery Rate (FDR) threshold of 0.05.

Tissue		Biological Process	Cellular Component	Molecular Function
Roots	bisque	Carbohydrate metabolic proc.		Cytoskeletal protein binding
		Cellulose metabolic proc.		Microtubule binding
		Cellulose biosynthetic proc.		UDP-glucosyltransferase activity
		Acetyl-CoA biosynthetic proc. from acetate		Tubulin binding
	black	Translation	Ribosome	Structural constituent of ribosome
		Peptide biosynthetic proc.	Non-membrane-bounded organelle	Structural molecule activity
		Amide biosynthetic proc.	Intracellular non-membrane-bounded organelle	RNA binding
		Peptide metabolic proc.	Ribonucleoprotein complex	Translation factor activity
	brown	Reactive oxygen species metabolic proc.	Organelle membrane	Glycosyltransferase activity
		Hydrogen peroxide metabolic proc.	Extracellular region	UDP-glycosyltransferase activity
		Response to oxidative stress	Proteasome complex	DNA secondary structure binding
		Sulfur compound metabolic proc.	Endoplasmic reticulum membrane	Minor groove of adenine-thymine-rich DNA binding
	darkgreen	Lipid metabolic proc.		Ubiquitin-protein transferase activity
		Transmembrane transport		Ubiquitin-like protein transferase activity
		Cellular lipid catabolic proc.		O-acyltransferase activity

		Fatty acid oxidation		Oxidoreductase activity
	darkred	Lipid metabolic proc.	Serine/threonine protein kinase complex	Acyltransferase activity
		Fatty acid biosynthetic proc.	Atg1/ULK1 kinase complex	Oxidoreductase activity
		Cellular lipid metabolic proc.	Protein kinase complex	Acyltransferase activity
		Lipid biosynthetic proc.		Heme oxygenase (decyclizing) activity
	floral-white	Carbohydrate metabolic proc.		Cytoskeletal protein binding
		Cellulose metabolic proc.		Microtubule binding
		Cellulose biosynthetic proc.		UDP-glucosyltransferase activity
		Acetyl-CoA biosynthetic proc. from acetate		Tubulin binding
	ivory	Organelle organization	Nucleus	ADP binding
		Vesicle-mediated transport	Nuclear protein-containing complex	ATP-dependent activity
		MRNA metabolic proc.	Membrane coat	Cytoskeletal protein binding
		Phospholipid metabolic proc.	Coated membrane	Cytoskeletal motor activity
	pale-turquoise	Hydrogen peroxide metabolic proc.	Extracellular region	Peroxidase activity
		Reactive oxygen species metabolic proc.	Apoplast	Oxidoreductase activity
		Response to oxidative stress	Intrinsic component of membrane	Antioxidant activity
		Transmembrane transport	External encapsulating structure	Glycosyltransferase activity
	palevio-letred	Transmembrane transport		UDP-glycosyltransferase activity
		ubiquitin-dependent protein catabolic proc.		Hydrolase activity
		Floral whorl development		Glycosyltransferase activity
		Stamen development		DNA-binding transcription factor activity
	royalblue	Small molecule metabolic proc.	Cytoplasm	Oxidoreductase activity
		Carboxylic acid metabolic proc.	Mitochondrion	Oxidoreductase activity
		Oxoacid metabolic proc.	Mitochondrial envelope	6-phosphofructokinase activity
		Pyruvate metabolic proc.	Mitochondrial membrane	Isocitrate dehydrogenase activity
Shoots	black	Alpha-amino acid catabolic proc.	Extracellular matrix	DNA-binding transcription factor activity
		Erythrose amino acid metabolic proc.		Transcription regulator activity
		L-phenylalanine metabolic proc.		Sequence-specific DNA binding
		Cellular amino acid catabolic proc.		Calcium ion binding
	blue	Amide biosynthetic proc.	Ribosome	RNA binding
		Translation	Non-membrane-bounded organelle	Structural constituent of ribosome
		Peptide biosynthetic proc.	Intracellular non-membrane-bounded organelle	Structural molecule activity
		Cellular amide metabolic proc.	Ribonucleoprotein complex	Catalytic activity

	brown	Transmembrane transport	Integral component of membrane	UDP-glycosyltransferase activity
		Vesicle-mediated transport	Peptidase complex	Glycosyltransferase activity
		Neg. reg. of cell death	Endoplasmic reticulum	Phosphoric ester hydrolase activity
		Reg. of cell death	Proteasome core complex	Transaminase activity
	darkgreen	Glycine decarboxylation	Glycine cleavage complex	GTPase activator activity
		Alpha-amino acid catabolic proc.		Microtubule binding
		Cellular amino acid catabolic proc.		GTPase regulator activity
		Vesicle-mediated transport		Nucleoside-triphosphatase regulator activity
	greenyellow	Cellular localization	Membrane coat	ADP binding
		Vesicle-mediated transport	Coated membrane	ATP-dependent activity
		Establishment of localization in cell	Cytoplasmic vesicle	Cytoskeletal protein binding
		Intracellular transport	Vesicle	Cytoskeletal motor activity
	lightyellow	Photosynthesis	Thylakoid	Peptidyl-prolyl cis-trans isomerase activity
		Photosynthesis	Photosystem	Cis-trans isomerase activity
		Photosynthesis	Photosynthetic membrane	Ion channel activity
		Generation of precursor metabolites and energy	Membrane protein complex	NAD binding
	midnightblue	Photosynthesis	Thylakoid	Metalloendopeptidase activity
		Terpenoid metabolic proc.	Photosynthetic membrane	Metallopeptidase activity
		Terpenoid biosynthetic proc.	Photosystem	Iron-sulfur cluster binding
		Isoprenoid biosynthetic proc.	Photosystem II	Metal cluster binding
	steelblue	Proton transmembrane transport	Proton-transporting V-type ATPase complex	Acid phosphatase activity
		Cation transmembrane transport	Proton-transporting two-sector ATPase complex	Oxidoreductase activity
		Inorganic ion transmembrane transport	Proton-transporting V-type ATPase	Dioxygenase activity
		Ion transmembrane transport	Membrane protein complex	Proton transmembrane transporter activity

Transcriptome profile changes in root

In root, many modules were found highly induced by N treatments, both at T1 and T2, with some modules showing interesting expression patterns between times sampling and N supply (LN, HN).

The black, grey60 and floralwhite modules showed a high positive correlation with both N treatments, although slightly different responses were detected. The darkgreen, bisque, and darkred showed an opposite trend, highly downregulated in response to N. The black module, including 1490 genes, was highly induced by N supply, with a lg2fc always higher at T1 HN in all four genotypes, except Appio, then showing genes expression decreases as a function of both N level and time sampling (Figure 9). GO enrichment of this module highlighted its role in translation, peptide biosynthesis and RNA processing. Nineteen transcription factors belonging to mTERF, MYB, and ERF were included, 26 hub-genes were identified. These were almost all ribosomal proteins or translation-associated factors like the eukaryotic translation initiation factor 3.

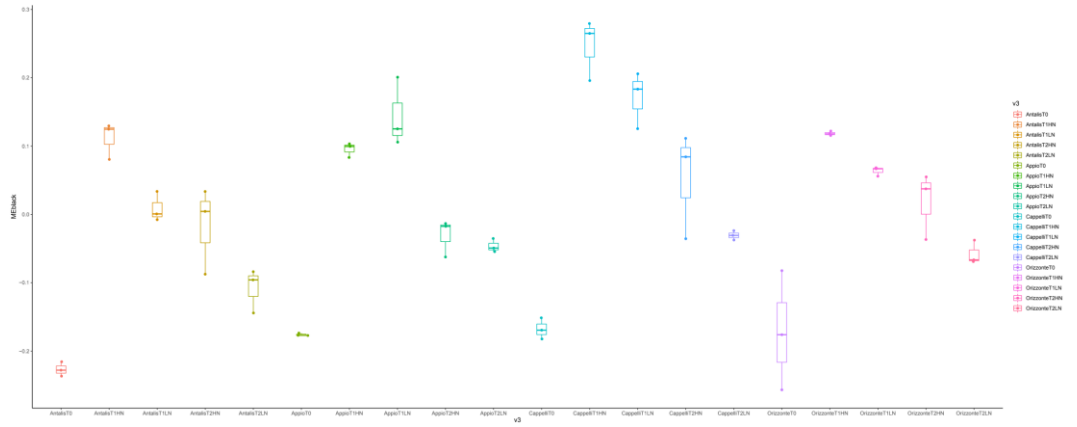

Figure 9 Expression profile (eigengene) of black module (root). N supply significantly enhanced gene transcripts, with a higher effect at T1 in HN condition. The induction decreased both with the N level and time. Colors were used to highlight genotypes (orange: Antalis, green: Appio, blue: Cappelli, and pink: Orizzonte) and shades of these four colors were used to highlight times sampling and N-treatments.

The floralwhite module, the smaller ones with 208 genes included, showed a significant upregulation at T2 in HN condition in all four genotypes. This module was involved in nicotianamine, amine and oxoacid metabolisms, as well as transmembrane transport.

Interestingly, the grey60 module showed a similar trend to the black module but with differences among genotypes. In particular, the genes included were highly downregulated at T1 in LN condition in Appio and Cappelli showing an opposite trend into Antalis and Orizzonte.

The royalblue module, including 1,330 genes, showed a rapid response to N supply (T1), both at high and low N (Figure 10). The GO terms enrichment highlighted its role in small molecules, oxoacid and carboxylic acid metabolisms. We detected a high number of transcription factors (45) with *bZIPs* and *MYBs* being the most abundant.

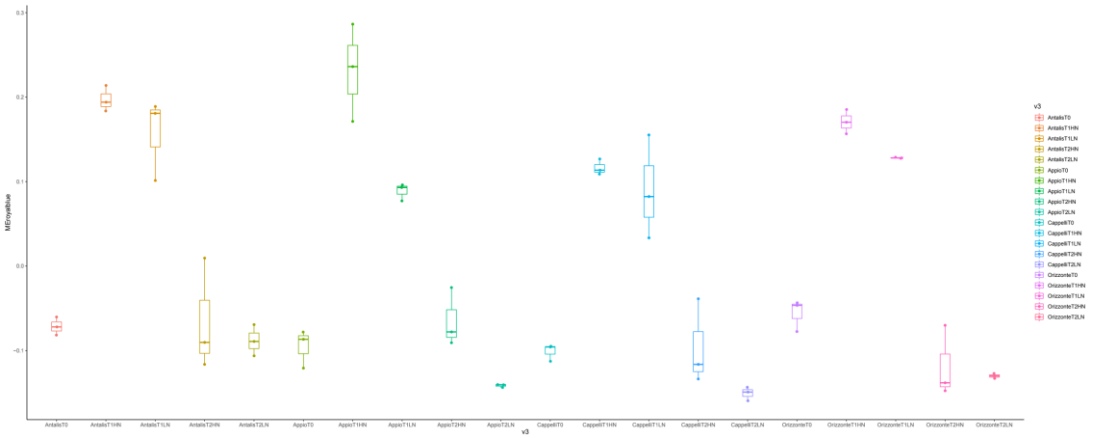

Figure 10 Expression profile (eigengene) of module royalblue (root). N supply significantly enhanced genes transcription, with a higher effect at T1 in HN condition. The induction decreased by both N level and time. Colors

were used to highlight genotypes (orange: Antalis, green: Appio, blue: Cappelli, and pink: Orizzonte) and shades of these four colors were used to highlight times sampling and N-treatments.

The darkred, darkgreen and bisque modules (including 1,074, 450 and 483 genes, respectively) exhibited an opposite trend, highly downregulated by N supply. In detail, the darkred module was highly downregulated in all the treatments with a slighter downregulation at T2 in LN condition, mainly in Cappelli and Appio with similar trend at T1. The darkgreen module was characterized by a very fast downregulation at T1, proportional to N level, with Appio showing a higher downregulation at LN compared to HN. Interestingly, both darkred and darkgreen modules were enriched in terms related to lipid metabolic process and transmembrane transport. Furthermore, darkred module was also involved in lipid transport while the darkgreen was highly enriched in ubiquitin-protein transferase activity. Finally, the bisque module was involved in carbohydrate metabolic process and cytoskeletal protein binding. The darkgreen and bisque modules were highly enriched in *MYBs* TF accounting for 30% and 22% of all TFs, respectively.

Remarkably, three large modules, brown, paleturquoise and palevioletred including 7,628, 855 and 4,612 genes, respectively, showed a differential response in the genotype Cappelli compared to the others (Figure 11). These modules were slightly modulated among genotypes, with brown module showing a low upregulation, while palevioletred and paleturqoise downregulated by N supply. In both modules, Cappelli showed a high upregulation, with an average lg2fc of 1.7 in comparison with the other three, except Appio at T1 in LN condition, which showed a similar upregulation to Cappelli. All three modules were involved in transmembrane transport as highlighted by the GO enrichment; both the brown and the paleturquoise modules were also enriched in oxidative stress response related terms. Furthermore, the brown module was also enriched in amino-acids transport related terms.

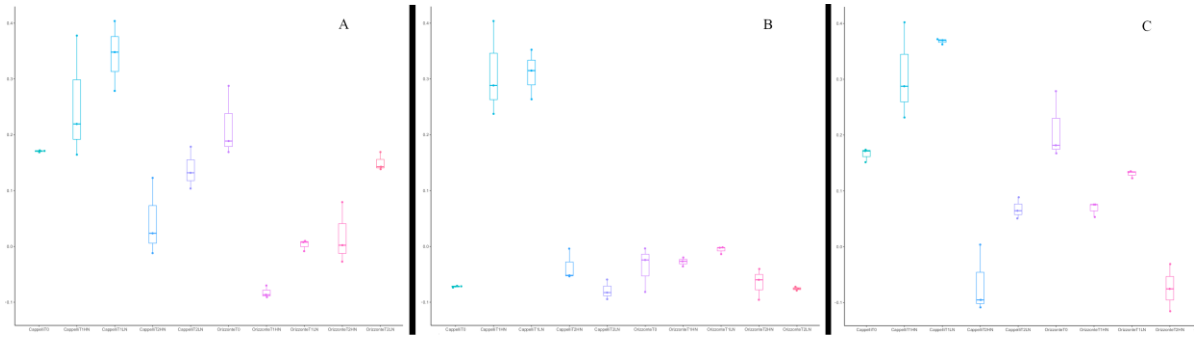

Figure 11 Expression profile (eigengenes) of module palevioletred (A), brown (B), and paleturquoise (C) in Cappelli (blue) and Orizzonte (pink) genotypes in root. N supply significantly enhanced genes transcription in Cappelli, mainly at T1. Colors were used to highlight genotypes (blue: Cappelli, and pink: Orizzonte) and shades of these four colors were used to highlight times sampling and N-treatments.

Transcriptome profile changes in shoot

In shoot, many modules were highly affected by N treatments, both at T1 and T2. In detail, four modules were correlated to both low and high N conditions (blue, midnightblue, lightyellow, and steelblue), while four were negatively correlated (black, brown, darkgreen, and greenyellow) (p-value ≤ 0.05 and cor > 0.5).

Among the upregulated modules, the midnightblue module (1,013 genes) showed the highest correlation coefficient with both low and high N conditions. The blue, midnightblue and lightyellow modules showed a similar profile among the genotypes, the first resulted upregulated at T1 in both N treatments, the second upregulated in all the conditions (T1 and T2 at low and high N) and the lightyellow at T1 (HN and LN) and T2 only at HN (Figure 12). Both module midnightblue and lightyellow are involved in photosynthesis processes, small molecule metabolism, and oxoacid metabolism, with many GO terms enriched included in these categories. Furthermore, the midnightblue module was also involved in isoprenoid and terpenoid biosynthesis and lipid metabolism, while the module lightyellow was also involved in carbohydrate metabolism. Finally, the blue module was highly enriched in peptide and amide biosynthesis, translation and RNA processing.

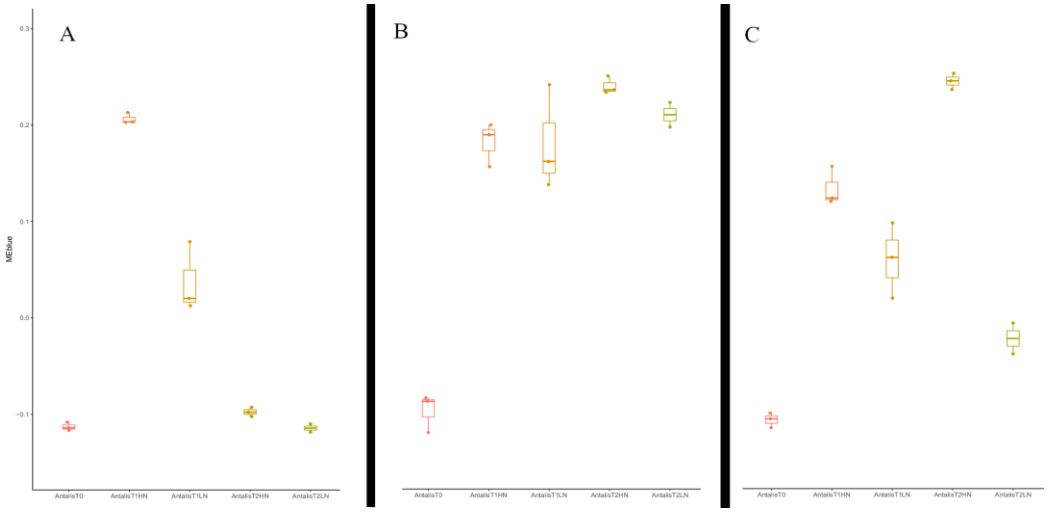

Figure 12 Expression profile (eigengenes) of blue (A), midnightblue (B), and lightyellow (C) modules in Antalis (shoot). N supply significantly enhanced the expression of genes included in blue module at T1 (both N conditions), at both T1 and T2 in midnight blue module and at T1 (LN and HN) and T2 (HN) in the lightyellow module.

Otherwise, four modules were downregulated by the N supply, mainly in the short-term response (T1) and high N treatment. These modules were involved in transcription regulation (black); transmembrane transport, vesicle mediated transport and lipid metabolism (brown); amino-acids catabolism, vesicle

mediated transport, and carbohydrate metabolism (darkgreen); cellular localization, nitrogen compound transport (greenyellow).

Two hundred fifty-two (252), 183, 15 and 83 transcription factors were identified among the genes included in black, brown, darkgreen and greenyellow modules, respectively. The two larger modules black (3,030 genes) and brown (3934) were enriched in WRKY (39 and 16), ERF (39 and 16) and MYB TF (33 and 20). In addition, the brown module was also enriched in the RADIALIS-like (19) TFs family.

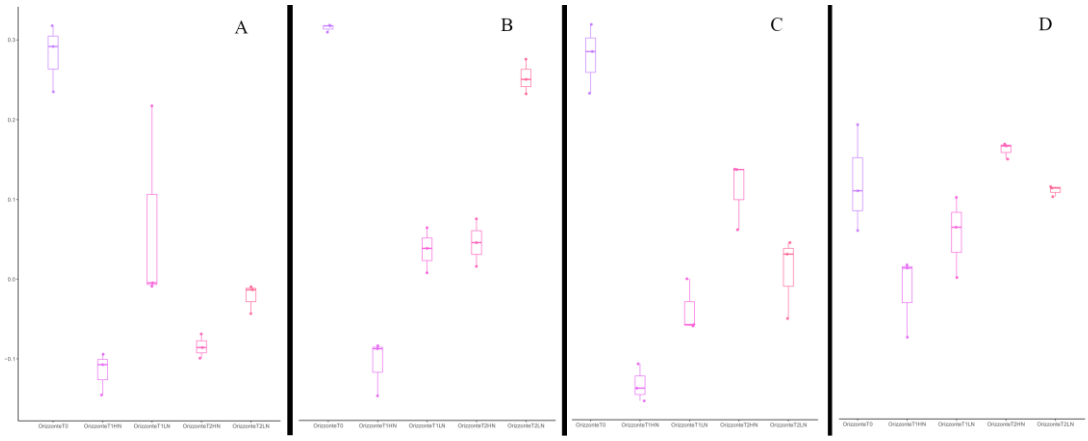

Figure 13 Expression profile (eigengenes) of black (A), brown (B), darkgreen (C), and greenyellow (D) modules in Orizzonte (shoot). N supply significantly downregulated gene expression at T1 mainly at HN.

Both the darkgreen (the smaller ones with 380 genes), and the greenyellow modules did not show any significantly enriched TF family. Among the N-reactive modules, the steelblue module with 140 genes upregulated showed a significant higher expression in Antalis, with highest gene expression at T0 at both low and high N. GO enrichment analysis revealed a specific role in cation and proton transmembrane transport. Four TFs were identified, 2 bHLH, a TCP, and a WRKY.

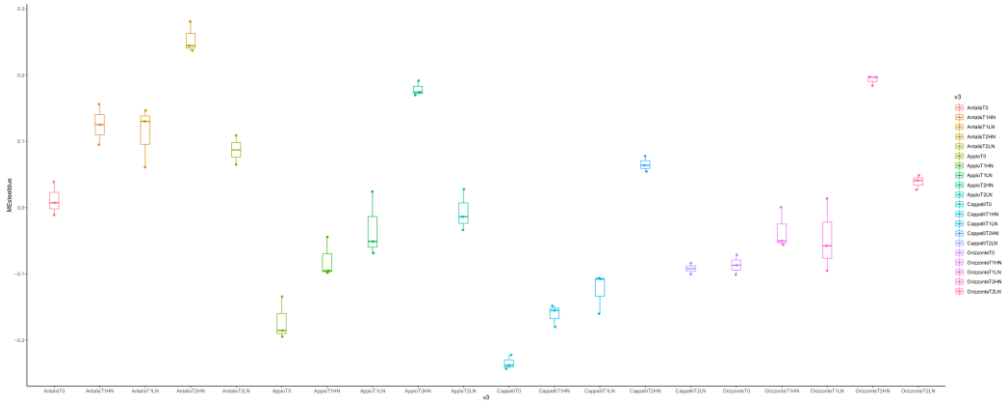

Figure 13 Expression profile (eigengene) of module steelblue (shoots). N supply significantly enhanced transcription, with a higher effect in the T2HN condition. Colors were used to highlight genotypes (orange:Antalis,

green:Appio, blue:Cappelli, and pink:Orizzonte) and shades of these four colors were used to highlight time-points and N-treatments.

Modulation of NPF and NRT2 nitrate transporters in response to N supply

Using the previously described NPF and NRT2 annotation, we were able to detect the expression of these important nitrate transporters. Seventeen and 3 TdNRT2 as well as 156 and 137 TdNPF genes resulted differentially expressed in at least one comparison in root and shoot, respectively.

Interestingly, TdNPF genes were distributed unevenly among the co-expression modules in root, with almost 55% in paleturquoise (43) and brown (44) modules showing a high variability among the genotypes. In shoot, TdNPF genes were spread evenly among the modules, indicating a more complex regulation of the gene family in the aboveground tissues; in detail, 34, 30, 24 and 12 *TdNPFs* were detected in the blue, brown, magenta and black modules, respectively, accounting for 73% of all the *TdNPFs*.

TdNRT2 genes were mainly modulated in root in response to N supply. Seventeen *TdNRT2* were distributed in seven modules, 6 in the brown, 2 in floralwhite, paleturquoise, royalblue and grey60 modules and only one in the black module; in shoots two out of three differentially expressed *TdNRT2s* were identified in the brown module.

A second supervised clustering using the expression data of *TdNRT2s* and *TdNPFs* in both tissues, independently, were performed to better describe the expression profiles of these important nitrate transporter genes. Two *TdNRT2s* groups were clearly distinguished in root (Figure 14). Group1 included ten genes members upregulated mainly in the rapid response to N supply at T1 (low and high N), then downregulated at T2. Group2 was mainly induced by HN condition, with a significant expression increase at T2 (Figure 14). In shoot, one NRT2 gene member resulted highly upregulated at T1 (HN), mainly in Cappelli, while two others were downregulated by high N supply at both time samplings (Figure 14).

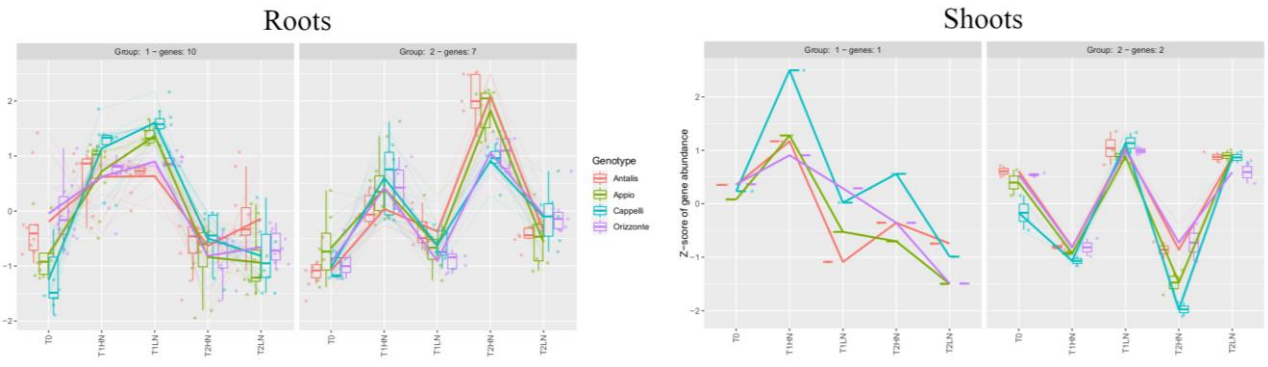

Figure 14. Clustering of 17 and 3 differentially expressed *TdNRT2s* in root and shoot, respectively. The analysis was performed using degPatterns and vst transformed expression data.

The TdNPF genes showed a lower induction in response to N compared to TdNRT2 family, both in root and shoot. In shoot, *TdNPFs* clustered in several groups, showing low variability among genotypes. In root, the two most abundant groups (Group2 and Group6) were mainly upregulated in Cappelli at T1 (HN and LN) and Appio at T1 (LN) (Figure 15). This result agrees with the expression profiles detected by the WGCNA, especially in palevioletred, brown, and paleturquoise modules. Interestingly, some TdNPFs groups showed differences in their constitutive gene expression among the genotypes.

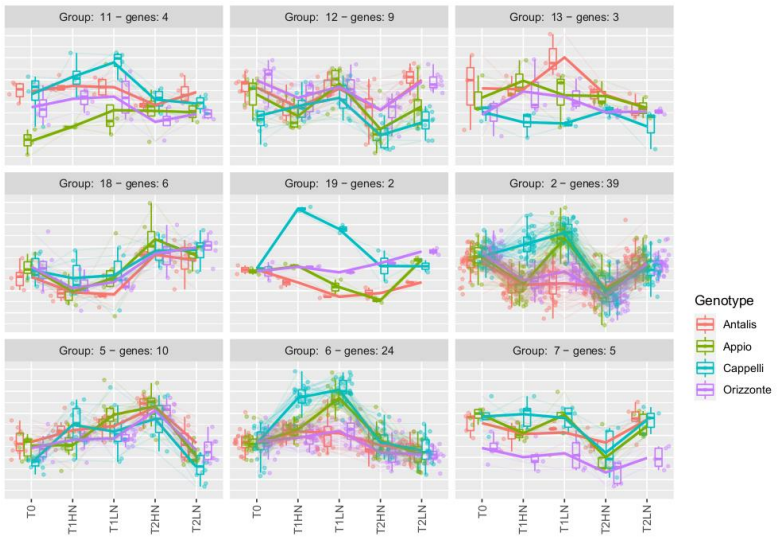

Figure 15 The main groups detected by the clustering by using 156 TdNPF genes differentially expressed in root. The analysis was performed using degPatterns and vst transformed expression data.

Differential expression of genes involved in N assimilation

Many genes are known to directly influence nitrate uptake and assimilation in plants. The expression modulation of these genes was detected by comparative transcriptomic analyses, resulting often related to NUE. Here, we detected 41 and 38 differentially expressed genes with significant differences among genotypes in root and shoot, respectively. Among these, several Glutamine Synthetases (GS), Glutamate Synthases (GOGAT), Asparagine Synthase (ASN), Nitrite Reductase (NiR), Nitrate Reductase (NR), and NAR2 were identified (Figure 16). The induction of these genes was higher in root, and Cappelli showed the most significant upregulation (lg2fc > 5) at T1 both in LN and HN conditions. In root, many Nitrate Reductases (NR) and Nitrite Reductase (NiR) were upregulated at T1 regardless of N levels, while at T2 they appeared downregulated in almost all genotypes, especially in Appio and Orizzonte. In shoot, N induced a lower number of these genes; The two NRs and 2 NiRs were upregulated at T2 (HN) in all the genotypes, with slightly higher levels in Orizzonte.

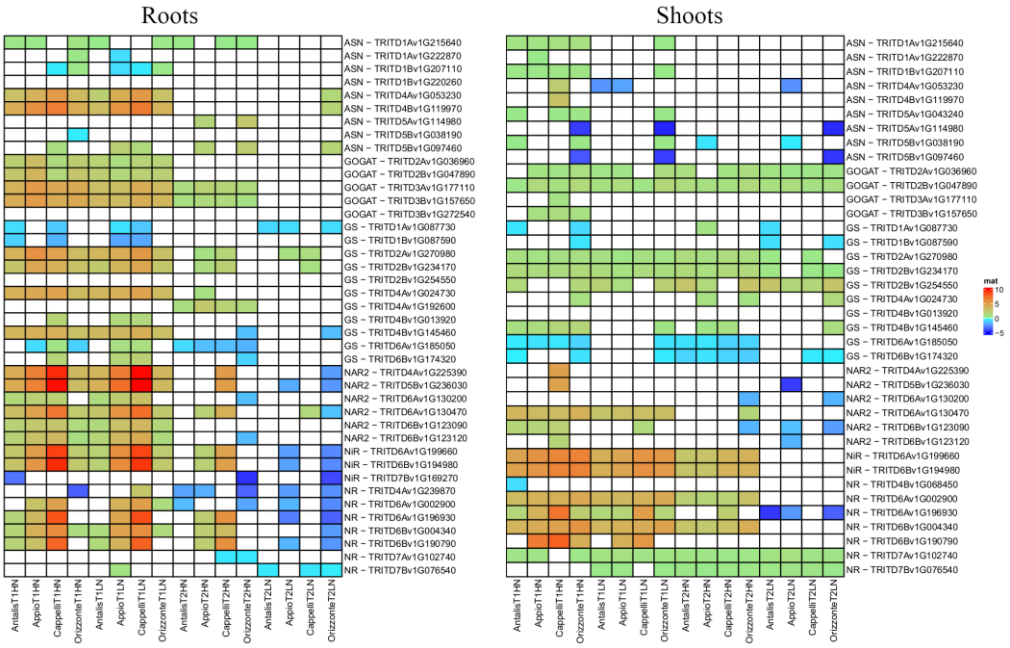

Figure 16 Heatmap showing the expression levels of genes involved in N metabolism differentially expressed in root. The colors indicate the log2FC between T0 and both other sampling times (T1 and T2), each N level and genotype. green-to-red: upregulated, cyan-to-blue: downregulated, white: not differentially expressed.

Transcription factors and protein kinases are essential for the regulation of gene expression. Nitrate can act as a signal molecule in the so-called nitrate-mediated signaling pathway. Changes in gene transcription can often be associated with differential expression of one or more transcription factors. Here, more than one thousand eight hundred (1,840) and 1,450 TFs were differentially expressed in root and shoot, respectively. The most abundant category was MYB (221 and 154 in root and shoot, respectively), followed by ERF (162, 105), WRKY (142, 108), bZIP (79, 56), and BHLH (42, 35). Furthermore, the WGCNA analysis allowed us to identify hub-genes among TFs, putatively involved in N-response. Among the highly induced modules (4 and 7 in shoot and root, respectively), 10 TF hub-genes (3 and 7) were highlighted (Figure 17). Interestingly, they were mainly upregulated in shoot at T1, with the higher differences in gene expression showed by Cappelli and Appio compared to the others. Moreover, the unique MYB detected as hub-gene was upregulated in root at T1 in both Cappelli (HN and LN) and Appio (LN). An AP2/B3 transcription factor was constitutively upregulated in all the genotypes and conditions, while *CCR4-NOT* was induced at T2 in all the genotypes under LN.

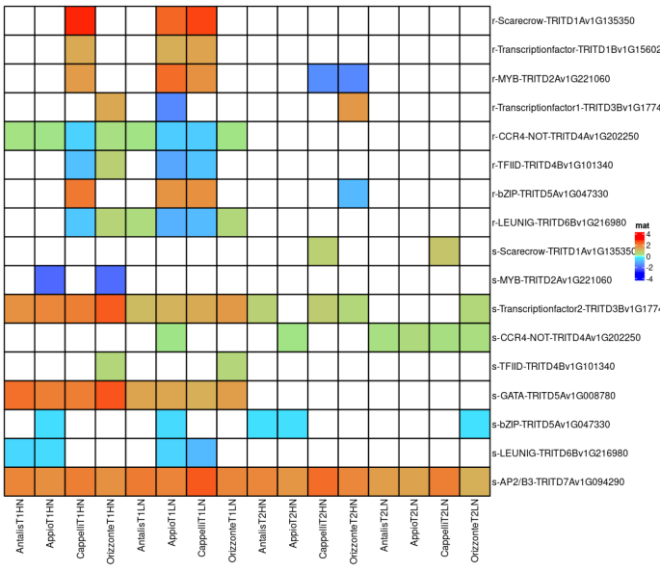

Figure 17 Heatmap showing the expression levels of transcription factors among the hub-genes of upregulated modules in both root (r-) and shoot (s-). The colors indicate the log2FC between T0 and both other sampling times (T1 and T2), each N level and genotype. green-to-red: upregulated, cyan-to-blue: downregulated, white: not differentially expressed.

Protein kinases are involved in nitrate signaling and often identified as key regulators of nitrate uptake in *Arabidopsis* through the phosphorylation of NRT proteins (Kumari et al., 2020). Many protein kinases were differentially expressed in response to N-supply in both roots and shoots. In our experiment, many receptor-like kinases (825 and 773 in root and shoot, respectively) as well as wall-associated kinases (41 and 38), MAP kinases (43 and 40), and histidine kinases (15 and 11) were identified. Nine and five protein kinases in root and shoot respectively were selected as hub-genes in the significant modules. In detail, in root we detected three Serine/threonine-protein kinases and a MAP kinase while in shoot a Serine/threonine-protein kinase and a Leucine-rich repeat protein kinase (LRR).

5.4 Discussion

Plant development and crop yield are deeply influenced by nitrogen availability into the soil and its efficient utilization by plants. A critical element for improving plant Nitrogen Use Efficiency (NUE) is to understand crop responses to N at both physiological and molecular levels, determining how N supply affects its uptake, transport and assimilation. The aim of our study was to detect significant differences of key gene expression between contrasting NUE genotypes to select candidate genes putatively involved in the complex trait. Thus, both short- (8h) and long-term (96h) transcriptomic responses of durum wheat to high and low N supply were investigated by RNA-seq analysis.

Our results highlighted distinct transcriptional profiles, confirming the significant differences detected for both NUE components (NUpE and NUtE), among genotypes. N supply modulated an average of

55% of the total genes in the durum wheat genome in each genotype, 60% and 51% of genes from root and shoot, respectively. Furthermore, each genotype showed a high number of genotype-specific induced genes ranging from 500 to 3,200 genes in Antalis and Appio, respectively. To face the high amount of DEGs and to highlight key genes showing significant differences among genotypes, a weighted gene co-expression network analysis (WGCNA) was adopted for clustering genes into co-expression modules. Afterwards, a GO enrichment analysis allowed us to functionally characterize these modules.

Twenty-eight and twenty-one modules were identified in root and shoot, respectively, among which, we detected three and one modules in root and shoot showing significantly different gene expressions among genotypes. These modules showed specific functional enrichment, highlighting the main pathways up- and down-regulated in response to N supply.

In root, genes involved in carbohydrate, peptide and amide metabolisms, cellulose biosynthesis, oxoacid and carboxylic acid metabolisms were highly induced, by contrast a significant genes downregulation related to lipid and fatty acid metabolisms was observed. In *Arabidopsis* seedlings, lipid metabolism was downregulated in response to NO_3^-, while both carbohydrates and oxoacids are involved in the C/N balance and in the amino acid biosynthesis (Castillo et al., 1996; Wang et al., 2003; Scheible et al., 2004; Zheng, 2009).

In shoot, genes involved in photosynthesis and terpenoid biosynthesis were the most upregulated by N supply. Interestingly, a severe downregulation of genes related to amino acid catabolism and vesicle-mediated transport, as well as transmembrane transport was detected. Amino acid catabolism following protein degradation is a secondary ammonia source (after direct ammonium uptake by plants) mainly in N-limited condition (Bernard and Habash, 2009). Interestingly, at T0 starved plants have fully activated the N recycling pathways but the repression of aminoacid catabolism was rapid and increasing with the N-level.

Some modules showed a different regulation in the older genotypes Cappelli and Appio, compared to Antalis and Orizzonte. In detail, Cappelli showed a significant upregulation of genes related to oxidative stress response and transmembrane transport in root. Plants nitrate starvation for 7 days before the NO_3^- resupply, may explain a high level of oxidative stress response genes at T0 but not after N-induction (T1 and T2). N-uptake is known to increase pH in the rhizosphere with an increase of H_2O_2 production in the epidermis of roots to favor the H^+/NO_3^- exchange (Chen et al., 2018). Furthermore, both nitric oxide (NO) and hydrogen peroxide are known to act as secondary messengers during root development and many other physiological processes (Liao et al., 2009; Niu et al., 2016).

Moreover, the high number of transmembrane transport proteins, mainly involved in proton and cation transmembrane and ion transport and included in these modules seems to confirm an active role of these genes in the N-uptake. In shoot, the steelblue module showed significant differences among genotypes with a higher upregulation at T0 in Antalis. We also detected other highly genotype-related modules in

both root and shoot and despite not directly involved in the N-induced plant responses, they might be involved in nitrate transport, sensing, and signaling.

As a signaling molecule, nitrate can regulate the expression of several genes. Both transcription factors and protein kinases are involved in the nitrate-mediated signaling pathway and their expression modulation has often been associated with higher NUE (Hu et al., 2009; Castaings et al., 2009; Nazish et al., 2021). Several MYB, WRKY, AP2-EREBP, bHLH, bZIP, ERF, NAC, GATA and DOF TF family members have been reported as main regulators of nitrogen metabolism in plants (Zhuo et al., 1999; Hao et al., 2011). *OsMYB305* overexpression in rice determined a higher N-content in root and shoot dry weight, while the higher NUE of rice *indica* subspecies compared to *japonica* was mainly attributed to the *OsMYB61* natural variation (Gao et al., 2020; Wang et al., 2020). Our dataset revealed that MYB, ERF, WRKY, bZIP, and BHLH were the most abundant TF families modulated in response to N in durum wheat. Furthermore, among the hub genes of N-responsive modules, we detected a member for each MYB, GATA, bZIP, and AP2/B3 TF families.

Many protein kinase families were also found involved in nitrate signaling and the regulation of nitrate uptake (Kumari et al., 2020). The first studied mechanism involving protein kinases is the phosphorylation and dephosphorylation of the nitrate transporter *AtNPF6.3* (=*CHL1*=*NRT1.1*) to regulate its dual-affinity (Liu et al., 2003). Many other reports have described many interactions between N-related genes and the protein kinases. Both NiR and NR were shown to be regulated by phosphorylation and dephosphorylation (Chandok et al., 1994; Redinbaugh et al., 1996; Ali et al., 2007; Zhou et al., 2020). In our condition, many families of protein kinases among DEGs and, more interestingly, among the hub genes were identified, among which, seven and four protein kinases in root and shoot, respectively.

Nitrate-related genes, involved in both N uptake and assimilation, were differentially expressed among our durum wheat genotypes. Among others, some members of NAR2 (=NRT3.1) nitrate transporter family, well known for their interaction with NRT2 proteins during nitrate uptake (Yan et al., 2011), were upregulated in root mainly at T1, showing a similar expression profile of NRT2 genes, as expected. The balance of nitrate reduction between root and shoot depends both on root/shoot biomass ratio and the activity of both tissues (Andrews, 1986; Gojon et al., 1994). Moreover, NR activity and its gene expression are also highly influenced by plant age (Cadergreen et al., 2003). Here, nitrate reductases were mainly distinguishable into two groups based on their expression. A first group included upregulated *NRs* in root and shoot at T1 in LN condition (short-term after N resupply), while the second one was strongly induced in shoot at T2 or in HN condition. Two out of the three NiR were upregulated in both root and shoot at T1 and only in shoot at T2 (HN condition). Remarkably, Cappelli showed the highest induction of many NAR2, NR and NiR genes, by contrast Orizzonte showed an opposite trend of genes expression, mainly at T2, with a significant *NR* and *NiR* downregulation in LN condition. Furthermore, Glutamate dehydrogenase (GDH), an important enzyme involved in Carbon/Nitrogen balance, was not detected as differentially expressed in both root and shoot. GDH is mainly involved in

the deamination of Glutamate to form ammonia or the amination of ammonia and 2-OG to form Glutamate. Here, no induction was detected, confirming its main role in ammonia assimilation when ammonia is uptaken from soil and in N remobilization during seed germination or during C or N starvation, as reported by works on Arabidopsis and tobacco (Miyashita et al., 2008; Liu et al., 2022).

NRT2 and NPF genes are usually involved in high- and low-affinity mechanisms of nitrate transporters, respectively, however many exceptions to this classification have been previously described in many plants (Hu et al., 2015; Wen et al., 2017; Wen and Kaiser, 2018). Our results showed a distinctive regulation of these genes in all the durum wheat genotypes, mainly in the older varieties Cappelli and Appio.

In root, both genotypes showed a significant *TdNPFs* upregulation in the short-term (8h) response to nitrate. Interestingly, the genes high induction was not affected by N-level in Cappelli, while Appio showed higher genes expression only at low N. Furthermore, two others upregulated TdNPFs were induced only in Cappelli at T1 (one at HN and the other at LN).

As above reported for NAR2 family, NRT2 genes showed two main trends of expression, the first group included *TdNRT2s* upregulated in the short-term response to nitrate regardless N concentration and the second one mainly upregulated at HN, with an increased transcript level over time. Our results did not show variability in the regulation of this gene family among genotypes, suggesting a highly conserved mechanism of *NRT2s* induction. This observation could also suggest that N uptake ability in durum wheat may not be directly attributable to the NRT2 transporters activity.

The four genotypes were highly distinct for gene expression regulation. The older variety Cappelli was the most diverse with many genes induced by N supply, mainly at T1 in root. Despite N-responsive genes showed limited expression differences among genotypes in shoot, however, we detected a small module including proton transmembrane transport genes significantly upregulated in the modern genotype Antalis. Interestingly, Cappelli showed the higher NUpE in the agronomic experiments while Antalis the higher NUE, making both upregulated genes and modules in these genotypes of particular interest for future studies.

5.5 Conclusions

In the present study, we have analyzed the differential transcriptome profiles of four durum wheat genotypes in response to two N concentrations both at 8 and 96 hours from the N-resupply. Our results provide useful information for better understanding the nitrate-mediated molecular mechanisms related to a more efficient N-use in durum wheat. The NUE contrasting genotypes appeared related to the significant distinct transcriptional profiles.

This is the first comparative transcriptomic analysis of durum wheat in response to variable N concentrations. The four distinguishable genotypes for NUE-related traits allowed us to highlight common pathways involved in durum wheat N-response and the genetic differences putatively involved in the phenotypic variation. In conclusion, this work provides valuable information to better

comprehend durum wheat response to N supply providing many candidate genes for NUE improvement.

Chapter 6: General conclusions and future perspectives

This research focused on improving our understanding on the genetics of Nitrogen Use Efficiency (NUE) in durum wheat. The results here obtained highlighted a high genetic variability underlying NUE within the species. Many studies on the molecular mechanisms underlying NUE were based on a two-genotype approach, comparing efficient and inefficient genotypes. Due to NUE complexity, the adoption of multiple genotypes showing contrasting phenotypes also for NUE components, such as NUpE and NUtE, could help to detect a more specific and higher level of genetic variability. Here, we performed two agronomic trials, by using ^{15}N in pots and different N supply in the field, to evaluate both NUpE and NUtE of nine durum wheat genotypes largely diversified for year of release, morphological and phenological traits, and yield potential allowing us to identify both NUE efficient and inefficient genotypes. Four genotypes were selected based on their N uptake, root system, N remobilization and utilization efficiencies. Senatore Cappelli, the oldest variety, showed the most differentiated response among the genotypes with the highest N uptake and a larger ability and speed in intercepting N when available. Unfortunately, this capacity did not reflect into a higher NUE, as expected from older varieties, because of the Senatore Cappelli inefficiency to N utilization and translocation from root to shoot. The most modern variety, Antalis was the most efficient in the N remobilization from flag leaves to the reproductive tissues, which determine a high NUE. Appio, instead, showed low values of N uptake, mainly when N was limited, a slow response to nitrate fertilization, and the lowest N remobilization from flag leaves to grain. Finally, Orizzonte was the most efficient in the N uptake per gram of root under limiting conditions with a highly efficient N translocation from root to shoot.

Our research also focused on the full characterization of both NPF and NRT2 genes in the durum wheat genome. The annotation of these gene families is of great relevance for the study of nitrate and nitrogen dynamics and their relationship with agronomic NUE. Here, we identified for the first time two hundred eleven (211) TdNPF and twenty (20) TdNRT2 genes, providing a deep annotation of their protein sequences and conserved domains. Many *TdNRT2s* were predicted to be under the regulation of MYB and MYC transcription factors, while some *TdNPFs* may be involved in the ABA signaling pathway. Interestingly, many genes in both families were retained after small-scale duplication events, suggesting a neo- or sub-functionalization of such members not already detected in *Arabidopsis* or other crops. These results suggest that the expansion of these families in wheat may be an important source of variability for the detection of NUE-related genes and potential candidates for maximizing NUE in wheat. Furthermore, using RNA-seq, we analyzed the effects of mycorrhizal inoculation on durum wheat under salt stress. This chapter allowed us to define the pipelines and methods for RNA-seq analysis on durum wheat, highlight key genes putatively involved in AMF-induced salt stress tolerance, identifying nitrate transporters expressed in durum wheat leaves and putatively involved also in plant

stress response. We detected a lower number of stress-related genes modulated by soil salinity in AMF inoculated compared to non-inoculated samples. The differentially regulated genes (DEGs) categories included the plant defensive genes against redox state (i.e., cytochrome P450, glutathione S-transferase, catalases) and involved in osmoregulation, osmolytes, and ions transport.

Finally, we analyzed the differential transcriptome profiles of the four selected durum wheat genotypes in response to low and high N supply at both 8 and 96 hours from the N-resupply. Our results provide useful information for a better understanding of the N-mediated molecular mechanisms related to a more efficient N-use in durum wheat. The four genotypes selected for contrasting NUpE and NUtE, NUE components, showed highly diversified transcriptome profiles, with almost 60% of durum wheat genes differentially expressed in at least one comparison. We were able to describe the main pathways and genes involved in the response to both high and low N, although the differences between treatments were lower compared to the expected. We further detected co-expression modules mainly upregulated in the high NUpE or high NutE genotypes in root and shoot, respectively, highlighting the putative regulators of these modules. Moreover, we precisely described the genotype specific induction of all the *TdNPFs* and *TdNRT2s* in response to N in both root and shoot using the previously extracted annotation. This allowed the detection of numerous groups of *TdNPFs* with highly different expression patterns among genotypes.

This is the first high depth comparative transcriptomic analysis on durum wheat in response to low and high N supply. The four distinguishable genotypes for NUE-related traits allowed us to highlight common pathways involved in durum wheat N-response and the genetic differences putatively involved in the phenotypic variation. In conclusion, this PhD thesis provides valuable information to better comprehend durum wheat response to N supply providing many candidate genes for NUE improvement. The genes here identified will serve as pool of candidate genes for NUE improvement in durum wheat, both for breeding and genetic engineering. Furthermore, our findings will also provide a highly detailed gene atlas for a deeper study of NUE in durum wheat.

Future studies will be focused on the narrowing of the candidate genes list. This will be performed using qPCR for the expression quantification of candidate genes on a wider set of genotypes and landraces, grown in several environmental conditions and N availability. Sampling times will follow the growing stages of the crop until grain filling and yield. Furthermore, the RNA-seq data could be implemented and integrated by proteomics and metabolomics profiling. Finally, *Arabidopsis* transgenic lines will be used for the functional characterization of the more interesting NUE-related candidate genes.

References

Ahmad P, Jaleel CA, Salem MA, Nabi G, Sharma S. Roles of enzymatic and nonenzymatic antioxidants in plants during abiotic stress. Crit Rev Biotechnol. 2010;30:161–75.

Akbudak, M. A., Filiz, E., & Çetin, D. (2022). Genome-wide identification and characterization of high-affinity nitrate transporter 2 (NRT2) gene family in tomato (Solanum lycopersicum) and their transcriptional responses to drought and salinity stresses. Journal of Plant Physiology, 153684.

Alaux P-L, Naveau F, Declerck S, Cranenbrouck S. Common mycorrhizal network induced JA/ET genes expression in healthy potato plants connected to potato plants infected by Phytophthora infestans. Front Plant Sci. 2020;11:602.

Ali, A., Sivakami, S., & Raghuram, N. (2007). Regulation of activity and transcript levels of NR in rice (Oryza sativa): Roles of protein kinase and G-proteins. Plant Science, 172(2), 406-413.

Almagro, A., Lin, S. H., & Tsay, Y. F. (2008). Characterization of the Arabidopsis nitrate transporter NRT1. 6 reveals a role of nitrate in early embryo development. The Plant Cell, 20(12), 3289-3299.

Almansouri M, Kinet J-M, Lutts S. Effect of salt and osmotic stresses on germination in durum wheat (Triticum durum Desf.). Plant Soil. 2001;231:243–54.

Alqarawi AA, Abd Allah EF, Hashem A. Alleviation of salt-induced adverse impact via mycorrhizal fungi in Ephedra aphylla Forssk. J Plant Interact. 2014;9:802–10.

Amagaya K, Shibuya T, Nishiyama M, Kato K, Kanayama Y. Characterization and expression analysis of the Ca2+/cation antiporter gene family in tomatoes. Plants. 2020;9:25.

Andrews, M. (1986). The partitioning of nitrate assimilation between root and shoot of higher plants. Plant, Cell & Environment, 9(7), 511-519.

Andrews, S. (2010). FastQC: a quality control tool for high throughput sequence data.

Annunziata MG, Ciarmiello LF, Woodrow P, Maximova E, Fuggi A, Carillo P. Durum wheat roots adapt to salinity remodeling the cellular content of nitrogen metabolites and sucrose. Front Plant Sci. 2017;7:2035.

Aroca R, Porcel R, Ruiz-Lozano JM. How does arbuscular mycorrhizal symbiosis regulate root hydraulic properties and plasma membrane aquaporins in Phaseolus vulgaris under drought, cold or salinity stresses? New Phytol. 2007;173:808–16.

Aslam, M., Travis, R. L., & Huffaker, R. C. (1992). Comparative kinetics and reciprocal inhibition of nitrate and nitrite uptake in roots of uninduced and induced barley (Hordeum vulgare L.) seedlings. Plant Physiology, 99(3), 1124-1133.

Asthir, B., Jain, D., Kaur, B., & Bain, N. S. (2017). Effect of nitrogen on starch and protein content in grain influence of nitrogen doses on grain starch and protein accumulation in diversified wheat genotypes. Journal of Environmental Biology, 38(3), 427.

Augé RM, Toler HD, Saxton AM. Arbuscular mycorrhizal symbiosis and osmotic adjustment in response to NaCl stress: a meta-analysis. Front Plant Sci. 2014;5:562.

Aziz, M. M., Palta, J. A., Siddique, K. H., & Sadras, V. O. (2017). Five decades of selection for yield reduced root length density and increased nitrogen uptake per unit root length in Australian wheat varieties. Plant and Soil, 413(1-2), 181-192.

Babst, B. A., Gao, F., Acosta-Gamboa, L. M., Karve, A., Schueller, M. J., & Lorence, A. (2019). Three NPF genes in Arabidopsis are necessary for normal nitrogen cycling under low nitrogen stress. Plant Physiology and Biochemistry, 143, 1-10.

Bagchi, R., Salehin, M., Adeyemo, O. S., Salazar, C., Shulaev, V., Sherrier, D. J., & Dickstein, R. (2012). Functional assessment of the Medicago truncatula NIP/LATD protein demonstrates that it is a high-affinity nitrate transporter. Plant physiology, 160(2), 906-916.

Bagchi, R., Salehin, M., Adeyemo, O. S., Salazar, C., Shulaev, V., Sherrier, D. J., & Dickstein, R. (2012). Functional assessment of the Medicago truncatula NIP/LATD protein demonstrates that it is a high-affinity nitrate transporter. Plant physiology, 160(2), 906-916.

Bai, H., Euring, D., Volmer, K., Janz, D., & Polle, A. (2013). The nitrate transporter (NRT) gene family in poplar. PloS one, 8(8), e72126.

Bailey, T. L., Johnson, J., Grant, C. E., & Noble, W. S. (2015). The MEME suite. Nucleic acids research, 43(W1), W39-W49.

Bajgain, P., Russell, B., & Mohammadi, M. (2018). Phylogenetic analyses and in-seedling expression of ammonium and nitrate transporters in wheat. Scientific reports, 8(1), 1-13.

Barraclough, P. B., Howarth, J. R., Jones, J., Lopez-Bellido, R., Parmar, S., Shepherd, C. E., & Hawkesford, M. J. (2010). Nitrogen efficiency of wheat: genotypic and environmental variation and prospects for improvement. European Journal of Agronomy, 33(1), 1-11.

Barros, L., Fernandes, Â., CFR Ferreira, I., Callejo, M., Matallana-González, M., Fernández-Ruiz, V., ... & Carrillo, J. M. (2020). Potential health claims of durum and bread wheat flours as functional ingredients. Nutrients, 12(2), 504.

Bateman, A., Coin, L., Durbin, R., Finn, R. D., Hollich, V., Griffiths-Jones, S., ... & Eddy, S. R. (2004). The Pfam protein families database. Nucleic acids research, 32(suppl_1), D138-D141.

Batistič O, Kudla J. Analysis of calcium signaling pathways in plants. Biochim Biophys Acta (BBA)-General Subj. 2012;1820:1283–93.

Begum N, Qin C, Ahanger MA, Raza S, Khan MI, Ashraf M, et al. Role of arbuscular mycorrhizal fungi in plant growth regulation: implications in abiotic stress tolerance. Front Plant Sci. 2019;10:1068.

Beltrano J, Ronco MG. Improved tolerance of wheat plants (Triticum aestivum L.) to drought stress and rewatering by the arbuscular mycorrhizal fungus Glomus claroideum: Effect on growth and cell membrane stability. Brazilian J Plant Physiol. 2008;20:29–37.

Bernard, S. M., & Habash, D. Z. (2009). The importance of cytosolic glutamine synthetase in nitrogen assimilation and recycling. New Phytologist, 182(3), 608-620.

Beusen, A. H. W., Bouwman, A. F., Heuberger, P. S. C., Van Drecht, G., & Van Der Hoek, K. W. (2008). Bottom-up uncertainty estimates of global ammonia emissions from global agricultural production systems. Atmospheric Environment, 42(24), 6067-6077.

Bi C, Yu Y, Dong C, Yang Y, Zhai Y, Du F, et al. The bZIP transcription factor TabZIP15 improves salt stress tolerance in wheat. Plant Biotechnol J. 2021;19:209.

Bitterlich M, Rouphael Y, Graefe J, Franken P. Arbuscular mycorrhizas: a promising component of plant production systems provided favorable conditions for their growth. Front Plant Sci. 2018;9:1329.

Bolger, A. M., Lohse, M., & Usadel, B. (2014). Trimmomatic: a flexible trimmer for Illumina sequence data. Bioinformatics, 30(15), 2114-2120.

Borrelli GM, Fragasso M, Nigro F, Platani C, Papa R, Beleggia R, et al. Analysis of metabolic and mineral changes in response to salt stress in durum wheat (Triticum turgidum ssp. durum) genotypes, which differ in salinity tolerance. Plant Physiol Biochem. 2018;133:57–70.

Bouguyon, E., Brun, F., Meynard, D., Kubeš, M., Pervent, M., Leran, S., ... & Gojon, A. (2015). Multiple mechanisms of nitrate sensing by Arabidopsis nitrate transceptor NRT1. 1. Nature Plants, 1(3), 1-8.

Bouguyon, E., Gojon, A., & Nacry, P. (2012, August). Nitrate sensing and signaling in plants. In Seminars in cell & developmental biology (Vol. 23, No. 6, pp. 648-654). Academic Press.

Bouwman, A. F., Boumans, L. J. M., & Batjes, N. H. (2002). Emissions of N2O and NO from fertilized fields: Summary of available measurement data. Global biogeochemical cycles, 16(4), 6-1.

Bouwman, Alexander F.; Boumans, L. J. M.; Batjes, Niels H. 2002. “Emissions of N2O and NO from Fertilized Fields: Summary of Available Measurement Data.” Global Biogeochemical Cycles 16(4): 6–1.

Brancourt-Hulmel, M., Doussinault, G., Lecomte, C., Bérard, P., Le Buanec, B., & Trottet, M. (2003). Genetic improvement of agronomic traits of winter wheat cultivars released in France from 1946 to 1992. Crop science, 43(1), 37-45.

Brancourt-Hulmel, Maryse; Doussinault, G.; Lecomte, Christophe; Bérard, P.; Le Buanec, B.; Trottet, Maxime. 2003. “Genetic Improvement of Agronomic Traits of Winter Wheat Cultivars Released in France from 1946 to 1992.” Crop Science 43(1): 37–45.

Brenchley, R., Spannagl, M., Pfeifer, M., Barker, G. L., D’Amore, R., Allen, A. M., ... & Hall, N. (2012). Analysis of the bread wheat genome using whole-genome shotgun sequencing. Nature, 491(7426), 705-710.

Brendolise, C., Espley, R. V., Lin-Wang, K., Laing, W., Peng, Y., McGhie, T., ... & Allan, A. C. (2017). Multiple copies of a simple MYB-binding site confers trans-regulation by specific flavonoid-related R2R3 MYBs in diverse species. Frontiers in plant science, 8, 1864.

Brini F, Hanin M, Lumbreras V, Amara I, Khoudi H, Hassairi A, et al. Overexpression of wheat dehydrin DHN-5 enhances tolerance to salt and osmotic stress in Arabidopsis thaliana. Plant Cell Rep. 2007;26:2017–26.

Brownlee, A. G., & Arst Jr, H. N. (1983). Nitrate uptake in Aspergillus nidulans and involvement of the third gene of the nitrate assimilation gene cluster. Journal of bacteriology, 155(3), 1138-1146.

Buchner, P., & Hawkesford, M. J. (2014). Complex phylogeny and gene expression patterns of members of the NITRATE TRANSPORTER 1/PEPTIDE TRANSPORTER family (NPF) in wheat. Journal of experimental botany, 65(19), 5697-5710.

Cabral C, Ravnskov S, Tringovska I, Wollenweber B. Arbuscular mycorrhizal fungi modify nutrient allocation and composition in wheat (Triticum aestivum L.) subjected to heat-stress. Plant Soil. 2016;408:385–99.

Cacco, G., Attinà, E., Gelsomino, A., & Sidari, M. (2000). Effect of nitrate and humic substances of different molecular size on kinetic parameters of nitrate uptake in wheat seedlings. Journal of plant nutrition and soil science, 163(3), 313-320.

Cai, C., Wang, J. Y., Zhu, Y. G., Shen, Q. R., Li, B., Tong, Y. P., & Li, Z. S. (2008). Gene structure and expression of the high-affinity nitrate transport system in rice roots. Journal of Integrative Plant Biology, 50(4), 443-451.

Calderini, Daniel F.; Torres-León, Santiago; Slafer, Gustavo A. 1995. "Consequences of Wheat Breeding on Nitrogen and Phosphorus Yield, Grain Nitrogen and Phosphorus Concentration and Associated Traits." Annals of Botany 76(3): 315–22.

Cameron, K. C., Di, H. J., & Moir, J. L. (2013). Nitrogen losses from the soil/plant system: a review. Annals of applied biology, 162(2), 145-173.

Cannon, S. B., Mitra, A., Baumgarten, A., Young, N. D., & May, G. (2004). The roles of segmental and tandem gene duplication in the evolution of large gene families in Arabidopsis thaliana. BMC plant biology, 4(1), 1-21.

Cantarella, H., Otto, R., Soares, J. R., & de Brito Silva, A. G. (2018). Agronomic efficiency of NBPT as a urease inhibitor: A review. Journal of advanced research, 13, 19-27.

Capriotti AL, Borrelli GM, Colapicchioni V, Papa R, Piovesana S, Samperi R, et al. Proteomic study of a tolerant genotype of durum wheat under salt-stress conditions. Anal Bioanal Chem. 2014;406:1423–35.

Castaings, L., Camargo, A., Pocholle, D., Gaudon, V., Texier, Y., Boutet-Mercey, S., ... & Krapp, A. (2009). The nodule inception-like protein 7 modulates nitrate sensing and metabolism in Arabidopsis. The Plant Journal, 57(3), 426-435.

Castillo, F., Dobao, M. M., Reyes, F., Blasco, R., Roldan, M. D., Gavira, M., ... & Martínez-Luque, M. (1996). Molecular and regulatory properties of the nitrate reducing systems of Rhodobacter. Current microbiology, 33(6), 341-346.

Cedergreen, N., & Madsen, T. V. (2003). Nitrate reductase activity in roots and shoots of aquatic macrophytes. Aquatic Botany, 76(3), 203-212.

Cerezo, M., Tillard, P., Filleur, S., Munos, S., Daniel-Vedele, F., & Gojon, A. (2001). Major alterations of the regulation of root NO3− uptake are associated with the mutation of Nrt2. 1 and Nrt2. 2 genes in Arabidopsis. Plant Physiology, 127(1), 262-271.

Chakrabortee S, Tripathi R, Watson M, Schierle GSK, Kurniawan DP, Kaminski CF, et al. Intrinsically disordered proteins as molecular shields. Mol Biosyst. 2012;8:210–9.

Chandrasekaran M, Chanratana M, Kim K, Seshadri S, Sa T. Impact of arbuscular mycorrhizal fungi on photosynthesis, water status, and gas exchange of plants under salt stress–a meta-analysis. Front Plant Sci. 2019;10:457.

Chao, J., Li, Z., Sun, Y., Aluko, O. O., Wu, X., Wang, Q., & Liu, G. (2021). MG2C: a user-friendly online tool for drawing genetic maps. Molecular Horticulture, 1(1), 1-4.

Chen J, Zhang H, Zhang X, Tang M. Arbuscular mycorrhizal symbiosis alleviates salt stress in black locust through improved photosynthesis, water status, and K+/Na+ homeostasis. Front Plant Sci. 2017;8:1739.

Chen, H., Zhang, Q., Cai, H., Zhou, W., & Xu, F. (2018). H2O2 mediates nitrate-induced iron chlorosis by regulating iron homeostasis in rice. Plant, Cell & Environment, 41(4), 767-781.

Chen, J. H., Jiang, H. W., Hsieh, E. J., Chen, H. Y., Chien, C. T., Hsieh, H. L., & Lin, T. P. (2012). Drought and salt stress tolerance of an Arabidopsis glutathione S-transferase U17 knockout mutant are attributed to the combined effect of glutathione and abscisic acid. Plant Physiology, 158(1), 340-351.

Chen, J., Zhang, Y., Tan, Y., Zhang, M., Zhu, L., Xu, G., & Fan, X. (2016). Agronomic nitrogen-use efficiency of rice can be increased by driving Os NRT 2.1 expression with the Os NAR 2.1 promoter. Plant Biotechnology Journal, 14(8), 1705-1715.

Chen, K. E., Chen, H. Y., Tseng, C. S., & Tsay, Y. F. (2020). Improving nitrogen use efficiency by manipulating nitrate remobilization in plants. Nature Plants, 6(9), 1126-1135.

Chiba, Y., Shimizu, T., Miyakawa, S., Kanno, Y., Koshiba, T., Kamiya, Y., & Seo, M. (2015). Identification of Arabidopsis thaliana NRT1/PTR FAMILY (NPF) proteins capable of transporting plant hormones. Journal of plant research, 128(4), 679-686.

Chung WS, Lee SH, Kim JC, Do Heo W, Kim MC, Park CY, et al. Identification of a calmodulin-regulated soybean Ca2+-ATPase (SCA1) that is located in the plasma membrane. Plant Cell. 2000;12:1393–407.

Congreves, K. A., Otchere, O., Ferland, D., Farzadfar, S., Williams, S., & Arcand, M. M. (2021). Nitrogen use efficiency definitions of today and tomorrow. Frontiers in Plant Science, 12.

Cormier, F., Foulkes, J., Hirel, B., Gouache, D., Moënne-Loccoz, Y., & Le Gouis, J. (2016). Breeding for increased nitrogen-use efficiency: a review for wheat (T. aestivum L.). Plant Breeding, 135(3), 255-278.

Corratgé-Faillie, C., & Lacombe, B. (2017). Substrate (un) specificity of Arabidopsis NRT1/PTR FAMILY (NPF) proteins. Journal of Experimental Botany, 68(12), 3107-3113.

Corso M, Doccula FG, de Melo JRF, Costa A, Verbruggen N. Endoplasmic reticulum-localized CCX2 is required for osmotolerance by regulating ER and cytosolic Ca2+ dynamics in Arabidopsis. Proc Natl Acad Sci. 2018;115:3966–71.

Crawford, N. M., & Glass, A. D. (1998). Molecular and physiological aspects of nitrate uptake in plants. Trends in plant science, 3(10), 389-395.

Curci, P. L., Cigliano, R. A., Zuluaga, D. L., Janni, M., Sanseverino, W., & Sonnante, G. (2017). Transcriptomic response of durum wheat to nitrogen starvation. Scientific reports, 7(1), 1-14.

De Angeli, A., Monachello, D., Ephritikhine, G., Frachisse, J. M., Thomine, S., Gambale, F., & Barbier-Brygoo, H. (2006). The nitrate/proton antiporter AtCLCa mediates nitrate accumulation in plant vacuoles. Nature, 442(7105), 939-942.

de Lacerda CF, Cambraia J, Oliva MA, Ruiz HA. Changes in growth and in solute concentrations in sorghum leaves and roots during salt stress recovery. Environ Exp Bot. 2005;54:69–76.

De Vita, P., & Taranto, F. (2019). Durum wheat (Triticum turgidum ssp. durum) breeding to meet the challenge of climate change. In Advances in plant breeding strategies: cereals (pp. 471-524). Springer, Cham.

De Vita, Pasquale; Nicosia, Orazio Li Destri; Nigro, Franca; Platani, Cristiano; Riefolo, Carmen; Di Fonzo, Natale; Cattivelli, Luigi. (2007). "Breeding Progress in Morpho-Physiological, Agronomical and Qualitative Traits of Durum Wheat Cultivars Released in Italy during the 20th Century." European Journal of Agronomy 26(1): 39–53.

Deng F, Zhang X, Wang W, Yuan R, Shen F. Identification of Gossypium hirsutum long non-coding RNAs (lncRNAs) under salt stress. BMC Plant Biol. 2018;18:1–14.

Dobin A, Davis CA, Schlesinger F, Drenkow J, Zaleski C, Jha S, et al. STAR: ultrafast universal RNA-seq aligner. Bioinformatics. 2013;29:15–21.

Dobriyal, Pariva; Qureshi, Ashi; Badola, Ruchi; Hussain, Syed Ainul. 2012. "A Review of the Methods Available for Estimating Soil Moisture and Its Implications for Water Resource Management." Journal of Hydrology 458(NA): 110–17.

Duan, J., Tian, H., & Gao, Y. (2016). Expression of nitrogen transporter genes in roots of winter wheat (Triticum aestivum L.) in response to soil drought with contrasting nitrogen supplies. Crop and Pasture Science, 67(2), 128-136.

Dubcovsky, J., & Dvorak, J. (2007). Genome plasticity a key factor in the success of polyploid wheat under domestication. Science, 316(5833), 1862-1866.

El-Amri SM, Al-Whaibi MH, Abdel-Fattah GM, Siddiqui MH. Role of mycorrhizal fungi in tolerance of wheat genotypes to salt stress. African J Microbiol Res. 2013;7:1286–95.

Estrada B, Aroca R, Maathuis FJM, Barea JM, RUIZ-LOZANO JM. Arbuscular mycorrhizal fungi native from a M editerranean saline area enhance maize tolerance to salinity through improved ion homeostasis. Plant Cell Environ. 2013;36:1771–82.

Evelin, H., Devi, T. S., Gupta, S., & Kapoor, R. (2019). Mitigation of salinity stress in plants by arbuscular mycorrhizal symbiosis: current understanding and new challenges. Frontiers in Plant Science, 10, 470.

Evelin, H., Giri, B., & Kapoor, R. (2013). Ultrastructural evidence for AMF mediated salt stress mitigation in Trigonella foenum-graecum. Mycorrhiza, 23(1), 71-86.

Fageria, N. K. (2014). Nitrogen harvest index and its association with crop yields. Journal of plant nutrition, 37(6), 795-810.

Fageria, N. K., Baligar, V. C., & Li, Y. C. (2008). The role of nutrient efficient plants in improving crop yields in the twenty first century. Journal of plant nutrition, 31(6), 1121-1157.

Fan, S. C., Lin, C. S., Hsu, P. K., Lin, S. H., & Tsay, Y. F. (2009). The Arabidopsis nitrate transporter NRT1. 7, expressed in phloem, is responsible for source-to-sink remobilization of nitrate. The Plant Cell, 21(9), 2750-2761.

Fan, X., Tang, Z., Tan, Y., Zhang, Y., Luo, B., Yang, M., ... & Xu, G. (2016). Overexpression of a pH-sensitive nitrate transporter in rice increases crop yields. Proceedings of the National Academy of Sciences, 113(26), 7118-7123.

FAO-AMIS, Food and Agriculture Organization of the United Nations - Agricultural Market Information System [WWW Document], URL http://statistics.amis-outlook.org/data/index.html#DOWNLOAD. (Accessed 2.20.2018).

Faris, J. D. (2014). Wheat domestication: Key to agricultural revolutions past and future. In Genomics of plant genetic resources (pp. 439-464). Springer, Dordrecht.

Feng, H., Fan, X., Yan, M., Liu, X., Miller, A. J., & Xu, G. (2011). Multiple roles of nitrate transport accessory protein NAR2 in plants. Plant signaling & behavior, 6(9), 1286-1289.

Fileccia V, Ruisi P, Ingraffia R, Giambalvo D, Frenda AS, Martinelli F. Arbuscular mycorrhizal symbiosis mitigates the negative effects of salinity on durum wheat. PLoS One. 2017;12:e0184158.

Forde, B. G. (2000). Nitrate transporters in plants: structure, function and regulation. Biochimica et Biophysica Acta (BBA)-Biomembranes, 1465(1-2), 219-235.

Forde, B. G., & Lea, P. J. (2007). Glutamate in plants: metabolism, regulation, and signalling. Journal of experimental botany, 58(9), 2339-2358.

Foulkes, M. J., Hawkesford, M. J., Barraclough, P. B., Holdsworth, M. J., Kerr, S., Kightley, S., & Shewry, P. R. (2009). Identifying traits to improve the nitrogen economy of wheat: Recent advances and future prospects. Field Crops Research, 114(3), 329-342.

Foulkes, M. J., Sylvester-Bradley, R., & Scott, R. K. (1998). Evidence for differences between winter wheat cultivars in acquisition of soil mineral nitrogen and uptake and utilization of applied fertilizer nitrogen. The Journal of Agricultural Science, 130(1), 29-44.

Fredes, I., Moreno, S., Díaz, F. P., & Gutiérrez, R. A. (2019). Nitrate signaling and the control of Arabidopsis growth and development. Current opinion in plant biology, 47, 112-118.

Fu, Y. B. (2015). Understanding crop genetic diversity under modern plant breeding. Theoretical and Applied Genetics, 128(11), 2131-2142.

Gaju, O., Allard, V., Martre, P., Le Gouis, J., Moreau, D., Bogard, M., ... & Foulkes, M. J. (2014). Nitrogen partitioning and remobilization in relation to leaf senescence, grain yield and grain nitrogen concentration in wheat cultivars. Field Crops Research, 155, 213-223.

Gaju, O., Allard, V., Martre, P., Snape, J. W., Heumez, E., LeGouis, J., ... & Foulkes, M. J. (2011). Identification of traits to improve the nitrogen-use efficiency of wheat genotypes. Field Crops Research, 123(2), 139-152.

Gangappa, S. N., & Botto, J. F. (2014). The BBX family of plant transcription factors. Trends in plant science, 19(7), 460-470.

Gao, Y., Xu, Z., Zhang, L., Li, S., Wang, S., Yang, H., ... & Zhou, Y. (2020). MYB61 is regulated by GRF4 and promotes nitrogen utilization and biomass production in rice. Nature communications, 11(1), 1-12.

Garg N, Pandey R. High effectiveness of exotic arbuscular mycorrhizal fungi is reflected in improved rhizobial symbiosis and trehalose turnover in Cajanus cajan genotypes grown under salinity stress. Fungal Ecol. 2016;21:57–67.

Garnett, Trevor; Conn, Vanessa M.; Kaiser, Brent N. 2009. "Root Based Approaches to Improving Nitrogen Use Efficiency in Plants." Plant, cell & environment 32(9): 1272–83.

Gastal, François; Lemaire, Gilles. 2002. "N Uptake and Distribution in Crops: An Agronomical and Ecophysiological Perspective." Journal of experimental botany 53(370): 789–99.

Ge, S. X., Jung, D., & Yao, R. (2020). ShinyGO: a graphical gene-set enrichment tool for animals and plants. Bioinformatics, 36(8), 2628-2629.

Geelen, D., Lurin, C., Bouchez, D., Frachisse, J. M., Lelièvre, F., Courtial, B., ... & Maurel, C. (2000). Disruption of putative anion channel gene AtCLC-a in Arabidopsis suggests a role in the regulation of nitrate content. The Plant Journal, 21(3), 259-267.

Gelli, M., Duo, Y., Konda, A. R., Zhang, C., Holding, D., & Dweikat, I. (2014). Identification of differentially expressed genes between sorghum genotypes with contrasting nitrogen stress tolerance by genome-wide transcriptional profiling. BMC genomics, 15(1), 1-16.

Giambalvo, D., Ruisi, P., Di Miceli, G., Frenda, A. S., & Amato, G. (2010). Nitrogen use efficiency and nitrogen fertilizer recovery of durum wheat genotypes as affected by interspecific competition. Agronomy Journal, 102(2), 707-715.

Gill SS, Tuteja N. Reactive oxygen species and antioxidant machinery in abiotic stress tolerance in crop plants. Plant Physiol Biochem. 2010;48:909–30.

Giovannetti M, Mosse B. An evaluation of techniques for measuring vesicular arbuscular mycorrhizal infection in roots. New Phytol. 1980; 84: 489–500.

Glass, A. D., Shaff, J. E., & Kochian, L. V. (1992). Studies of the uptake of nitrate in barley: IV. Electrophysiology. Plant Physiology, 99(2), 456-463.

Goel, P., Sharma, N. K., Bhuria, M., Sharma, V., Chauhan, R., Pathania, S., ... & Singh, A. K. (2018). Transcriptome and co-expression network analyses identify key genes regulating nitrogen use efficiency in Brassica juncea L. Scientific Reports, 8(1), 1-18.

Gojon, A., Krouk, G., Perrine-Walker, F., & Laugier, E. (2011). Nitrate transceptor (s) in plants. Journal of experimental botany, 62(7), 2299-2308.

Gojon, A., Plassard, C., & Bussi, C. (1994). Root/shoot distribution of NO3-. Assimilation in herbaceous and woody species.

Golldack D, Li C, Mohan H, Probst N. Tolerance to drought and salt stress in plants: unraveling the signaling networks. Front Plant Sci. 2014;5:151.

Gomez, I., Pedreño, J. N., Moral, R., Iborra, M. R., Palacios, G., & Mataix, J. (1996). Salinity and nitrogen fertilization affecting the macronutrient content and yield of sweet pepper plants. Journal of plant nutrition, 19(2), 353-359.

Gondim FA, Gomes-Filho E, Costa JH, Alencar NLM, Prisco JT. Catalase plays a key role in salt stress acclimation induced by hydrogen peroxide pretreatment in maize. Plant Physiol Biochem. 2012;56:62–71.

Goyal, S. S., & Huffaker, R. C. (1986). The uptake of NO3−, NO2−, and NH4+ by intact wheat (Triticum aestivum) seedlings: I. Induction and kinetics of transport systems. Plant Physiology, 82(4), 1051-1056.

Grindlay, Douglas J.C. 1997. “REVIEW Towards an Explanation of Crop Nitrogen Demand Based on the Optimization of Leaf Nitrogen per Unit Leaf Area.” The Journal of Agricultural Science 128(4): 377–96.

Guarda, G., Padovan, S., & Delogu, G. (2004). Grain yield, nitrogen-use efficiency and baking quality of old and modern Italian bread-wheat cultivars grown at different nitrogen levels. European Journal of Agronomy, 21(2), 181-192.

Guo, B. B., Liu, B. C., He, L., Wang, Y. Y., Feng, W., Zhu, Y. J., ... & Guo, T. C. (2019A). Root and nitrate-N distribution and optimization of N input in winter wheat. Scientific Reports, 9(1), 1-12.

Guo, H., Tian, Z., Sun, S., Li, Y., Jiang, D., Cao, W., & Dai, T. (2019B). Preanthesis root growth and nitrogen uptake improved wheat grain yield and nitrogen use efficiency. Agronomy Journal, 111(6), 3048-3056.

Gustafson, P., Raskina, O., Ma, X., & Nevo, E. (2009). Wheat evolution, domestication, and improvement. Wheat: science and trade. Wiley, Danvers, 5-30.

Gutiérrez, R. A., Gifford, M. L., Poultney, C., Wang, R., Shasha, D. E., Coruzzi, G. M., & Crawford, N. M. (2007). Insights into the genomic nitrate response using genetics and the Sungear Software System. Journal of Experimental Botany, 58(9), 2359-2367.

Guttieri, M. J., Frels, K., Regassa, T., Waters, B. M., & Baenziger, P. S. (2017). Variation for nitrogen use efficiency traits in current and historical great plains hard winter wheat. Euphytica, 213(4), 1-18.

Habash, D. Z., Baudo, M., Hindle, M., Powers, S. J., Defoin-Platel, M., Mitchell, R., ... & Nachit, M. M. (2014). Systems responses to progressive water stress in durum wheat. PLoS One, 9(9), e108431.

Han, Y. L., Song, H. X., Liao, Q., Yu, Y., Jian, S. F., Lepo, J. E., ... & Zhang, Z. H. (2016). Nitrogen use efficiency is mediated by vacuolar nitrate sequestration capacity in roots of Brassica napus. Plant Physiology, 170(3), 1684-1698.

Hao, Q. N., Zhou, X. A., Sha, A. H., Wang, C., Zhou, R., & Chen, S. L. (2011). Identification of genes associated with nitrogen-use efficiency by genome-wide transcriptional analysis of two soybean genotypes. BMC genomics, 12(1), 1-15.

Hatje, K., Keller, O., Hammesfahr, B., Pillmann, H., Waack, S., & Kollmar, M. (2011). Cross-species protein sequence and gene structure prediction with fine-tuned Webscipio 2.0 and Scipio. BMC research notes, 4(1), 1-20.

Hawkins, J., & Bodén, M. (2006). Detecting and sorting targeting peptides with neural networks and support vector machines. Journal of bioinformatics and computational biology, 4(01), 1-18.

Herridge, D. F., Peoples, M. B., & Boddey, R. M. (2008). Global inputs of biological nitrogen fixation in agricultural systems. Plant and soil, 311(1), 1-18.

Hildebrandt, U., Schmelzer, E., & Bothe, H. (2002). Expression of nitrate transporter genes in tomato colonized by an arbuscular mycorrhizal fungus. Physiologia Plantarum, 115(1), 125-136.

Hirel, B., Tétu, T., Lea, P. J., & Dubois, F. (2011). Improving nitrogen use efficiency in crops for sustainable agriculture. Sustainability, 3(9), 1452-1485.

Ho, C. H., Lin, S. H., Hu, H. C., & Tsay, Y. F. (2009). CHL1 functions as a nitrate sensor in plants. Cell, 138(6), 1184-1194.

Ho, J., Tumkaya, T., Aryal, S., Choi, H., & Claridge-Chang, A. (2019). Moving beyond P values: data analysis with estimation graphics. Nature methods, 16(7), 565-566.

Horton, P., Park, K. J., Obayashi, T., Fujita, N., Harada, H., Adams-Collier, C. J., & Nakai, K. (2007). WoLF PSORT: protein localization predictor. Nucleic acids research, 35(suppl_2), W585-W587.

Hsu, P. K., & Tsay, Y. F. (2013). Two phloem nitrate transporters, NRT1. 11 and NRT1. 12, are important for redistributing xylem-borne nitrate to enhance plant growth. Plant Physiology, 163(2), 844-856.

Hu, B., Wang, W., Ou, S., Tang, J., Li, H., Che, R., ... & Chu, C. (2015). Variation in NRT1. 1B contributes to nitrate-use divergence between rice subspecies. Nature Genetics, 47(7), 834-838.

Hu, D. G., Ma, Q. J., Sun, C. H., Sun, M. H., You, C. X., & Hao, Y. J. (2016). Overexpression of MdSOS2L1, a CIPK protein kinase, increases the antioxidant metabolites to enhance salt tolerance in apple and tomato. Physiologia plantarum, 156(2), 201-214.

Hu, H. C., Wang, Y. Y., & Tsay, Y. F. (2009). AtCIPK8, a CBL-interacting protein kinase, regulates the low-affinity phase of the primary nitrate response. The Plant Journal, 57(2), 264-278.

Hu, H., Dai, M., Yao, J., Xiao, B., Li, X., Zhang, Q., & Xiong, L. (2006). Overexpressing a NAM, ATAF, and CUC (NAC) transcription factor enhances drought resistance and salt tolerance in rice. Proceedings of the National Academy of Sciences, 103(35), 12987-12992.

Huang, J. G., Yang, M., Liu, P., YANG, G. D., WU, C. A., & ZHENG, C. C. (2009). GhDREB1 enhances abiotic stress tolerance, delays GA-mediated development and represses cytokinin signalling in transgenic Arabidopsis. Plant, cell & environment, 32(8), 1132-1145.

Huang, Y., Zhao, H., Gao, F., Yao, P., Deng, R., Li, C., ... & Wu, Q. (2018). A R2R3-MYB transcription factor gene, FtMYB13, from Tartary buckwheat improves salt/drought tolerance in Arabidopsis. Plant Physiology and Biochemistry, 132, 238-248.

Huda KMK, Banu MSA, Garg B, Tula S, Tuteja R, Tuteja N. Os ACA 6, a P-type IIB Ca2+ ATP ase promotes salinity and drought stress tolerance in tobacco by ROS scavenging and enhancing the expression of stress-responsive genes. Plant J. 2013;76:997–1015.

Huggins, D. R., & Pan, W. L. (1993). Nitrogen efficiency component analysis: an evaluation of cropping system differences in productivity. *Agronomy Journal*, *85*(4), 898-905.

Hussain, A. B. I. D., Ghaudhry, M. R., Wajad, A., Ahmed, A., Rafiq, M. U. H. A. M. M. A. D., Ibrahim, M. U. H. A. M. M. A. D., & Goheer, A. R. (2004). Influence of water stress on growth, yield and radiation use efficiency of various wheat cultivars. Intl. J. Agric. Biol, 6, 1074-1079.

Ierna, A., Lombardo, G. M., & Mauromicale, G. (2016). Yield, nitrogen use efficiency and grain quality in durum wheat as affected by nitrogen fertilization under a Mediterranean environment. Experimental Agriculture, 52(2), 314-329.

Ingraffia, R., Amato, G., Frenda, A. S., & Giambalvo, D. (2019). Impacts of arbuscular mycorrhizal fungi on nutrient uptake, N2 fixation, N transfer, and growth in a wheat/faba bean intercropping system. PLoS One, 14(3), e0213672.

Ingraffia, R., Amato, G., Sosa-Hernández, M. A., Frenda, A. S., Rillig, M. C., & Giambalvo, D. (2020). Nitrogen type and availability drive mycorrhizal effects on wheat performance, nitrogen uptake and recovery, and production sustainability. Frontiers in plant science, 760.

International Wheat Genome Sequencing Consortium. (2014). A chromosome-based draft sequence of the hexaploid bread wheat (Triticum aestivum) genome. Science, 345(6194).

Jahromi, F., Aroca, R., Porcel, R., & Ruiz-Lozano, J. M. (2008). Influence of salinity on the in vitro development of Glomus intraradices and on the in vivo physiological and molecular responses of mycorrhizal lettuce plants. Microbial Ecology, 55(1), 45-53.

Jørgensen, M. E., Xu, D., Crocoll, C., Ernst, H. A., Ramírez, D., Motawia, M. S., ... & Halkier, B. A. (2017). Origin and evolution of transporter substrate specificity within the NPF family. Elife, 6, e19466.

Ju, X. T., Xing, G. X., Chen, X. P., Zhang, S. L., Zhang, L. J., Liu, X. J., ... & Zhang, F. S. (2009). Reducing environmental risk by improving N management in intensive Chinese agricultural systems. Proceedings of the National Academy of Sciences, 106(9), 3041-3046.

Kamiji, Yoshiaki; Pang, Jiayin; Milroy, Stephen P.; Palta, Jairo A. 2014. “Shoot Biomass in Wheat Is the Driver for Nitrogen Uptake under Low Nitrogen Supply, but Not under High Nitrogen Supply.” Field Crops Research 165(NA): 92–98.

Kant, S. (2018, February). Understanding nitrate uptake, signaling and remobilisation for improving plant nitrogen use efficiency. In Seminars in Cell & Developmental Biology (Vol. 74, pp. 89-96). Academic Press.

Kaur, A., Pati, P. K., Pati, A. M., & Nagpal, A. K. (2017). In-silico analysis of cis-acting regulatory elements of pathogenesis-related proteins of Arabidopsis thaliana and Oryza sativa. PloS one, 12(9), e0184523.

Kautz, Timo; Amelung, Wulf; Ewert, Frank; Gaiser, Thomas; Horn, Rainer; Jahn, Reinhold; Javaux, M.; Kemna, Andreas; Kuzyakov, Yakov; Munch, J.C.; Pätzold, Stefan; Peth, Stephan; Scherer, Heinrich W.; Schloter, Michael; Schneider, Heike U.; Vanderborght, Jan; Vetterlein, Doris; Walter, Achim; Wiesenberg, Guido L. B.; Köpke, Ulrich. 2013. “Nutrient Acquisition from Arable Subsoils in Temperate Climates: A Review.” Soil Biology and Biochemistry 57(NA): 1003–22.

Keneni, G., Bekele, E., Imtiaz, M., & Dagne, K. (2012). Genetic vulnerability of modern crop cultivars: causes, mechanism and remedies. Int J Plant Res, 2(3), 69-79.

Khan MS. The role of DREB transcription factors in abiotic stress tolerance of plants. Biotechnol Biotechnol Equip. 2011;25:2433–42.

Khassanova G, Kurishbayev A, Jatayev S, Zhubatkanov A, Zhumalin A, Turbekova A, et al. Intracellular vesicle trafficking genes, RabC-GTP, are highly expressed under salinity and rapid dehydration but down-regulated by drought in leaves of chickpea (Cicer arietinum L.). Front Genet. 2019;10:40.

Kim H-S, Lee JH, Kim JJ, Kim C-H, Jun S-S, Hong Y-N. Molecular and functional characterization of CaLEA6, the gene for a hydrophobic LEA protein from Capsicum annuum. Gene. 2005;344:115–23.

Kinnersley AM, Turano FJ. Gamma aminobutyric acid (GABA) and plant responses to stress. CRC Crit Rev Plant Sci. 2000;19:479–509.

Kirkegaard, John A.; Lilley, J. M.; Howe, G. N.; Graham, J. M. 2007. “Impact of Subsoil Water Use on Wheat Yield.” Australian Journal of Agricultural Research 58(4): 303–15.

Konishi, M., & Yanagisawa, S. (2010). Identification of a nitrate-responsive cis-element in the Arabidopsis NIR1 promoter defines the presence of multiple cis-regulatory elements for nitrogen response. The Plant Journal, 63(2), 269-282.

Kosová, K., Urban, M. O., Vítámvás, P., & Prášil, I. T. (2016). Drought stress response in common wheat, durum wheat, and barley: transcriptomics, proteomics, metabolomics, physiology, and breeding for an enhanced drought tolerance. In Drought Stress Tolerance in Plants, Vol 2 (pp. 277-314). Springer, Cham.

Kotur, Z., & Glass, A. D. (2015). A 150 kDa plasma membrane complex of AtNRT 2.5 and AtNAR 2.1 is the major contributor to constitutive high-affinity nitrate influx in A rabidopsis thaliana. Plant, cell & environment, 38(8), 1490-1502.

Kristensen, H. L., & Thorup-Kristensen, K. (2004A). Uptake of15N labeled nitrate by root systems of sweet corn, carrot and white cabbage from 0.2–2.5 meters depth. Plant and Soil, 265(1), 93-100.

Kristensen, H. L., & Thorup-Kristensen, K. (2004B). Root growth and nitrate uptake of three different catch crops in deep soil layers. Soil Science Society of America Journal, 68, 529-537.

Krogh, A., Larsson, B., Von Heijne, G., & Sonnhammer, E. L. (2001). Predicting transmembrane protein topology with a hidden Markov model: application to complete genomes. Journal of molecular biology, 305(3), 567-580.

Kronzucker, H. J., Siddiqi, M. Y., & Glass, A. D. (1995). Kinetics of NO3-influx in spruce. Plant Physiology, 109(1), 319-326.

Krouk, G., Mirowski, P., LeCun, Y., Shasha, D. E., & Coruzzi, G. M. (2010). Predictive network modeling of the high-resolution dynamic plant transcriptome in response to nitrate. Genome biology, 11(12), 1-19.

Kumari, S., & Raghuram, N. (2020). Protein phosphatases in N response and NUE in crops. Protein Phosphatases and Stress Management in Plants, 233-244.

Kyriakou, V., Garagounis, I., Vourros, A., Vasileiou, E., & Stoukides, M. (2020). An electrochemical haber-bosch process. Joule, 4(1), 142-158.

Lamichhane, Suman; Murata, Chiaki; Griffey, Carl A.; Thomason, Wade Everett; Fukao, Takeshi. 2021. “Physiological and Molecular Traits Associated with Nitrogen Uptake under Limited Nitrogen in Soft Red Winter Wheat.” Plants (Basel, Switzerland) 10(1): 165-NA.

Langfelder, P., & Horvath, S. (2008). WGCNA: an R package for weighted correlation network analysis. BMC bioinformatics, 9(1), 1-13.

Le Gouis, J., Béghin, D., Heumez, E., & Pluchard, P. (2000). Genetic differences for nitrogen uptake and nitrogen utilisation efficiencies in winter wheat. European Journal of Agronomy, 12(3-4), 163-173.

Lezhneva, L., Kiba, T., Feria-Bourrellier, A. B., Lafouge, F., Boutet-Mercey, S., Zoufan, P., ... & Krapp, A. (2014). The Arabidopsis nitrate transporter NRT 2.5 plays a role in nitrate acquisition and remobilization in nitrogen-starved plants. The Plant Journal, 80(2), 230-241.

Li, M., Tian, H., & Gao, Y. (2021). A genome-wide analysis of NPF and NRT2 transporter gene families in bread wheat provides new insights into the distribution, function, regulation and evolution of nitrate transporters. Plant and Soil, 1-17.

Li, T., Liao, K., Xu, X., Gao, Y., Wang, Z., Zhu, X., ... & Xuan, Y. (2017). Wheat Ammonium Transporter (AMT) Gene family: diversity and possible role in host–pathogen interaction with stem rust. Frontiers in plant science, 8, 1637.

Li, W., He, X., Chen, Y., Jing, Y., Shen, C., Yang, J., ... & Tong, Y. (2020). A wheat transcription factor positively sets seed vigour by regulating the grain nitrate signal. New Phytologist, 225(4), 1667-1680.

Li, W., Wang, Y., Okamoto, M., Crawford, N. M., Siddiqi, M. Y., & Glass, A. D. (2007). Dissection of the AtNRT2. 1: AtNRT2. 2 inducible high-affinity nitrate transporter gene cluster. Plant physiology, 143(1), 425-433.

Liao, M., Fillery, I. R., & Palta, J. A. (2004). Early vigorous growth is a major factor influencing nitrogen uptake in wheat. Functional Plant Biology, 31(2), 121-129.

Liao, W. B., Xiao, H. L., & Zhang, M. L. (2010). Effect of nitric oxide and hydrogen peroxide on adventitious root development from cuttings of ground-cover chrysanthemum and associated biochemical changes. Journal of Plant Growth Regulation, 29(3), 338-348.

Liao, W., Xiao, H., & Zhang, M. (2009). Role and relationship of nitric oxide and hydrogen peroxide in adventitious root development of marigold. Acta Physiologiae Plantarum, 31(6), 1279-1289.

Limaux, F., Recous, S., Meynard, J. M., & Guckert, A. (1999). Relationship between rate of crop growth at date of fertiliser N application and fate of fertiliser N applied to winter wheat. Plant and Soil, 214(1), 49-59.

Lin, S. H., Kuo, H. F., Canivenc, G., Lin, C. S., Lepetit, M., Hsu, P. K., ... & Tsay, Y. F. (2008). Mutation of the Arabidopsis NRT1. 5 nitrate transporter causes defective root-to-shoot nitrate transport. The Plant Cell, 20(9), 2514-2528.

Lindemose, S., O'Shea, C., Jensen, M. K., & Skriver, K. (2013). Structure, function and networks of transcription factors involved in abiotic stress responses. International journal of molecular sciences, 14(3), 5842-5878.

Liu, J., Fu, J., Tian, H., & Gao, Y. (2015). In-season expression of nitrate and ammonium transporter genes in roots of winter wheat (Triticum aestivum L.) genotypes with different nitrogen-uptake efficiencies. Crop and Pasture Science, 66(7), 671-678.

Liu, K. H., & Tsay, Y. F. (2003). Switching between the two action modes of the dual-affinity nitrate transporter CHL1 by phosphorylation. The EMBO journal, 22(5), 1005-1013.

Liu, K. H., Huang, C. Y., & Tsay, Y. F. (1999). CHL1 is a dual-affinity nitrate transporter of Arabidopsis involved in multiple phases of nitrate uptake. The Plant Cell, 11(5), 865-874

Liu, K. H., Niu, Y., Konishi, M., Wu, Y., Du, H., Chung, H. S., ... & Sheen, J. (2017). Discovery of nitrate–CPK–NLP signalling in central nutrient–growth networks. Nature, 545(7654), 311-316.

Liu, K., Xu, H., Liu, G., Guan, P., Zhou, X., Peng, H., ... & Du, J. (2018). QTL mapping of flag leaf-related traits in wheat (Triticum aestivum L.). Theoretical and applied genetics, 131(4), 839-849.

Liu, X., Hu, B., & Chu, C. (2022). Nitrogen assimilation in plants: current status and future prospects. *Journal of Genetics and Genomics*, *49*(5), 394-404.

Lohse, M., Nagel, A., Herter, T., May, P., Schroda, M., Zrenner, R., ... & Usadel, B. (2014). Mercator: a fast and simple web server for genome scale functional annotation of plant sequence data. Plant, cell & environment, 37(5), 1250-1258.

Longo, A., Miles, N. W., & Dickstein, R. (2018). Genome mining of plant NPFs reveals varying conservation of signature motifs associated with the mechanism of transport. Frontiers in plant science, 1668.

Lopes, M. S., Cortadellas, N., Kichey, T., Dubois, F., Habash, D. Z., & Araus, J. L. (2006). Wheat nitrogen metabolism during grain filling: comparative role of glumes and the flag leaf. Planta, 225(1), 165-181.

López-Bellido, L., López-Bellido, R. J., & López-Bellido, F. J. (2006). Fertilizer nitrogen efficiency in durum wheat under rainfed Mediterranean conditions: Effect of split application. Agronomy journal, 98(1), 55-62.

Loussaert, D., Clapp, J., Mongar, N., O'Neill, D. P., & Shen, B. (2018). Nitrate assimilation limits nitrogen use efficiency (NUE) in maize (Zea mays L.). Agronomy, 8(7), 110.

Love, M. I., Huber, W., & Anders, S. (2014). Moderated estimation of fold change and dispersion for RNA-seq data with DESeq2. Genome biology, 15(12), 1-21.

Lu, C., & Tian, H. (2017). Global nitrogen and phosphorus fertilizer use for agriculture production in the past half century: shifted hot spots and nutrient imbalance. Earth System Science Data, 9(1), 181-192.

Lv, R., Han, L., Xiao, B., Xiao, C., Yang, Z., Wang, H., ... & Yang, C. (2019). An extracted tetraploid wheat harbouring the BBAA component of common wheat shows anomalous shikimate and sucrose metabolism. BMC plant biology, 19(1), 1-11.

Lynch, M., & Conery, J. S. (2000). The evolutionary fate and consequences of duplicate genes. science, 290(5494), 1151-1155.

Ma, Q., Sun, Q., Zhang, X., Li, F., Ding, Y., Tao, R., ... & Zhu, X. (2022). Controlled-release nitrogen fertilizer management influences grain yield in winter wheat by regulating flag leaf senescence post-anthesis and grain filling. Food and Energy Security, e361.

Maccaferri, M., Harris, N. S., Twardziok, S. O., Pasam, R. K., Gundlach, H., Spannagl, M., ... & Cattivelli, L. (2019). Durum wheat genome highlights past domestication signatures and future improvement targets. Nature genetics, 51(5), 885-895.

Maccaferri, M., Ricci, A., Salvi, S., Milner, S. G., Noli, E., Martelli, P. L., ... & Tuberosa, R. (2015). A high-density, SNP-based consensus map of tetraploid wheat as a bridge to integrate durum and bread wheat genomics and breeding. Plant biotechnology journal, 13(5), 648-663.

MacKown, C. T., & McClure, P. R. (1988). Development of accelerated net nitrate uptake: effects of nitrate concentration and exposure time. Plant physiology, 87(1), 162-166.

Maeda, S. I., Konishi, M., Yanagisawa, S., & Omata, T. (2014). Nitrite transport activity of a novel HPP family protein conserved in cyanobacteria and chloroplasts. Plant and Cell Physiology, 55(7), 1311-1324.

Mansour, M. M. F. (2000). Nitrogen containing compounds and adaptation of plants to salinity stress. Biologia plantarum, 43(4), 491-500.

Marchive, C., Roudier, F., Castaings, L., Bréhaut, V., Blondet, E., Colot, V., ... & Krapp, A. (2013). Nuclear retention of the transcription factor NLP7 orchestrates the early response to nitrate in plants. Nature communications, 4(1), 1-9.

Marcussen, T., Sandve, S. R., Heier, L., Spannagl, M., Pfeifer, M., Jakobsen, K. S., ... & International Wheat Genome Sequencing Consortium. (2014). Ancient hybridizations among the ancestral genomes of bread wheat. science, 345(6194).

Mauceri, A., Abenavoli, M. R., Toppino, L., Panda, S., Mercati, F., Aci, M. M., ... & Lupini, A. (2021). Transcriptomics reveal new insights into molecular regulation of nitrogen use efficiency in Solanum melongena. *Journal of experimental botany*, *72*(12), 4237-4253.

Mauceri, A., Aci, M. M., Toppino, L., Panda, S., Meir, S., Mercati, F., ... & Sunseri, F. (2022). Uncovering Pathways Highly Correlated to NUE through a Combined Metabolomics and Transcriptomics Approach in Eggplant. *Plants*, *11*(5), 700.

Miflin, B. J., & Habash, D. Z. (2002). The role of glutamine synthetase and glutamate dehydrogenase in nitrogen assimilation and possibilities for improvement in the nitrogen utilization of crops. Journal of experimental botany, 53(370), 979-987.

Miller, A. J., Fan, X., Orsel, M., Smith, S. J., & Wells, D. M. (2007). Nitrate transport and signalling. *Journal of experimental Botany*, *58*(9), 2297-2306.

Min, X., Siddiqi, M. Y., Guy, R. D., Glass, A. D., & Kronzucker, H. J. (2000). A comparative kinetic analysis of nitrate and ammonium influx in two early-successional tree species of temperate and boreal forest ecosystems. Plant, Cell & Environment, 23(3), 321-328.

Mistry, J., Finn, R. D., Eddy, S. R., Bateman, A., & Punta, M. (2013). Challenges in homology search: HMMER3 and convergent evolution of coiled-coil regions. Nucleic acids research, 41(12), e121-e121.

Miyashita, Y., & Good, A. G. (2008). NAD (H)-dependent glutamate dehydrogenase is essential for the survival of Arabidopsis thaliana during dark-induced carbon starvation. *Journal of Experimental Botany*, *59*(3), 667-680.

Mokhele, B., Zhan, X., Yang, G., & Zhang, X. (2012). Nitrogen assimilation in crop plants and its affecting factors. Canadian Journal of Plant Science, 92(3), 399-405.

Moll, R. H., Kamprath, E. J., & Jackson, W. A. (1982). Analysis and interpretation of factors which contribute to efficiency of nitrogen utilization 1. Agronomy journal, 74(3), 562-564.

Morere-Le Paven, M. C., Viau, L., Hamon, A., Vandecasteele, C., Pellizzaro, A., Bourdin, C., ... & Limami, A. M. (2011). Characterization of a dual-affinity nitrate transporter MtNRT1. 3 in the model legume Medicago truncatula. Journal of Experimental Botany, 62(15), 5595-5605.

Motzo, Rosella; Fois, Simonetta; Giunta, Francesco. 2004. "Relationship between Grain Yield and Quality of Durum Wheats from Different Eras of Breeding." Euphytica 140(3): 147–54.

Munns R, Tester M. Mechanisms of salinity tolerance. Annu Rev Plant Biol. 2008;59:651–81.

Muños, S., Cazettes, C., Fizames, C., Gaymard, F., Tillard, P., Lepetit, M., ... & Gojon, A. (2004). Transcript profiling in the chl1-5 mutant of Arabidopsis reveals a role of the nitrate transporter NRT1. 1 in the regulation of another nitrate transporter, NRT2. 1. The Plant Cell, 16(9), 2433-2447.

Muurinen, S., Slafer, G. A., & Peltonen-Sainio, P. (2006). Breeding effects on nitrogen use efficiency of spring cereals under northern conditions. Crop Science, 46(2), 561-568.

Muvunyi BP, Yan Q, Wu F, Min X, Yan ZZ, Kanzana G, et al. Mining late embryogenesis abundant (LEA) family genes in Cleistogenes songorica, a xerophyte perennial desert plant. Int J Mol Sci. 2018;19:3430.

Navarro JM, Pérez-Tornero O, Morte A. Alleviation of salt stress in citrus seedlings inoculated with arbuscular mycorrhizal fungi depends on the rootstock salt tolerance. J Plant Physiol. 2014;171:76–85.

Nazish, T., Arshad, M., Jan, S. U., Javaid, A., Khan, M. H., Naeem, M. A., ... & Ali, M. (2021). Transporters and transcription factors gene families involved in improving nitrogen use efficiency (NUE) and assimilation in rice (Oryza sativa L.). Transgenic Research, 1-20.

Nie, L., Feng, J., Fan, P., Chen, X., Guo, J., Lv, S., ... & Li, Y. (2015). Comparative proteomics of root plasma membrane proteins reveals the involvement of calcium signalling in NaCl-facilitated nitrate uptake in Salicornia europaea. Journal of Experimental Botany, 66(15), 4497-4510.

Nigro, D., Gadaleta, A., Mangini, G., Colasuonno, P., Marcotuli, I., Giancaspro, A., ... & Blanco, A. (2019). Candidate genes and genome-wide association study of grain protein content and protein deviation in durum wheat. Planta, 249(4), 1157-1175.

Niu, L., & Liao, W. (2016). Hydrogen peroxide signaling in plant development and abiotic responses: crosstalk with nitric oxide and calcium. Frontiers in Plant Science, 7, 230.

O'Brien, J. A., Vega, A., Bouguyon, E., Krouk, G., Gojon, A., Coruzzi, G., & Gutiérrez, R. A. (2016). Nitrate transport, sensing, and responses in plants. Molecular plant, 9(6), 837-856.

Orsel, M., Filleur, S., Fraisier, V., & Daniel-Vedele, F. (2002A). Nitrate transport in plants: which gene and which control?. Journal of Experimental Botany, 53(370), 825-833.

Orsel, M., Krapp, A., & Daniel-Vedele, F. (2002B). Analysis of the NRT2 nitrate transporter family in Arabidopsis. Structure and gene expression. Plant physiology, 129(2), 886-896.

Ortiz-MonasterioR, J. I., Sayre, K. D., Rajaram, S., & McMahon, M. (1997). Genetic progress in wheat yield and nitrogen use efficiency under four nitrogen rates. Crop Science, 37(3), 898-904.

Ouziad F, Wilde P, Schmelzer E, Hildebrandt U, Bothe H. Analysis of expression of aquaporins and Na+/H+ transporters in tomato colonized by arbuscular mycorrhizal fungi and affected by salt stress. Environ Exp Bot. 2006;57:177–86.

Palta, J. A., & Yang, J. C. (2014). Crop root system behaviour and yield. Field Crops Research, 165, 1-149.

Palta, J. A., Chen, X., Milroy, S. P., Rebetzke, G. J., Dreccer, M. F., & Watt, M. (2011). Large root systems: are they useful in adapting wheat to dry environments?. Functional Plant Biology, 38(5), 347-354.

Pandian BA, Sathishraj R, Djanaguiraman M, Prasad P V, Jugulam M. Role of cytochrome P450 enzymes in plant stress response. Antioxidants. 2020;9:454.

Pang, J., Milroy, S. P., Rebetzke, G. J., & Palta, J. A. (2015). The influence of shoot and root size on nitrogen uptake in wheat is affected by nitrate affinity in the roots during early growth. Functional Plant Biology, 42(12), 1179-1189.

Pang, J., Palta, J. A., Rebetzke, G. J., & Milroy, S. P. (2013). Wheat genotypes with high early vigour accumulate more nitrogen and have higher photosynthetic nitrogen use efficiency during early growth. Functional Plant Biology, 41(2), 215-222.

Patro, R., Duggal, G., Love, M. I., Irizarry, R. A., & Kingsford, C. (2017). Salmon provides fast and bias-aware quantification of transcript expression. Nature methods, 14(4), 417-419.

Paux, E., Sourdille, P., Salse, J., Saintenac, C., Choulet, F., Leroy, P., ... & Feuillet, C. (2008). A physical map of the 1-gigabase bread wheat chromosome 3B. science, 322(5898), 101-104.

Peng, J. H., Sun, D., & Nevo, E. (2011). Domestication evolution, genetics and genomics in wheat. Molecular Breeding, 28(3), 281-301.

Phillips JM, Hayman DS. Improved procedures for clearing and staining parasitic and vesicular-arbuscular mycorrhizal fungi for rapid assessment of infection. Trans Br Mycol Soc. 1970; 55: 158–161.

Pilbeam, C. J., McNeill, A. M., Harris, H. C., & Swift, R. S. (1997). Effect of fertilizer rate and form on the recovery of 15N-labelled fertilizer applied to wheat in Syria. The Journal of Agricultural Science, 128(4), 415-424.

Popova, O. V., Dietz, K. J., & Golldack, D. (2003). Salt-dependent expression of a nitrate transporter and two amino acid transporter genes in Mesembryanthemum crystallinum. Plant molecular biology, 52(3), 569-578.

Porcel, R., Aroca, R., Azcon, R., & Ruiz-Lozano, J. M. (2016). Regulation of cation transporter genes by the arbuscular mycorrhizal symbiosis in rice plants subjected to salinity suggests improved salt tolerance due to reduced Na+ root-to-shoot distribution. Mycorrhiza, 26(7), 673-684.

Porcel, R., Redondo-Gómez, S., Mateos-Naranjo, E., Aroca, R., Garcia, R., & Ruiz-Lozano, J. M. (2015). Arbuscular mycorrhizal symbiosis ameliorates the optimum quantum yield of photosystem II and reduces non-photochemical quenching in rice plants subjected to salt stress. Journal of plant physiology, 185, 75-83.

Pozo MJ, Jung SC, López-Ráez JA, Azcón-Aguilar C. Impact of arbuscular mycorrhizal symbiosis on plant response to biotic stress: the role of plant defence mechanisms. In: Arbuscular mycorrhizas: physiology and function. Springer; 2010. p. 193–207.

Qi YC, Liu WQ, Qiu LY, Zhang SM, Ma L, Zhang H. Overexpression of glutathione S-transferase gene increases salt tolerance of Arabidopsis. Russ J plant Physiol. 2010;57:233–40.

Qin, T., Zhao, H., Cui, P., Albesher, N., & Xiong, L. (2017). A nucleus-localized long non-coding RNA enhances drought and salt stress tolerance. Plant physiology, 175(3), 1321-1336.

Qin, Y., Tian, Y., & Liu, X. (2015). A wheat salinity-induced WRKY transcription factor TaWRKY93 confers multiple abiotic stress tolerance in Arabidopsis thaliana. Biochemical and Biophysical Research Communications, 464(2), 428-433.

Quan, X., Zeng, J., Ye, L., Chen, G., Han, Z., Shah, J. M., & Zhang, G. (2016). Transcriptome profiling analysis for two Tibetan wild barley genotypes in responses to low nitrogen. BMC plant biology, 16(1), 1-16.

Qudeimat E, Faltusz AMC, Wheeler G, Lang D, Holtorf H, Brownlee C, et al. A PIIB-type Ca2+-ATPase is essential for stress adaptation in Physcomitrella patens. Proc Natl Acad Sci. 2008;105:19555–60.

R Core Team (2021). R: A language and environment for statistical computing. R Foundation for Statistical Computing, Vienna, Austria. URL https://www.R-project.org/.

Rashid, M., Bera, S., Medvinsky, A. B., Sun, G. Q., Li, B. L., & Chakraborty, A. (2018). Adaptive regulation of nitrate transceptor NRT1. 1 in fluctuating soil nitrate conditions. Iscience, 2, 41-50.

Rasmussen, Irene Skovby; Dresbøll, Dorte Bodin; Thorup-Kristensen, Kristian. 2015. "Winter Wheat Cultivars and Nitrogen (N) Fertilization—Effects on Root Growth, N Uptake Efficiency and N Use Efficiency." European Journal of Agronomy 68(NA): 38–49.

Raudvere U, Kolberg L, Kuzmin I, Arak T, Adler P, Peterson H, et al. g: Profiler: a web server for functional enrichment analysis and conversions of gene lists (2019 update). Nucleic Acids Res. 2019;47:W191–8.

Raun, W. R., & Johnson, G. V. (1999). Improving nitrogen use efficiency for cereal production. Agronomy journal, 91(3), 357-363.

Redillas MCFR, Park S-H, Lee JW, Kim YS, Jeong JS, Jung H, et al. Accumulation of trehalose increases soluble sugar contents in rice plants conferring tolerance to drought and salt stress. Plant Biotechnol Rep. 2012;6:89–96.

Redinbaugh, M. G., Huber, S. C., Huber, J. L., Hendrix, K. W., & Campbell, W. H. (1996). Nitrate reductase expression in maize leaves (Zea mays) during dark-light transitions. Complex effects of protein phosphatase inhibitors on enzyme activity, protein synthesis and transcript levels. Physiologia Plantarum, 98(1), 67-76.

Rehman RU, Di Sansebastiano G-P. Plant Rab GTPases in membrane trafficking and signalling. Plant Signal Underst Mol crosstalk. 2014;:51–73.

Renault H, Roussel V, El Amrani A, Arzel M, Renault D, Bouchereau A, et al. The Arabidopsis pop2-1 mutant reveals the involvement of GABA transaminase in salt stress tolerance. BMC Plant Biol. 2010;10:1–16.

Rengasamy P. World salinization with emphasis on Australia. J Exp Bot. 2006;57:1017–23.

Rharrabti, Y., Villegas, D., García del Moral, L. F., Aparicio, N., Elhani, S., & Royo, C. (2001). Environmental and genetic determination of protein content and grain yield in durum wheat under Mediterranean conditions. Plant Breeding, 120(5), 381-388.

Riveras, E., Alvarez, J. M., Vidal, E. A., Oses, C., Vega, A., & Gutiérrez, R. A. (2015). The calcium ion is a second messenger in the nitrate signaling pathway of Arabidopsis. Plant physiology, 169(2), 1397-1404.

Robertson, G. P., & Vitousek, P. M. (2009). Nitrogen in agriculture: balancing the cost of an essential resource. Annual review of environment and resources, 34, 97-125.

Rolly, N. K., & Yun, B. W. (2021). Regulation of Nitrate (NO3) Transporters and Glutamate Synthase-Encoding Genes under Drought Stress in Arabidopsis: The Regulatory Role of AtbZIP62 Transcription Factor. Plants, 10(10), 2149.

Ruisi, P., Frangipane, B., Amato, G., Frenda, A. S., Plaia, A., Giambalvo, D., & Saia, S. (2015). Nitrogen uptake and nitrogen fertilizer recovery in old and modern wheat genotypes grown in the presence or absence of interspecific competition. Frontiers in plant science, 6, 185.

Ruisi, P., Giambalvo, D., Saia, S., Di Miceli, G., Frenda, A. S., Plaia, A., & Amato, G. (2014). Conservation tillage in a semiarid Mediterranean environment: results of 20 years of research. Italian Journal of Agronomy, 9(1), 1-7.

Ruisi, P., Giambalvo, D., Saia, S., Di Miceli, G., Frenda, A. S., Plaia, A., & Amato, G. (2014). Conservation tillage in a semiarid Mediterranean environment: results of 20 years of research. Italian Journal of Agronomy, 9(1), 1-7.

Ruisi, P., Saia, S., Badagliacca, G., Amato, G., Frenda, A. S., Giambalvo, D., & Di Miceli, G. (2016). Long-term effects of no tillage treatment on soil N availability, N uptake, and 15N-fertilizer recovery of durum wheat differ in relation to crop sequence. Field crops research, 189, 51-58.

Ruiz-Lozano, J. M., Porcel, R., Azcón, C., & Aroca, R. (2012). Regulation by arbuscular mycorrhizae of the integrated physiological response to salinity in plants: new challenges in physiological and molecular studies. Journal of Experimental Botany, 63(11), 4033-4044.

Ryan, J., Ibrikci, H., Sommer, R., & McNeill, A. (2009). Nitrogen in rainfed and irrigated cropping systems in the Mediterranean region. Advances in Agronomy, 104, 53-136.

Sa, G., Yao, J., Deng, C., Liu, J., Zhang, Y., Zhu, Z., ... & Chen, S. (2019). Amelioration of nitrate uptake under salt stress by ectomycorrhiza with and without a Hartig net. New Phytologist, 222(4), 1951-1964.

Saha J, Brauer EK, Sengupta A, Popescu SC, Gupta K, Gupta B. Polyamines as redox homeostasis regulators during salt stress in plants. Front Environ Sci. 2015;3:21.

Sairam RK, Deshmukh PS, Shukla DS. Tolerance to drought and temperature stress in relation to increased antioxidant enzyme activity in wheat. J Agron Crop Sci. 1997; 178: 171–177.

Salse, J., Bolot, S., Throude, M., Jouffe, V., Piegu, B., Quraishi, U. M., ... & Feuillet, C. (2008). Identification and characterization of shared duplications between rice and wheat provide new insight into grass genome evolution. The Plant Cell, 20(1), 11-24.

Sanaa, M., Van Cleemput, O., Baert, L., & Mhiri, A. (1992). Field study of the fate of labelled fertilizer nitrogen applied to wheat on calcareous Tunisian soils. Pédologie (Gent), 42(3), 245-255.

Sánchez-Barrena MJ, Martínez-Ripoll M, Zhu J-K, Albert A. The structure of the Arabidopsis thaliana SOS3: molecular mechanism of sensing calcium for salt stress response. J Mol Biol. 2005;345:1253–64.

Scheible, W. R., Morcuende, R., Czechowski, T., Fritz, C., Osuna, D., Palacios-Rojas, N., ... & Stitt, M. (2004). Genome-wide reprogramming of primary and secondary metabolism, protein synthesis, cellular growth processes, and the regulatory infrastructure of Arabidopsis in response to nitrogen. Plant physiology, 136(1), 2483-2499.

Severini, Alan David; Wasson, Anton; Evans, John R.; Richards, Richard A.; Watt, Michelle. (2020). "Root Phenotypes at Maturity in Diverse Wheat and Triticale Genotypes Grown in Three Field Experiments: Relationships to Shoot Selection, Biomass, Grain Yield, Flowering Time, and Environment." Field Crops Research 255(NA): 107870-NA.

Shabala, S. (2013). Learning from halophytes: physiological basis and strategies to improve abiotic stress tolerance in crops. Annals of botany, 112(7), 1209-1221.

Shahid SA, Zaman M, Heng L. Soil salinity: historical perspectives and a world overview of the problem. In: Guideline for salinity assessment, mitigation and adaptation using nuclear and related techniques. Springer; 2018. p. 43–53.

Shannon P, Markiel A, Ozier O, Baliga NS, Wang JT, Ramage D, et al. Cytoscape: a software environment for integrated models of biomolecular interaction networks. Genome Res. 2003;13:2498–504.

Shi W, Hao L, Li J, Liu D, Guo X, Li H. The Gossypium hirsutum WRKY gene GhWRKY39-1 promotes pathogen infection defense responses and mediates salt stress tolerance in transgenic Nicotiana benthamiana. Plant Cell Rep. 2014;33:483–98.

Siddiqi, M. Y., Glass, A. D., Ruth, T. J., & Rufty, T. W. (1990). Studies of the uptake of nitrate in barley: I. Kinetics of 13NO3− influx. Plant Physiology, 93(4), 1426-1432.

Sievers, F., Wilm, A., Dineen, D., Gibson, T. J., Karplus, K., Li, W., ... & Higgins, D. G. (2011). Fast, scalable generation of high-quality protein multiple sequence alignments using Clustal Omega. Molecular systems biology, 7(1), 539.

Simpson, R. J., Lambers, H., & Dalling, M. J. (1983). Nitrogen redistribution during grain growth in wheat (Triticum aestivum L.): IV. Development of a quantitative model of the translocation of nitrogen to the grain. Plant Physiology, 71(1), 7-14.

Singh, A., Kanwar, P., Yadav, A. K., Mishra, M., Jha, S. K., Baranwal, V., ... & Pandey, G. K. (2014). Genome-wide expressional and functional analysis of calcium transport elements during abiotic stress and development in rice. The FEBS journal, 281(3), 894-915.

Singh, J., Kunhikrishnan, A., Bolan, N. S., & Saggar, S. (2013). Impact of urease inhibitor on ammonia and nitrous oxide emissions from temperate pasture soil cores receiving urea fertilizer and cattle urine. Science of the total Environment, 465, 56-63.

Singh, M., Singh, A., Prasad, S. M., & Singh, R. K. (2017). Regulation of plants metabolism in response to salt stress: an omics approach. Acta Physiologiae Plantarum, 39(2), 1-17.

Singh, R. P., Jha, P., & Jha, P. N. (2015). The plant-growth-promoting bacterium Klebsiella sp. SBP-8 confers induced systemic tolerance in wheat (Triticum aestivum) under salt stress. Journal of plant physiology, 184, 57-67.

Slafer, Gustavo A.; Andrade, Fernando H.; Feingold, Sergio E. 1990. "Genetic Improvement of Bread Wheat (Triticum Aestivum L.) in Argentina : Relationships between Nitrogen and Dry Matter." Euphytica 50(1): 63–71.

Smith, S. E., & Read, D. J. (2010). Mycorrhizal symbiosis. Academic press.

Sol, S., Valkov, V. T., Rogato, A., Noguero, M., Gargiulo, L., Mele, G., ... & Chiurazzi, M. (2019). Disruption of the Lotus japonicus transporter LjNPF2. 9 increases shoot biomass and nitrate content without affecting symbiotic performances. BMC plant biology, 19(1), 1-14.

Stein H, Honig A, Miller G, Erster O, Eilenberg H, Csonka LN, et al. Elevation of free proline and proline-rich protein levels by simultaneous manipulations of proline biosynthesis and degradation in plants. Plant Sci. 2011;181:140–50.

Sun M, Jia B, Cui N, Wen Y, Duanmu H, Yu Q, et al. Functional characterization of a Glycine soja Ca 2+ ATPase in salt–alkaline stress responses. Plant Mol Biol. 2016;90:419–34.

Sun, Y., Zhang, T., Xu, X., Yang, Y., Tong, H., Mur, L. A. J., & Yuan, H. (2021). Transcriptomic Characterization of Nitrate-Enhanced Stevioside Glycoside Synthesis in Stevia (Stevia rebaudiana) Bertoni. International journal of molecular sciences, 22(16), 8549.

Supek F, Bošnjak M, Škunca N, Šmuc T. REVIGO summarizes and visualizes long lists of gene ontology terms. PLoS One. 2011;6:e21800.

Swarbreck, S. M., Wang, M., Wang, Y., Kindred, D., Sylvester-Bradley, R., Shi, W., ... & Griffiths, H. (2019). A roadmap for lowering crop nitrogen requirement. Trends in Plant Science, 24(10), 892-904.

Sylvester-Bradley, R., & Kindred, D. R. (2009). Analysing nitrogen responses of cereals to prioritize routes to the improvement of nitrogen use efficiency. Journal of experimental botany, 60(7), 1939-1951.

Tal, I., Zhang, Y., Jørgensen, M. E., Pisanty, O., Barbosa, I. C., Zourelidou, M., ... & Shani, E. (2016). The Arabidopsis NPF3 protein is a GA transporter. Nature communications, 7(1), 1-11.

Talaat NB, Shawky BT. Protective effects of arbuscular mycorrhizal fungi on wheat (Triticum aestivum L.) plants exposed to salinity. Environ Exp Bot. 2014;98:20–31.

Tang, W., Ye, J., Yao, X., Zhao, P., Xuan, W., Tian, Y., ... & Wan, J. (2019). Genome-wide associated study identifies NAC42-activated nitrate transporter conferring high nitrogen use efficiency in rice. Nature communications, 10(1), 1-11.

Taranto, F., D'Agostino, N., Rodriguez, M., Pavan, S., Minervini, A. P., Pecchioni, N., ... & De Vita, P. (2020). Whole genome scan reveals molecular signatures of divergence and selection related to important traits in durum wheat germplasm. Frontiers in genetics, 11, 217.

Team, R. Core. (2013). R: A language and environment for statistical computing.

Thimm, O., Bläsing, O., Gibon, Y., Nagel, A., Meyer, S., Krüger, P., ... & Stitt, M. (2004). MAPMAN: a user-driven tool to display genomics data sets onto diagrams of metabolic pathways and other biological processes. The Plant Journal, 37(6), 914-939.

Thomas PD, Campbell MJ, Kejariwal A, Mi H, Karlak B, Daverman R, et al. PANTHER: a library of protein families and subfamilies indexed by function. Genome Res. 2003;13:2129–41.

Thorup-Kristensen, Kristian; Cortasa, Montserrat Salmerón; Loges, Ralf. 2009. "Winter Wheat Roots Grow Twice as Deep as Spring Wheat Roots, Is This Important for N Uptake and N Leaching Losses?" Plant and Soil 322(1): 101–14.

Tian, H., Yuan, X., Duan, J., Li, W., Zhai, B., & Gao, Y. (2017). Influence of nutrient signals and carbon allocation on the expression of phosphate and nitrogen transporter genes in winter wheat (Triticum aestivum L.) roots colonized by arbuscular mycorrhizal fungi. PLoS One, 12(2), e0172154.

Tilman, D., Cassman, K. G., Matson, P. A., Naylor, R., & Polasky, S. (2002). Agricultural sustainability and intensive production practices. Nature, 418(6898), 671-677.

Todd, C. D., Zeng, P., Huete, A. M. R., Hoyos, M. E., & Polacco, J. C. (2004). Transcripts of MYB-like genes respond to phosphorous and nitrogen deprivation in Arabidopsis. Planta, 219(6), 1003-1009.

Tong, J., Walk, T. C., Han, P., Chen, L., Shen, X., Li, Y., ... & Qin, L. (2020). Genome-wide identification and analysis of high-affinity nitrate transporter 2 (NRT2) family genes in rapeseed (Brassica napus L.) and their responses to various stresses. BMC plant biology, 20(1), 1-16.

Troccoli, A., Borrelli, G. M., De Vita, P., Fares, C., & Di Fonzo, N. (2000). Mini review: durum wheat quality: a multidisciplinary concept. Journal of Cereal Science, 32(2), 99-113.

Trueman, L. J., Richardson, A., & Forde, B. G. (1996). Molecular cloning of higher plant homologues of the high-affinity nitrate transporters of Chlamydomonas reinhardtii and Aspergillus nidulans. Gene, 175(1-2), 223-231.

Tsay, Y. F., Chiu, C. C., Tsai, C. B., Ho, C. H., & Hsu, P. K. (2007). Nitrate transporters and peptide transporters. FEBS letters, 581(12), 2290-2300.

Tsay, Y. F., Schroeder, J. I., Feldmann, K. A., & Crawford, N. M. (1993). The herbicide sensitivity gene CHL1 of Arabidopsis encodes a nitrate-inducible nitrate transporter. Cell, 72(5), 705-713.

Tzfadia, O., Diels, T., De Meyer, S., Vandepoele, K., Aharoni, A., & Van de Peer, Y. (2016). CoExpNetViz: comparative co-expression networks construction and visualization tool. Frontiers in plant science, 6, 1194.

Ueda A, Yamamoto-Yamane Y, Takabe T. Salt stress enhances proline utilization in the apical region of barley roots. Biochem Biophys Res Commun. 2007;355:61–6.

Vicente, R., Bolger, A. M., Martínez-Carrasco, R., Pérez, P., Gutiérrez, E., Usadel, B., & Morcuende, R. (2019). De novo transcriptome analysis of durum wheat flag leaves provides new insights into the regulatory response to elevated CO2 and high temperature. Frontiers in plant science, 10, 1605.

Vimal SR, Singh JS, Arora NK, Singh S. Soil-plant-microbe interactions in stressed agriculture management: a review. Pedosphere. 2017;27:177–92.

von der Fecht-Bartenbach, J., Bogner, M., Dynowski, M., & Ludewig, U. (2010). CLC-b-mediated NO− 3/H+ exchange across the tonoplast of Arabidopsis vacuoles. Plant and Cell Physiology, 51(6), 960-968.

von Wirén, N., Gazzarrini, S., & Frommer, W. B. (1997). Regulation of mineral nitrogen uptake in plants. Plant and Soil, 196(2), 191-199.

Von Wittgenstein, N. J., Le, C. H., Hawkins, B. J., & Ehlting, J. (2014). Evolutionary classification of ammonium, nitrate, and peptide transporters in land plants. BMC evolutionary biology, 14(1), 1-17.

Wang, C., Liu, W., Li, Q., Ma, D., Lu, H., Feng, W., ... & Guo, T. (2014). Effects of different irrigation and nitrogen regimes on root growth and its correlation with above-ground plant parts in high-yielding wheat under field conditions. Field Crops Research, 165, 138-149.

Wang, D., Xu, T., Yin, Z., Wu, W., Geng, H., Li, L., ... & Lian, X. (2020). Overexpression of OsMYB305 in rice enhances the nitrogen uptake under low-nitrogen condition. Frontiers in plant science, 11, 369.

Wang, J., Hüner, N., & Tian, L. (2019A). Identification and molecular characterization of the Brachypodium distachyon NRT2 family, with a major role of BdNRT2. 1. Physiologia plantarum, 165(3), 498-510.

Wang, J., Li, Y., Zhu, F., Ming, R., & Chen, L. Q. (2019B). Genome-wide analysis of nitrate transporter (NRT/NPF) family in sugarcane Saccharum spontaneum L. Tropical Plant Biology, 12(3), 133-149.

Wang, J., Song, K., Sun, L., Qin, Q., Sun, Y., Pan, J., & Xue, Y. (2019C). Morphological and transcriptome analysis of wheat seedlings response to low nitrogen stress. Plants, 8(4), 98.

Wang, J., Wu, X. F., Tang, Y., Li, J. G., & Zhao, M. L. (2021A). RNA-Seq Provides New Insights into the Molecular Events Involved in “Ball-Skin versus Bladder Effect” on Fruit Cracking in Litchi. International journal of molecular sciences, 22(1), 454.

Wang, Q., Liu, C., Dong, Q., Huang, D., Li, C., Li, P., & Ma, F. (2018A). Genome-wide identification and analysis of apple NITRATE TRANSPORTER 1/PEPTIDE TRANSPORTER family (NPF) genes reveals MdNPF6. 5 confers high capacity for nitrogen uptake under low-nitrogen conditions. International journal of molecular sciences, 19(9), 2761.

Wang, R., Guan, P., Chen, M., Xing, X., Zhang, Y., & Crawford, N. M. (2010). Multiple regulatory elements in the Arabidopsis NIA1 promoter act synergistically to form a nitrate enhancer. Plant physiology, 154(1), 423-432.

Wang, R., Okamoto, M., Xing, X., & Crawford, N. M. (2003). Microarray analysis of the nitrate response in Arabidopsis roots and shoots reveals over 1,000 rapidly responding genes and new linkages to glucose, trehalose-6-phosphate, iron, and sulfate metabolism. Plant physiology, 132(2), 556-567.

Wang, X. F., An, J. P., Liu, X., Su, L., You, C. X., & Hao, Y. J. (2018B). The nitrate-responsive protein MdBT2 regulates anthocyanin biosynthesis by interacting with the MdMYB1 transcription factor. Plant Physiology, 178(2), 890-906.

Wang, X., Cai, X., Xu, C., & Wang, Q. (2021B). Identification and characterization of the NPF, NRT2 and NRT3 in spinach. Plant Physiology and Biochemistry, 158, 297-307.

Wang, Y. Y., Cheng, Y. H., Chen, K. E., & Tsay, Y. F. (2018C). Nitrate transport, signaling, and use efficiency. Annual Review of Plant Biology, 69, 85-122.

Wang, Y. Y., Hsu, P. K., & Tsay, Y. F. (2012A). Uptake, allocation and signaling of nitrate. Trends in plant science, 17(8), 458-467.

Wang, Y., Gu, W., Meng, Y., Xie, T., Li, L., Li, J., & Wei, S. (2017). γ-Aminobutyric acid imparts partial protection from salt stress injury to maize seedlings by improving photosynthesis and upregulating osmoprotectants and antioxidants. Scientific reports, 7(1), 1-13.

Wang, Y., Tang, H., DeBarry, J. D., Tan, X., Li, J., Wang, X., ... & Paterson, A. H. (2012B). MCScanX: a toolkit for detection and evolutionary analysis of gene synteny and collinearity. Nucleic acids research, 40(7), e49-e49.

Wang, Y., Ying, H., Yin, Y., Zheng, H., & Cui, Z. (2019D). Estimating soil nitrate leaching of nitrogen fertilizer from global meta-analysis. Science of the total Environment, 657, 96-102.

Wang, Yingcheng; Ying, Hao; Yin, Yulong; Zheng, Huifang; Cui, Zhenling. (2018D). Estimating Soil Nitrate Leaching of Nitrogen Fertilizer from Global Meta-Analysis. The Science of the total environment 657(NA): 96–102.

Wang, Y., Wang, M., Li, Y., Wu, A., & Huang, J. (2018D). Effects of arbuscular mycorrhizal fungi on growth and nitrogen uptake of Chrysanthemum morifolium under salt stress. *PLoS One*, *13*(4), e0196408.

Wen S, Zhang Y, Deng Y, Chen G, Yu Y, Wei Q. (2020A) Genomic identification and expression analysis of the BBX transcription factor gene family in Petunia hybrida. Mol Biol Rep. ;47:6027–41.

Wen, J., Li, P. F., Ran, F., Guo, P. C., Zhu, J. T., Yang, J., ... & Du, H. (2020B). Genome-wide characterization, expression analyses, and functional prediction of the NPF family in Brassica napus. BMC genomics, 21(1), 1-17.

Wen, Z., Tyerman, S. D., Dechorgnat, J., Ovchinnikova, E., Dhugga, K. S., & Kaiser, B. N. (2017). Maize NPF6 proteins are homologs of Arabidopsis CHL1 that are selective for both nitrate and chloride. The Plant Cell, 29(10), 2581-2596.

Wen, Z., & Kaiser, B. N. (2018). Unraveling the functional role of NPF6 transporters. Frontiers in Plant Science, 9, 973.

Wickham H, Wickham MH. The ggplot package. Google Sch http//ftp uni-bayreuth de/math/statlib/R/CRAN/doc/packages/ggplot pdf. 2007.

Williams KP, Lau BY. RNAcentral: A comprehensive database of non-coding RNA sequences. Nucleic Acids Res. 2016;45 SAND-2017-0752J.

Wu X, Jia Q, Ji S, Gong B, Li J, Lü G, et al. Gamma-aminobutyric acid (GABA) alleviates salt damage in tomato by modulating Na+ uptake, the GAD gene, amino acid synthesis and reactive oxygen species metabolism. BMC Plant Biol. 2020;20:1–21.

Xiang Y, Huang Y, Xiong L. Characterization of stress-responsive CIPK genes in rice for stress tolerance improvement. Plant Physiol. 2007;144:1416–28.

Xu, G., Fan, X., & Miller, A. J. (2012). Plant nitrogen assimilation and use efficiency. Annual review of plant biology, 63, 153-182.

Xu, N., Yu, B., Chen, R., Li, S., Zhang, G., & Huang, J. (2020). OsNAR2. 2 plays a vital role in the root growth and development by promoting nitrate uptake and signaling in rice. Plant Physiology and Biochemistry, 149, 159-169.

Xu, Z., Wang, C., Xue, F., Zhang, H., & Ji, W. (2015). Wheat NAC transcription factor TaNAC29 is involved in response to salt stress. Plant Physiology and Biochemistry, 96, 356-363.

Xuan, W., Beeckman, T., & Xu, G. (2017). Plant nitrogen nutrition: sensing and signaling. Current Opinion in Plant Biology, 39, 57-65.

Yan, M., Fan, X., Feng, H., Miller, A. J., Shen, Q., & Xu, G. (2011). Rice OsNAR2. 1 interacts with OsNRT2. 1, OsNRT2. 2 and OsNRT2. 3a nitrate transporters to provide uptake over high and low concentration ranges. Plant, Cell & Environment, 34(8), 1360-1372.

Yáñez-Cuna, J. O., Kvon, E. Z., & Stark, A. (2013). Deciphering the transcriptional cis-regulatory code. Trends in Genetics, 29(1), 11-22.

Yin, L. P., Li, P., Wen, B., Taylor, D., & Berry, J. O. (2007). Characterization and expression of a high-affinity nitrate system transporter gene (TaNRT2. 1) from wheat roots, and its evolutionary relationship to other NTR2 genes. Plant Science, 172(3), 621-631.

You, H., Liu, Y., Minh, T. N., Lu, H., Zhang, P., Li, W., ... & Li, Q. (2020). Genome-wide identification and expression analyses of nitrate transporter family genes in wild soybean (Glycine soja). Journal of Applied Genetics, 61(4), 489-501.

Yu, G., Wang, L. G., Han, Y., & He, Q. Y. (2012). clusterProfiler: an R package for comparing biological themes among gene clusters. Omics: a journal of integrative biology, 16(5), 284-287.

Yu, P., Li, X., Yuan, L., & Li, C. (2014). A novel morphological response of maize (Zea mays) adult roots to heterogeneous nitrate supply revealed by a split-root experiment. Physiologia Plantarum, 150(1), 133-144.

Zamboni, A., Astolfi, S., Zuchi, S., Pii, Y., Guardini, K., Tononi, P., & Varanini, Z. (2014). Nitrate induction triggers different transcriptional changes in a high and a low nitrogen use efficiency maize inbred line. Journal of integrative plant biology, 56(11), 1080-1094.

Zhang, H., Wang, X., You, M., & Liu, C. (1999). Water-yield relations and water-use efficiency of winter wheat in the North China Plain. Irrigation Science, 19(1), 37-45.

Zhang, L., Zhao, G., Xia, C., Jia, J., Liu, X., & Kong, X. (2012). Overexpression of a wheat MYB transcription factor gene, TaMYB56-B, enhances tolerances to freezing and salt stresses in transgenic Arabidopsis. Gene, 505(1), 100-107.

Zhang, W., Han, Z., Guo, Q., Liu, Y., Zheng, Y., Wu, F., & Jin, W. (2014). Identification of maize long non-coding RNAs responsive to drought stress. PloS one, 9(6), e98958.

Zhang, X., Chen, S., Sun, H., Wang, Y., & Shao, L. (2009). Root size, distribution and soil water depletion as affected by cultivars and environmental factors. Field Crops Research, 114(1), 75-83.

Zhang, X., Dong, J., Deng, F., Wang, W., Cheng, Y., Song, L., ... & Shen, F. (2019). The long non-coding RNA lncRNA973 is involved in cotton response to salt stress. BMC Plant Biology, 19(1), 1-16.

Zhang, X., Li, F., Ding, Y., Ma, Q., Yi, Y., Zhu, M., ... & Zhu, X. (2021A). Transcriptome Analysis of Two Near-Isogenic Lines with Different NUE under Normal Nitrogen Conditions in Wheat. Biology, 10(8), 787.

Zhang, Z., Li, Z., Wang, W., Jiang, Z., Guo, L., Wang, X., ... & Chu, C. (2021B). Modulation of nitrate-induced phosphate response by the MYB transcription factor RLI1/HINGE1 in the nucleus. Molecular Plant, 14(3), 517-529.

Zhao, H., Jiang, J., Li, K., & Liu, G. (2017). Populus simonii× Populus nigra WRKY70 is involved in salt stress and leaf blight disease responses. Tree physiology, 37(6), 827-844.

Zhao, L., Chen, P., Liu, P., Song, Y., & Zhang, D. (2021). Genetic Effects and Expression Patterns of the Nitrate Transporter (NRT) Gene Family in Populus tomentosa. Frontiers in plant science, 12, 754.

Zheng, Z. L. (2009). Carbon and nitrogen nutrient balance signaling in plants. Plant signaling & behavior, 4(7), 584-591.

Zhou, Y., Yang, P., Cui, F., Zhang, F., Luo, X., & Xie, J. (2016). Transcriptome analysis of salt stress responsiveness in the seedlings of Dongxiang wild rice (Oryza rufipogon Griff.). PloS one, 11(1), e0146242.

Zhu, X., Song, F., Liu, S., Liu, F., & Li, X. (2018). Arbuscular mycorrhiza enhances nutrient accumulation in wheat exposed to elevated CO2 and soil salinity. Journal of Plant Nutrition and Soil Science, 181(6), 836-846.

Zhuo, D., Okamoto, M., Vidmar, J. J., & Glass, A. D. (1999). Regulation of a putative high-affinity nitrate transporter (Nrt2; 1At) in roots of Arabidopsis thaliana. The Plant Journal, 17(5), 563-568.

Zou, X., Liu, M. Y., Wu, W. H., & Wang, Y. (2020). Phosphorylation at Ser28 stabilizes the Arabidopsis nitrate transporter NRT2. 1 in response to nitrate limitation. Journal of Integrative Plant Biology, 62(6), 865-876.